THE SENSITIVITY OF BUCKLING OF AXIALLY COMPRESSED FIBER-REINFORCED CYLINDRICAL SHELLS TO SMALL GEOMETRIC IMPERFECTIONS

By

Michael F. Card

Thesis submitted to the Graduate Faculty of the

Virginia Polytechnic Institute

in partial fulfillment for the degree of

DOCTOR OF PHILOSOPHY

in

ENGINEERING MECHANICS

June 1969

NOV 1969
RECEIVED
NASA STI FACILITY
INPUT BRANCH

N69-40244
(ACCESSION NUMBER)
167
(PAGES)
TMX-61914
(NASA CR OR TMX OR AD NUMBER)
(THRU)
1
(CODE)
32
(CATEGORY)
FACILITY FORM 602

Reproduced by the
CLEARINGHOUSE
for Federal Scientific & Technical
Information Springfield Va. 22151

THE SENSITIVITY OF BUCKLING OF AXIALLY COMPRESSED FIBER-REINFORCED CYLINDRICAL SHELLS TO SMALL GEOMETRIC IMPERFECTIONS

by

Michael F. Card

ABSTRACT

An index of imperfection sensitivity is obtained by investigating the character of the initial postbuckling region for a geometrically perfect cylindrical shell. Using techniques of perturbation theory, equations governing postbuckling behavior of a multilayered, orthotropic cylinder are developed. The theory considers the effects of nonlinear deformations induced by loading prior to buckling. Solutions for postbuckling displacements are obtained by converting the governing equations and boundary conditions to a system of second-order differential equations, which are then written in terms of finite differences at stations along the length of the cylinder. The resulting algebraic equations are solved by matrix algebra exploiting Gaussian elimination. A computer program was developed to solve the resulting large systems of simultaneous equations and to perform the numerical differentiation and integration necessary to calculate the imperfection sensitivity index.

Relative values of the imperfection sensitivity index are investigated for three types of fiber-reinforced cylinders: helically wrapped glass-epoxy and boron-epoxy cylinders, and aluminum cylinders overwrapped with boron-epoxy. The helical wrap angle was varied in cylinders of fixed geometry to identify wrapping configurations of minimum imperfection

sensitivity. Sensitivity indices were obtained from the present theory as well as from an extension of existing theory. Agreement between sensitivity indices predicted by the two theories was reasonably good. Computed results for buckling of the three types of cylinders suggest that substantial differences (up to 27 percent) can exist between classical and consistent theory predictions for buckling, depending on the wrapping configuration. The differences are a result of load-induced prebuckling deformations which are retained in consistent buckling theories but are omitted in classical theories.

Sensitivity indices computed for the three types of cylinders suggest that 45° wraps in helically wound glass-epoxy and boron-epoxy shells are desirable. For wraps possessing small imperfection sensitivity, boron-epoxy cylinders are less imperfection-sensitive than glass-epoxy cylinders. The most attractive configuration identified in the study was a circumferentially overwound boron-aluminum shell which was found to have a positive postbuckling slope.

The behavior of fiber-reinforced cylinders was investigated experimentally by conducting compressive buckling tests on twelve 30-inch-diameter glass-epoxy shells with variable wrap configurations. Elastic constants computed from test data were in good agreement with analytical predictions. Depending on wrap configuration, compressive buckling loads varied from 50 to 90 percent of consistent theory predictions. Comparisons of imperfection sensitivity indices with test data show that the indices are in fair agreement with experimental buckling data trends. The theoretical and experimental studies reported herein suggest that

certain fiber orientations can enhance the compressive buckling strength of geometrically similar cylinders due to the fiber configuration's reduced sensitivity to geometric imperfections in the cylinder wall.

THE SENSITIVITY OF BUCKLING OF AXIALLY COMPRESSED FIBER-REINFORCED CYLINDRICAL SHELLS TO SMALL GEOMETRIC IMPERFECTIONS

by

Michael F. Card

Thesis submitted to the Graduate Faculty of the

Virginia Polytechnic Institute

in partial fulfillment of the degree of

DOCTOR OF PHILOSOPHY

in

Engineering Mechanics

APPROVED:

Chairman, Dr. Daniel Frederick

Dr. Thomas Davis

Dr. Ricardo Chicurel

Prof. Charles Smith

Dr. Leonard McFadden

June 1969

Blacksburg, Virginia

II. TABLE OF CONTENTS

HEADING		PAGE
I.	TITLE	i
II.	TABLE OF CONTENTS	ii
III.	LIST OF TABLES AND FIGURES	iv
IV.	INTRODUCTION	1
V.	LIST OF SYMBOLS	5
VI.	IMPERFECTION SENSITIVITY INDEX	8
VII.	DERIVATION OF GOVERNING EQUATIONS	12
	Assumptions	12
	Equilibrium Equations	13
	Perturbation Procedure	17
	Zeroth Perturbation	19
	First Perturbation	26
	Second Perturbation	29
	Third Perturbation	33
	Determination of b	39
VIII.	NUMERICAL SOLUTION OF POSTBUCKLING EQUATIONS	41
	General Solution	41
	Boundary Conditions	46
	Solution for First Perturbation	50
	Solution for Second Perturbation	53
	Evaluation of b	56
	Program SICK	60

HEADING PAGE

IX. INVESTIGATION OF RELATIVE IMPERFECTION SENSITIVITY OF FIBER-REINFORCED CYLINDERS 62

Glass-Epoxy Cylinders 63

Boron-Epoxy Cylinders 68

Boron-Aluminum Cylinders 72

X. EXPERIMENTAL INVESTIGATION 78

Test Specimens 78

Test Procedure 82

Test Results 83

Comparison of Theory and Experiment 91

XI. CONCLUDING REMARKS 97

XII. ACKNOWLEDGMENTS 100

XIII. REFERENCES 101

XIV. VITA 105

XV. APPENDIX A 106

III. LIST OF TABLES AND FIGURES

TABLE PAGE

I. Elastic Constants for Materials Used in Imperfection Sensitivity Study 156

II. Test Cylinder Constituent Properties 157

III. Test Cylinder Dimensions and Experimental Results 158

FIGURE

1. Real geometry of measured imperfections in a large cylinder (ref. 28) 9

2. Geometry of fiber-reinforced cylinders 16

3. Buckling loads for glass-epoxy cylinders ($R/t = 100$, $A/R = 0.7$, $v_f = 0.65$) 64

4. Imperfection sensitivity indices for glass-epoxy cylinders 67

5. Buckling loads for boron-epoxy cylinders ($R/t = 100$, $A/R = 0.7$, $v_f = 0.50$) 69

6. Imperfection sensitivity indices for boron-epoxy cylinders 71

7. Buckling loads for boron-aluminum cylinders ($R/t = 100$, $A/R = 0.7$, $v_f = 0.50$) 74

8. Imperfection sensitivity indices for boron-aluminum cylinders 75

9. Photomicrographs of wall of test cylinders 79

FIGURE PAGE

10. Stress-strain curve for 3-inch-diameter ERL-2256 epoxy block loaded in compression 81

11. Sample plot of cylinder test data 84

12. Extensional moduli for test cylinders with alternating helical and circumferential wraps (cylinders 1 to 6) . . 86

13. Poisson's ratio associated with radial expansion induced by axial loading of test cylinders with alternating helical and circumferential wraps (cylinders 1 to 6) 87

14. Extensional moduli for test cylinders with helical wraps (cylinders 7 to 12) 88

15. Poisson's ratio associated with radial expansion induced by axial loading of test cylinders with helical wraps (cylinders 7 to 12) 89

16. Buckled test cylinder 90

17. Comparison of theoretical and experimental buckling loads for test cylinders with alternating helical and circumferential wraps 92

18. Imperfection sensitivity indices for test cylinders with alternating helical and circumferential wraps 92

19. Comparison of theoretical and experimental buckling loads for test cylinders with helical wraps 95

20. Imperfection sensitivity indices for test cylinders with helical wraps 95

21. Flow diagram for program SICK 109

IV. INTRODUCTION

The purpose of the dissertation is to investigate the sensitivity of fiber-reinforced cylinders to small imperfections in the geometry of the wall of the cylinder. The development of boron and high-modulus glass fibers as reinforcement suggests that fiber-wound or fiber-reinforced shells possess great technological potential. Recent experience at NASA (refs. 1 to 4) and elsewhere has indicated that the state of the art of these new materials is such that their elastic behavior can be predicted with reasonable engineering accuracy. Furthermore, efficiency studies of cylindrical shells loaded in axial compression (ref. 5) have shown that they are competitive with the best metallic shells as lightweight load-carrying members. Thus, studies of filamentary shells are of current technological interest.

If fibrous shells are ever to be accepted as reliable load-bearing elements, their structural behavior must be thoroughly understood. One of the most important factors in the buckling behavior of a shell is its sensitivity to small deviations from perfect geometry. The sensitivity of axially loaded cylindrical shells to initial imperfections has long been suspected to be a major cause of lack of agreement between theoretical predictions and experimental buckling data for shells loaded in axial compression. Recent tests on carefully manufactured cylindrical specimens (refs. 6 to 8) indicate that shells of near-perfect geometry can develop loads which approach predictions for idealized shells. The problem, however, still remains to find some method of making practical shell structures more predictable and, hence, more reliable.

By the nature of their construction, fiber-reinforced shells usually possess orthotropic material characteristics. In studies of the behavior of orthotropic shells, there is some evidence that, given the proper orthotropy and geometry, orthotropic shells can behave with relatively low sensitivity to small initial imperfections. For example, buckling data for axially loaded longitudinally stiffened cylindrical shells (which can be considered to be a class of orthotropic shells) have been shown by the author to be in good agreement with theoretical predictions for ideal cylinders (ref. 9). Furthermore, postbuckling studies (refs. 10 to 14) have indicated that minimum postbuckling loads for orthotropic cylinders can be much higher than isotropic cylinders with similar radius-thickness ratios. These observations have been used in attempts to predict "knockdown factors" (reductions in theoretical predictions) to correlate buckling theory and experiment (ref. 15). The insensitivity of orthotropic shells has not been established in general and, in fact, imperfection sensitivity of stiffened shells in certain geometric ranges has been noted in references 16 and 17.

An interesting peculiarity of fiber-reinforced shells is the fact that by suitable layering, two-dimensional isotropic relations for the elastic constants of the shell wall can be obtained. Thus, by varying the orientation of fibers in a shell of fixed geometry, one can encounter for a shell with specified length, radius, and total thickness, an isotropic configuration among configurations of varying degrees of orthotropy. Hence, the designer of fiber-reinforced shells, as opposed to metallic shells, has at his disposal an additional degree-of-freedom—orthotropy.

Based on the limited evidence of the reduced sensitivity of certain orthotropic shells to initial imperfections, we are confronted with the following interesting possibility in design. It is conceivable that for certain geometries we can find two fiber-reinforced shells, one possessing orthotropy, the other isotropy, such that the isotropic shell will buckle at a higher load theoretically. However, because of the greater sensitivity of the isotropic shell to initial imperfections, the orthotropic shell practically will carry a higher load and, even more important, may be more predictable in its behavior.

The goal of the present research is to study the relative imperfection sensitivity of fiber-reinforced cylinders in order to identify which fiber configurations are least sensitive to initial geometric imperfections. The investigation is accomplished by studying the behavior of a perfect shell in its initial postbuckling region. An index of imperfection sensitivity as suggested by Koiter (refs. 16 to 24) is determined by perturbing the shell displacements in the neighborhood of the bifurcation point. The effects of nonlinear displacements induced by loading prior to buckling are considered. The theory is derived by employing principles of perturbation theory and represents an extension to cylindrical shells of the plate postbuckling theory developed by Stein (ref. 25). Relative values of the sensitivity index are found for helically wrapped cylinders of glass-epoxy, boron-epoxy, and boron-aluminum loaded in axial compression. Wrapping configurations were varied to discover configurations of minimum imperfection sensitivity.

A series of compression tests was conducted on twelve glass-epoxy, filament-wound cylinders to investigate experimental buckling behavior. Theoretical imperfection sensitivity trends are compared with the experimental results.

V. LIST OF SYMBOLS

A	cylinder length
A_{21}, A_{31}	square matrices associated with left-hand side of equations (31) and (40), respectively
a	coefficient in load-displacement expansion (eq. (9))
b	imperfection sensitivity index
C_{ij}	extensional stiffness of cylinder wall (see eq. (5))
c_1, c_2	constants in homogeneous solutions (see eqs. (27) and (36))
$\vec{D}$	postbuckling displacement vector defined in equation (45)
D_{ij}	bending stiffness of cylinder wall (see eq. (5))
D_{21}, D_{31}, E_{31}	column vectors associated with right-hand sides of secular equations (see eqs. (31), (40), and (71) to (74))
E_x, E_y	equivalent Young's moduli for helically wrapped layer of cylinder wall
$\overline{E}_x$	effective Young's modulus for contraction of composite cylinder wall
$F_1, F_2, G_1, G_2, G_{12}, G$	constants associated with axisymmetric prebuckling solution for w (eq. (18))
G_{xy}	equivalent shear modulus for helically wrapped layer of cylinder wall
K_{ij}	stiffness of cylinder wall associated with coupling between extension and bending (see eq. (5))
M_x, M_y, M_{xy}	moment resultants
N_x, N_y, N_{xy}	stress resultants

n	number of full waves in cylinder buckle pattern in circumferential direction
$P_1 = \dfrac{C_{12}R}{C_{11}C_{22} - C_{12}^2}$	
R	radius of cylinder measured to arbitrary reference surface
t	total wall thickness of cylindrical shell
$\overline{U}_1, \overline{V}_1, \overline{W}_1$	displacement functions of x associated with first perturbation (eigenvector components)
U_1, V_1, W_1	normalized eigenvector components
u, v, w	displacements of shell wall in x-, y-, and z-directions, respectively
Z	column vector formed from u, v, w, and M_x evaluated at each finite difference station
x, y, z	surface and normal coordinates for shell
α	helical wrap angle
β, γ	cylinder prestress parameters (see eq. (18))
γ_{xy}	shear strain in shell at reference surface
Δ	distance between adjacent finite difference stations
$\delta\Pi$	virtual work for an axially loaded cylinder
ϵ	normal strain
$\kappa_x, \kappa_y, \kappa_{xy}$	curvatures
Λ_{ij}	structural constants defined in equation (51)
λ	magnitude of applied compressive load at ends of cylinder

μ	Poisson's ratio for isotropic material
μ_x, μ_y	equivalent Poisson's ratios for helically wrapped, orthotropic layer
$\bar{\mu}_x$	effective Poisson's ratio for composite cylinder wall
ξ	perturbation parameter, measure of amplitude of initial postbuckling displacements
$\bar{\xi}$	amplitude of initial imperfection
σ	normal stress
τ	shear stress

Superscripts:

i	ith layer of cylinder wall
*	evaluated at $\lambda = \lambda_{cr}$
T	transpose of a column vector

Subscripts:

0,1,2,3	prebuckling, first, second, or third perturbation, respectively (when used on load, strain, or displacement variables)
s	imperfect cylinder buckling
x,y	longitudinal and circumferential directions, respectively
cr	at buckling
iso	isotropic
exp	experimental

Primes are used to denote ordinary differentiation with respect to the variable x. A subscript preceded by a comma denotes partial differentiation with respect to the subscript.

VI. IMPERFECTION SENSITIVITY INDEX

There are several studies of the sensitivity of shells to initial imperfections available in the literature (see, e.g., refs. 26 and 27). The majority of these studies are restricted by the adoption of an initial imperfection of specified geometry. Practically speaking, however, real initial imperfections have a somewhat random character. An example of this fact is shown in figure 1. Measured radial displacements from perfect geometry are shown for a 10-foot diameter ring-stiffened cylindrical shell (ref. 28). The initial radial displacement w_i divided by the shell thickness t is plotted against length for various circumferential stations about 6 inches apart. It is evident that considerable judgment and ingenuity is required to represent such initial imperfections analytically. Thus, in the present state of the art, it seems impractical to hope for an analysis which will yield the exact reduction in buckling load for a wide range of realistic imperfection geometries. However, a method of assessing relative sensitivities of shells to initial imperfections does exist.

In his doctoral dissertation, Koiter (ref. 19) proposed a theoretical method of obtaining an estimate of the sensitivity of a broad class of shells to initial imperfections. In the Koiter theory, it is postulated that the sensitivity of a structure to small initial imperfections can be assessed by a knowledge of the perfect structure's behavior in the initial postbuckling region. In his thesis, Koiter demonstrates that for imperfections having the shape of the perfect shell buckling mode,

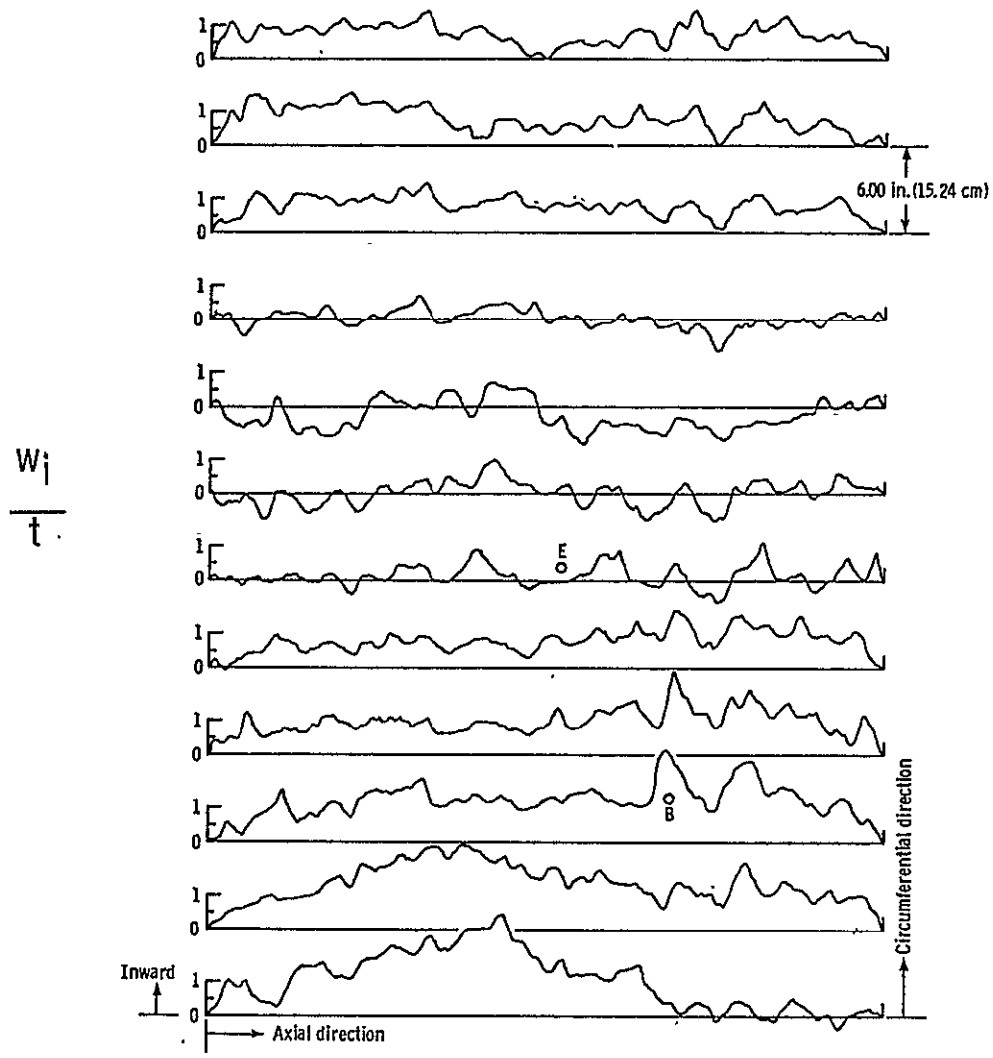

Figure 1.- Real geometry of measured imperfections in a large cylinder (ref. 28).

the sensitivity of the shell could be investigated with a knowledge of either of two fundamental parameters.

These parameters were identified by expanding the applied load λ as a function of a scalar perturbation parameter ξ. The parameter ξ is arbitrary and physically can be considered to be any convenient, suitably small measure of the growth of displacements in the shell just after buckling. The expansion of load in terms of this scalar measure of postbuckling displacement can be written as

$$\lambda = \lambda_{cr} + a\lambda_{cr}\xi + b\lambda_{cr}\xi^2 + \ldots$$

where λ_{cr} is the bifurcation or buckling load. Koiter has demonstrated that when small initial imperfections are taken into account, the relationship between the buckling load of the shell in the presence of the imperfection and the buckling load for a perfect shell is related to the parameters a and b. For example, Koiter has shown for a shell governed by "cubic" behavior ($a = 0$), the relationship between the buckling load λ_s in the presence of an initial imperfection of magnitude $\bar{\xi}$ and the buckling load for a perfect shell λ_{cr} is given by

$$\left(1 - \frac{\lambda_s}{\lambda_{cr}}\right)^{3/2} = \frac{3\sqrt{3}}{2} \left|\bar{\xi}\right| \sqrt{-b}\left(\frac{\lambda_s}{\lambda_{cr}}\right)$$

The above relationship is restricted to the so-called "classical" theory of buckling in which the effects of deformations prior to buckling are ignored. Recent results (refs. 23 and 24), in which these effects are

considered, also conclude that b is a measure number of the reduction in buckling load due to imperfections.

Thus, depending on the type of shell, either a or b is a fundamental parameter in assessing relative sensitivity to small imperfections, that is, the imperfection sensitivity index. Hence, the goal of employing Koiter's theory to assess imperfection sensitivity is to understand the character of the postbuckling behavior of the structure in the neighborhood of a singularity, namely, the point of buckling. This type of consideration is somewhat analogous to studies in the theory of nonlinear vibrations where one examines the character of singularities in vibrating systems (e.g., refs. 29 and 30). In fact, in this field there is even Poincaré's "index of singularity." Koiter's work relates the character of the singularity occurring at buckling (bifurcation) to the structure's sensitivity to initial imperfections.

VII. DERIVATION OF GOVERNING EQUATIONS

Assumptions

In developing the theoretical estimate of imperfection sensitivity of the cylinder, several basic assumptions are made. The cylinder is assumed to be composed of several orthotropic layers, each with one of its principal axes of orthotropy alined with the cylinder axis. The effects of transverse shear are ignored. At the onset of loading, the cylinder is assumed to be perfectly cylindrical so that its shape is changed only by deformations induced by load. The cylinder is assumed to buckle into a unique buckling mode, so that the behavior of the shell can be investigated in the neighborhood of a bifurcation point. For a cylinder, this restriction precludes consideration of cylinders that "buckle" in an axisymmetric mode. Axisymmetric "buckling" in a cylinder is simply unchecked growth of the axisymmetric deformations induced by loading and is often described as collapse rather than buckling. Since no bifurcation occurs, the present theory cannot assess relative imperfection sensitivity for this phenomenon.

The theory is developed by adopting the Koiter parameters to obtain the sensitivity index of a perfect cylinder. The development of the theory differs from that existing in the literature (refs. 16 to 24) in that the index is identified by employing perturbation techniques similar to those of reference 25. Nonlinear equilibrium equations formulated from Donnell-von Karman strain displacement relations are perturbed about the bifurcation point to find equations governing the behavior of the

shell in the initial postbuckling region. The perturbation is shown to produce secular terms which are constrained to vanish. The constraint conditions yield relationships between the sensitivity index and the buckling mode. The sensitivity index is then computed by using the constraint condition together with a suitable definition of the perturbation parameter.

Equilibrium Equations

Nonlinear equilibrium equations are formulated using the Donnell-von Karman strain displacement relations. Under the assumptions, the virtual work expression for a multilayered orthotropic cylinder loaded in axial compression can be written as follows:

$$\delta\Pi = \int_0^A \int_0^{2\pi R} (N_x \delta\epsilon_x + N_y \delta\epsilon_y + N_{xy}\delta\gamma_{xy} + M_x \delta\kappa_x + M_y \delta\kappa_y + M_{xy}\delta\kappa_{xy})dx\, dy$$
$$+ \int_0^{2\pi R} \lambda\delta u \Big|_0^A dy = 0 \tag{1}$$

where

$$\left.\begin{aligned}
N_x &= C_{11}\epsilon_x + C_{12}\epsilon_y + K_{11}\kappa_x + K_{12}\kappa_y \\
N_y &= C_{12}\epsilon_x + C_{22}\epsilon_y + K_{12}\kappa_x + K_{22}\kappa_y \\
N_{xy} &= C_{66}\gamma_{xy} + K_{66}\kappa_{xy} \\
M_x &= K_{11}\epsilon_x + K_{12}\epsilon_y + D_{11}\kappa_x + D_{12}\kappa_y \\
M_y &= K_{12}\epsilon_x + K_{22}\epsilon_y + D_{12}\kappa_x + D_{22}\kappa_y \\
M_{xy} &= K_{66}\gamma_{xy} + D_{66}\kappa_{xy}
\end{aligned}\right\} \tag{2}$$

with

$$\left.\begin{aligned} \epsilon_x &= u_{,x} + \frac{1}{2} w_{,x}^2 & \kappa_x &= - w_{,xx} \\ \epsilon_y &= v_{,y} + \frac{w}{R} + \frac{1}{2} w_{,y}^2 & \kappa_y &= - w_{,yy} \\ \gamma_{xy} &= u_{,y} + v_{,x} + w_{,x} w_{,y} & \kappa_{xy} &= - 2w_{,xy} \end{aligned}\right\} \tag{3}$$

In equations (2), C_{ij}, D_{ij}, and K_{ij} are structural stiffnesses of the multilayered wall associated with extension, bending and coupling between bending and extension, respectively. If the stress-strain relations for the ith cylinder layer are written as

$$\left.\begin{aligned} \sigma_x^i &= \frac{E_x^i}{1 - \mu_x^i \mu_y^i}\left(\epsilon_x^i + \mu_y^i \epsilon_y^i\right) \\ \sigma_y^i &= \frac{E_y^i}{1 - \mu_x^i \mu_y^i}\left(\epsilon_y^i + \mu_x^i \epsilon_x^i\right) \\ \tau_{xy}^i &= G_{xy}^i \gamma_{xy}^i \end{aligned}\right\} \tag{4}$$

then, the structural stiffnesses can be defined by the following integrals:

$$
\left.
\begin{aligned}
C_{11} &= \int_{wall} \frac{E_x^i}{1 - \mu_x^i \mu_y^i}\, dz \qquad
C_{12} = \int_{wall} \frac{\mu_y^i E_x^i}{1 - \mu_x^i \mu_y^i}\, dz \qquad
C_{22} = \int_{wall} \frac{E_y^i}{1 - \mu_x^i \mu_y^i}\, dz \\
K_{11} &= \int_{wall} \frac{E_x^i}{1 - \mu_x^i \mu_y^i}\, z\, dz \qquad
K_{12} = \int_{wall} \frac{\mu_y^i E_x^i}{1 - \mu_x^i \mu_y^i}\, z\, dz \qquad
K_{22} = \int_{wall} \frac{E_y^i}{1 - \mu_x^i \mu_y^i}\, z\, dz \\
D_{11} &= \int_{wall} \frac{E_x^i}{1 - \mu_x^i \mu_y^i}\, z^2 dz \qquad
D_{12} = \int_{wall} \frac{\mu_y^i E_x^i}{1 - \mu_x^i \mu_y^i}\, z^2 dz \qquad
D_{22} = \int_{wall} \frac{E_y^i}{1 - \mu_x^i \mu_y^i}\, z^2 dz
\end{aligned}
\right\} \tag{5}
$$

The integrals appearing in equations (5) can be evaluated for an arbitrary reference surface by using equations (83) and (85) of reference 31. The elastic constants for fiber-reinforced structures appearing in equations (4) can be predicted analytically from the constituent properties of the fiber and matrix. The constants for a layer in which the fibers are unidirectional can be obtained from any of references 32 to 35. For layers with fibers oriented at angles $\pm\alpha$ (see fig. 2), an "equivalent" orthotropic layer is defined through compatibility considerations and the transformation equations of orthotropic elasticity (see refs. 35 to 37). The formulae employed herein are summarized in appendix B of reference 1.

Equation (1) can be expressed as a function of the displacement variables u, v, and w. Integration by parts yields the following equilibrium equations which are valid in the postbuckling region:

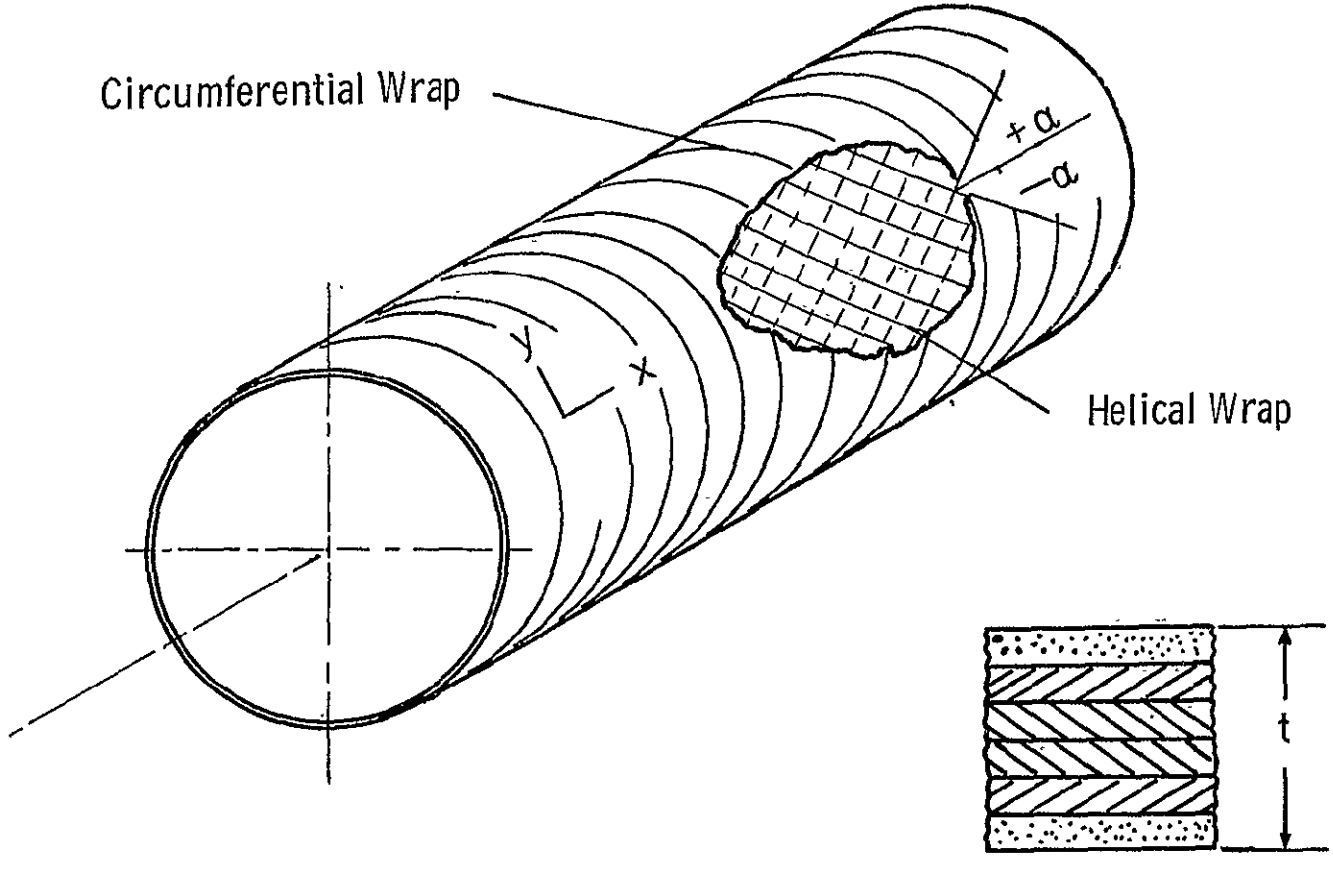

Figure 2.- Geometry of fiber-reinforced cylinders.

$$\left.\begin{aligned} &N_{x,x} + N_{xy,y} = 0 \\ &N_{xy,x} + N_{y,y} = 0 \\ &-M_{x,xx} - 2M_{xy,xy} - M_{y,yy} + \frac{N_y}{R} - N_x w_{,xx} - 2N_{xy} w_{,xy} - N_y w_{,yy} = 0 \end{aligned}\right\} \quad (6)$$

The boundary conditions resulting from the variations, with the load specified and the cylinder supported at the ends, can be written as

$$\left.\begin{aligned} &N_x + \lambda = 0 \\ &N_{xy} = 0 \quad \text{or} \quad v = 0 \\ &M_x = 0 \quad \text{or} \quad w_{,x} = 0 \\ &w = 0 \end{aligned}\right\} \quad (7)$$

Perturbation Procedure

Following the Koiter procedure, the displacements are expanded as

$$\left.\begin{aligned} u &= u_0(\xi) + u_1\xi + u_2\xi^2 + \ldots \\ v &= v_0(\xi) + v_1\xi + v_2\xi^2 + \ldots \\ w &= w_0(\xi) + w_1\xi + w_2\xi^2 + \ldots \end{aligned}\right\} \quad (8)$$

where the subscript 0 denotes the axisymmetric state of deformation induced by load and ξ is the perturbation parameter.

The applied compressive load λ is expanded as

$$\lambda = \lambda_{cr} + a\lambda_{cr}\xi + b\lambda_{cr}\xi^2 + \ldots \quad (9)$$

where λ_{cr} is the applied load at buckling. At this point, it should be observed that Koiter's work was based on classical buckling analysis so that the dependence of the axisymmetric deformations (u_o, v_o, w_o) on ξ is not clearly noted. Fitch (ref. 24) has recently generalized Koiter's work to include the effects of deformations prior to buckling. In Fitch's work, the dependence of the axisymmetric deformations on ξ can be found by expanding these deformations in a Taylor series about the buckling load λ_{cr}. Thus,

$$\left.\begin{aligned} u_o &= u_o^* + (\lambda - \lambda_{cr})u_{o,\lambda}^* + \frac{1}{2}(\lambda - \lambda_{cr})^2 u_{o,\lambda\lambda}^* + \cdots \\ v_o &= v_o^* + (\lambda - \lambda_{cr})v_{o,\lambda}^* + \frac{1}{2}(\lambda - \lambda_{cr})^2 v_{o,\lambda\lambda}^* + \cdots \\ w_o &= w_o^* + (\lambda - \lambda_{cr})w_{o,\lambda}^* + \frac{1}{2}(\lambda - \lambda_{cr})^2 w_{o,\lambda\lambda}^* + \cdots \end{aligned}\right\} \tag{10}$$

where the $*$ denotes quantities evaluated at $\lambda = \lambda_{cr}$. For example,

$$w_{o,x\lambda}^* = \left.\frac{\partial^2 w_o}{\partial x \partial \lambda}\right|_{\lambda = \lambda_{cr}}$$

Using equations (9) and (10)

$$\left.\begin{aligned} u &= u_o^* + (a\lambda_{cr}u_{o,\lambda}^* + u_1)\xi + \left(\frac{1}{2}a^2\lambda_{cr}^2 u_{o,\lambda\lambda}^* + b\lambda_{cr}u_{o,\lambda}^* + u_2\right)\xi^2 + \cdots \\ v &= v_o^* + (a\lambda_{cr}v_{o,\lambda}^* + v_1)\xi + \left(\frac{1}{2}a^2\lambda_{cr}^2 v_{o,\lambda\lambda}^* + b\lambda_{cr}v_{o,\lambda}^* + v_2\right)\xi^2 + \cdots \\ w &= w_o^* + (a\lambda_{cr}w_{o,\lambda}^* + w_1)\xi + \left(\frac{1}{2}a^2\lambda_{cr}^2 w_{o,\lambda\lambda}^* + b\lambda_{cr}w_{o,\lambda}^* + w_2\right)\xi^2 + \cdots \end{aligned}\right\} \tag{11}$$

Zeroth Perturbation

If equations (11) are substituted into the equilibrium equations (6) and the boundary conditions (7), a series of equations corresponding to powers of ξ are obtained. The equations corresponding to the zeroth power of ξ can be written as follows

ξ^o:

$$N^{*\prime}_{x_o} = 0 \tag{12a}$$

$$N^{*\prime}_{xy_o} = 0 \tag{12b}$$

$$- M^{*\prime\prime}_{x_o} + \frac{N^*_{y_o}}{R} - N^*_{x_o} w^{*\prime\prime}_o = 0 \tag{12c}$$

with boundary conditions

$$N^*_{x_o} + \lambda_{cr} = 0 \tag{13a}$$

$$N^*_{xy_o} = 0 \quad \text{or} \quad v^*_o = 0 \tag{13b}$$

$$w^*_o = 0 \tag{13c}$$

$$M^*_{x_o} = 0 \quad \text{or} \quad w^{*\prime}_o = 0 \tag{13d}$$

with

$$\left.\begin{aligned} \epsilon^*_{x_o} &= u_o^{*\prime} + \frac{1}{2}(w_o^{*\prime})^2 \\ \epsilon^*_{y_o} &= \frac{w_o^*}{R} \\ \kappa^*_{x_o} &= - w_o^{*\prime\prime} \end{aligned}\right\} \tag{14}$$

where the prime denotes ordinary differentiation with respect to x. The stress resultants of equations (12) and (13) are defined by substituting equations (14) into the constitutive relations of equations (2).

Equations (12) and (13) can be identified as equations determining the axisymmetric deformations occuring in the cylinder prior to buckling. The asterisk indicates that the deformations resulting from these equations must be evaluated at the inception of buckling, that is, at $\lambda = \lambda_{cr}$.

Solutions to equations (12) can be obtained by integrating equation (12a) and applying boundary condition (13a) so that

$$N^*_{x_o} = - \lambda_{cr} \tag{15}$$

From the definition of $N^*_{x_o}$, it follows that

$$\epsilon^*_{x_o} = u_o^{*\prime} + \frac{1}{2}(w_o^{*\prime})^2 = \frac{K_{11}}{C_{11}} w_o^{*\prime\prime} - \frac{C_{12}}{C_{11}} \frac{w_o^*}{R} - \frac{\lambda_{cr}}{C_{11}} \tag{16}$$

Integration of equation (12b) together with either of boundary conditions (13b) imply that both v_o^* and $N^*_{xy_o}$ are zero everywhere. Substitution

of equation (16) into equation (12c) yields the following ordinary differential equation in w_o^*,

$$\left(D_{11} - \frac{K_{11}^2}{C_{11}}\right) w_o^{*''''} + \left[\frac{2}{R}\left(\frac{K_{11}C_{12}}{C_{11}} - K_{12}\right) + \lambda_{cr}\right] w_o^{*''} + \frac{1}{R^2}\left(C_{22} - \frac{C_{12}^2}{C_{11}}\right) w_o^*$$

$$= \frac{1}{R}\frac{C_{12}}{C_{11}}\lambda_{cr} \tag{17}$$

For simply supported shells ($M_{\bar{x}_o}^* = 0$) with boundary conditions applied at $\bar{x} = \pm A/2$ when A is the cylinder length, the solution of (17) can be written as

$$w_o^* = F_1 \sinh \beta\bar{x} \sin \gamma\bar{x} + F_2 \cosh \beta\bar{x} \cos \gamma\bar{x} + \lambda_{cr} P_1 \tag{18}$$

where

$$\beta = \sqrt{\frac{1}{2R}\left(\sqrt{\frac{C_{11}\,C_{22} - C_{12}^2}{D_{11}\,C_{11} - K_{11}^2}} - \frac{K_{11}C_{12} - K_{12}C_{11} + \frac{\lambda_{cr}}{2} C_{11}R}{D_{11}C_{11} - K_{11}^2}\right)}$$

$$\gamma = \sqrt{\frac{1}{2R}\left(\sqrt{\frac{C_{11}\,C_{22} - C_{12}^2}{D_{11}\,C_{11} - K_{11}^2}} + \frac{K_{11}C_{12} - K_{12}C_{11} + \frac{\lambda_{cr}}{2} C_{11}R}{D_{11}C_{11} - K_{11}^2}\right)}$$

$$P_1 = \frac{C_{12}R}{C_{11}C_{22} - C_{12}^2}$$

$$F_1 = \frac{G_1 \cosh \frac{\beta A}{2} \cos \frac{\gamma A}{2} - G_2 \sinh \frac{\beta A}{2} \sin \frac{\gamma A}{2}}{2\left(D_{11} - \frac{K_{11}^2}{C_{11}}\right)\beta\gamma\left(\sinh^2 \frac{\beta A}{2} \sin^2 \frac{\gamma A}{2} + \cosh^2 \frac{\beta A}{2} \cos^2 \frac{\gamma A}{2}\right)}$$

$$F_2 = \frac{G_2 \cosh \frac{\beta A}{2} \cos \frac{\gamma A}{2} + G_1 \sinh \frac{\beta A}{2} \sin \frac{\gamma A}{2}}{2\left(D_{11} - \frac{K_{11}^2}{C_{11}}\right)\beta\gamma\left(\sinh^2 \frac{\beta A}{2} \sin^2 \frac{\gamma A}{2} + \cosh^2 \frac{\beta A}{2} \cos^2 \frac{\gamma A}{2}\right)}$$

with

$$G_1 = \lambda_{cr}\left[\frac{K_{11}}{C_{11}} + R\,\frac{C_{12}}{C_{11}}\left(\frac{D_{11}C_{11} - K_{12}^2}{C_{11}C_{22} - C_{12}^2}\right)\left(\beta^2 - \gamma^2\right)\right]$$

$$G_2 = 2\beta\gamma R\,\frac{C_{12}}{C_{11}}\left(\frac{D_{11}C_{11} - K_{12}^2}{C_{11}C_{22} - C_{12}^2}\right)$$

For clamped boundary conditions, the radial displacement w_o^* is given by (18) with

$$F_1 = \lambda_{cr}P_1 \frac{\beta \sinh \frac{\beta A}{2} \cos \frac{\gamma A}{2} - \gamma \cosh \frac{\beta A}{2} \sin \frac{\gamma A}{2}}{\beta \sin \frac{\gamma A}{2} \cos \frac{\gamma A}{2} + \gamma \sinh \frac{\beta A}{2} \cosh \frac{\beta A}{2}}$$

$$F_2 = -\lambda_{cr}P_1 \frac{\gamma \sinh \frac{\beta A}{2} \cos \frac{\gamma A}{2} + \beta \cosh \frac{\beta A}{2} \sin \frac{\gamma A}{2}}{\beta \sin \frac{\gamma A}{2} \cos \frac{\gamma A}{2} + \gamma \sinh \frac{\beta A}{2} \cosh \frac{\beta A}{2}} \tag{19}$$

Note, in general, that quantities such as $w^*_{o,\lambda}$ can be found from equations (18) and (19) by replacing λ_{cr} by λ, performing the indicated partial differentiation and evaluating the result at $\lambda = \lambda_{cr}$. For the quantity $w^*_{o,x\lambda}$, the result can be written as

$$\begin{aligned} w^*_{o,x\lambda} = {} & \cosh \beta\bar{x} \sin \gamma\bar{x}(F_1\beta - F_2\gamma)_{,\lambda} + \sinh \beta\bar{x} \cos \gamma\bar{x}(F_1\gamma + F_2\beta)_{,\lambda} \\ & + \bar{x} \sinh \beta\bar{x} \sin \gamma\bar{x}\left[\beta_{,\lambda}(F_1\beta - F_2\gamma) - \gamma_{,\lambda}(F_1\gamma + F_2\beta)\right] \\ & + \bar{x} \cosh \beta\bar{x} \cos \gamma\bar{x}\left[\beta_{,\lambda}(F_1\gamma + F_2\beta) + \gamma_{,\lambda}(F_1\beta - F_2\gamma)\right] \end{aligned} \tag{20}$$

with

$$\gamma_{,\lambda} = \frac{C_{11}}{8\gamma(D_{11}C_{11} - K_{11}^2)}$$

$$\beta_{,\lambda} = \frac{-C_{11}}{8\beta(D_{11}C_{11} - K_{11}^2)}$$

For simple support boundary conditions, if

$$F_1 = \frac{G_{12}}{G} \quad \text{and} \quad F_2 = \frac{G_{21}}{G}$$

$$
\left.
\begin{aligned}
F_{1,\lambda} = {} & \frac{G_{1,\lambda}}{G} \cosh \frac{\beta A}{2} \cos \frac{\gamma A}{2} - \frac{G_{2,\lambda}}{G} \sinh \frac{\beta A}{2} \sin \frac{\gamma A}{2} \\
& + \frac{A}{2G} \sinh \frac{\beta A}{2} \cos \frac{\gamma A}{2}(G_1\beta_{,\lambda} - G_2\gamma_{,\lambda}) - \frac{A}{2G} \cosh \frac{\beta A}{2} \sin \frac{\gamma A}{2}(G_1\gamma_{,\lambda} + G_2\beta_{,\lambda}) \\
& - \frac{2G_{12}}{G^2}(\gamma\beta)_{,\lambda}\left(\sinh^2 \frac{\beta A}{2} \sin^2 \frac{\gamma A}{2} + \cosh^2 \frac{\beta A}{2} \cos^2 \frac{\gamma A}{2}\right) \\
& - \frac{2G_{12}}{G^2} \gamma\beta A\left(\beta_{,\lambda} \sinh \frac{\beta A}{2} \cosh \frac{\beta A}{2} - \gamma_{,\lambda} \sin \frac{\gamma A}{2} \cos \frac{\gamma A}{2}\right) \\
F_{2,\lambda} = {} & - \frac{G_{1,\lambda}}{G} \sinh \frac{\beta A}{2} \sin \frac{\gamma A}{2} - \frac{G_{2,\lambda}}{G} \cosh \frac{\beta A}{2} \cos \frac{\gamma A}{2} \\
& + \frac{A}{2G} \cosh \frac{\beta A}{2} \sin \frac{\gamma A}{2}(G_2\gamma_{,\lambda} - G_1\beta_{,\lambda}) - \frac{A}{2G} \sinh \frac{\beta A}{2} \cos \frac{\gamma A}{2}(G_1\gamma_{,\lambda} + G_2\beta_{,\lambda}) \\
& + \frac{2G_{21}}{G^2}(\gamma\beta)_{,\lambda}\left(\sinh^2 \frac{\beta A}{2} \sin^2 \frac{\gamma A}{2} + \cosh^2 \frac{\beta A}{2} \cos^2 \frac{\gamma A}{2}\right) \\
& + \frac{2G_{21}}{G^2} \gamma\beta A\left(\beta_{,\lambda} \sinh \frac{\beta A}{2} \cosh \frac{\beta A}{2} - \gamma_{,\lambda} \sin \frac{\gamma A}{2} \cos \frac{\gamma A}{2}\right)
\end{aligned}
\right\} \quad (21)
$$

with

$$G_{1,\lambda} = P_1\left[\beta^2 - \gamma^2 + 2\lambda_{cr}(\beta\beta_{,\lambda} - \gamma\gamma_{,\lambda}) - \frac{K_{11}}{D_{11}C_{11} - K_{11}^2}\right]$$

$$G_{2,\lambda} = P_1\left[2\lambda_{cr}(\beta\gamma)_{,\lambda} + 2\gamma\beta\right]$$

For clamped boundary conditions, if

$$F_1 = \frac{\lambda_{cr}P_1G_{12}}{G} \quad \text{and} \quad F_2 = -\frac{\lambda_{cr}P_1G_{21}}{G}$$

$$\begin{aligned} F_{1,\lambda} = {} & \frac{P_1G_{12}}{G} + \frac{\lambda_{cr}P_1}{G}\left(\beta_{,\lambda} \sinh\frac{\beta A}{2}\cos\frac{\gamma A}{2} - \gamma_{,\lambda}\cosh\frac{\beta A}{2}\sin\frac{\gamma A}{2}\right) \\ & + \frac{A}{2}\frac{\lambda_{cr}P_1}{G}\left[\cosh\frac{\beta A}{2}\cos\frac{\gamma A}{2}(\beta\beta_{,\lambda} - \gamma\gamma_{,\lambda}) - \sinh\frac{\beta A}{2}\sin\frac{\gamma A}{2}(\beta\gamma)_{,\lambda}\right] \\ & - \frac{\lambda_{cr}P_1G_{12}}{2G^2}(\beta_{,\lambda}\sin\gamma A + A\beta\gamma_{,\lambda}\cos\gamma A + \gamma_{,\lambda}\sinh\beta A + A\gamma\beta_{,\lambda}\cosh\beta A) \end{aligned}$$

$$
\left.
\begin{aligned}
F_{2,\lambda} = &- \frac{P_1 G_{21}}{G} - \frac{\lambda_{cr} P_1}{G}\left(\beta_{,\lambda} \cosh \frac{\beta A}{2} \sin \frac{\gamma A}{2} + \gamma_{,\lambda} \sinh \frac{\beta A}{2} \cos \frac{\gamma A}{2}\right) \\
&- \frac{A}{2} \frac{\lambda_{cr} P_1}{G}\left[\sinh \frac{\beta A}{2} \sin \frac{\gamma A}{2}(\beta\beta_{,\lambda} - \gamma\gamma_{,\lambda}) + \cosh \frac{\beta A}{2} \cos \frac{\gamma A}{2}(\beta\gamma)_{,\lambda}\right] \\
&+ \frac{\lambda_{cr} P_1 G_{21}}{2G^2}(\beta_{,\lambda} \sin \gamma A + A\beta\gamma_{,\lambda} \cos \gamma A + \gamma_{,\lambda} \sinh \beta A + A\gamma\beta_{,\lambda} \cosh \beta A)
\end{aligned}
\right\} \quad (22)
$$

It should be noted that equations (18) through (22) were developed by exploiting symmetry of the boundary conditions using a coordinate $\bar{x}$ with origin at the middle of the cylinder. For subsequent developments, a more convenient coordinate is x whose origin is at the end of the cylinder. Equations (18) through (20) may be written for this coordinate by using the transformation $\bar{x} = x - A/2$.

First Perturbation

The equations corresponding to the first power of ξ can be written as follows:

$$
\left.
\begin{aligned}
&N_{x_1,x} + N_{xy_1,y} = 0 \\
&N_{xy_1,x} + N_{y_1,y} = 0 \\
&- M_{x_1,xx} - 2M_{xy_1,xy} - M_{y_1,yy} + \frac{N_{y_1}}{R} - N^*_{x_o} w_{1,xx} - N_{x_1} w^*_{o,xx} - N^*_{y_o} w_{1,yy} = 0
\end{aligned}
\right\} \quad (23)
$$

with boundary conditions

$$\left.\begin{aligned} N_{x_1} &= 0 \\ v_1 = 0 \quad \text{or} \quad N_{xy_1} &= 0 \\ w_1 &= 0 \\ M_{x_1} = 0 \quad \text{or} \quad w_{1,x} &= 0 \end{aligned}\right\} \tag{24}$$

In equations (23) and (24) and subsequent perturbations

$$\left.\begin{aligned} \epsilon_{x_i} &= u_{i,x} + w^*_{o,x}\, w_{i,x} \\ \epsilon_{y_i} &= v_{i,y} + \frac{w_i}{R} \\ \gamma_{xy_i} &= u_{i,y} + v_{i,x} + w^*_{o,x}\, w_{i,y} \\ \kappa_{x_i} &= - w_{i,xx} \\ \kappa_{y_i} &= - w_{i,yy} \\ \kappa_{xy_i} &= - 2w_{i,xy} \end{aligned}\right\} i = 1,2,3, \ldots . \tag{25}$$

and the corresponding stress resultants are obtained by substituting equations (25) into the constitutive relations (2).

To obtain equations (23), the equilibrium equations resulting from the zeroth perturbation (eqs. (12)), were used to eliminate terms such as $a\lambda_{cr}N^*_{x_o,x}$ obtained from the perturbation. Also in obtaining the boundary conditions exploitation was made of the fact that terms

having the functional form $a\lambda_{cr}f^*_{o,\lambda}$ vanish at the boundary if f^*_o is zero there. Equations (23) and (24) are similar to the usual equations governing buckling of a prestressed cylinder except for the absence of a free buckling parameter. The buckling parameter is absent since, in the present problem, the displacements of the shell have been expanded about a single, known point of bifurcation. Thus, as opposed to the usual buckling problem in which a multitude of eigenvectors are possible solutions, only one eigenvector is an admissible solution of (23) - namely that corresponding to $N^*_{x_o} = -\lambda_{cr}$. If both the buckling load λ_{cr} as well as the number of circumferential waves n in the buckle pattern are established by a conventional buckling analysis (e.g., ref. 38) equations (23) and (24) can be converted into a set of ordinary simultaneous differential equations and boundary conditions by the following substitution:

$$\left.\begin{aligned} u_1 &= \overline{U}_1(x) \cos \frac{ny}{R} \\ v_1 &= \overline{V}_1(x) \sin \frac{ny}{R} \\ w_1 &= \overline{W}_1(x) \cos \frac{ny}{R} \end{aligned}\right\} \tag{26}$$

As was done in reference 38, the eigenvector corresponding to $N^*_{x_o} = -\lambda_{cr}$ can be found by the method of finite differences and determinant plotting. The components of the resulting eigenvector can be expressed as

$$\left.\begin{aligned} u_1 &= c_1 U_1(x) \cos \frac{ny}{R} \\ v_1 &= c_1 V_1(x) \sin \frac{ny}{R} \\ w_1 &= c_1 W_1(x) \cos \frac{ny}{R} \end{aligned}\right\} \tag{27}$$

where c_1 is an arbitrary constant and U_1, V_1, and W_1 are suitably normalized components.

Second Perturbation

The equations corresponding to the second power of ξ can be written as follows:

$$N_{x_2,x} + N_{xy_2,x} = - a\lambda_{cr}\left[C_{11}(w^*_{o,x\lambda}\, w_{1,x})_{,x} + C_{66} w^*_{o,x\lambda}\, w_{1,yy}\right]$$

$$- \frac{1}{2}(C_{11}\, w^2_{1,x} + C_{12}\, w^2_{1,y})_{,x} - C_{66}(w_{1,x} w_{1,y})_{,y} \tag{28a}$$

$$N_{xy_2,x} + N_{y_2,y} = - a\lambda_{cr}\left[C_{66}(w^*_{o,x\lambda}\, w_{1,y})_{,x} + C_{12}\, w^*_{o,x\lambda}\, w_{1,xy}\right]$$

$$- \frac{1}{2}(C_{12}\, w^2_{1,x} + C_{22}\, w^2_{1,y})_{,y} - C_{66}(w_{1,x} w_{1,y})_{,x} \tag{28b}$$

$$
\begin{aligned}
&- M_{x_2,xx} - 2M_{xy_2,xy} - M_{y_2,yy} + \frac{N_{y_2}}{R} - N^*_{x_0}\, w_{2,xx} - N_{x_2}\, w^*_{0,xx} - N^*_{y_0}\, w_{2,yy} \\
&= a\lambda_{cr}\Big[N_{x_1}\, w^*_{0,xx\lambda} + N^*_{x_0,\lambda}\, w_{1,xx} + N^*_{y_0,\lambda}\, w_{1,yy} + C_{11} w^*_{0,x\lambda}\, w^*_{0,xx}\, w_{1,x} - \frac{C_{12}}{R}\, w^*_{0,x\lambda}\, w_{1,x} \\
&\quad + K_{11}(w^*_{0,x\lambda}\, w_{1,x})_{,xx} + K_{12} w^*_{0,x\lambda}\, w_{1,xyy} + 2K_{66}(w^*_{0,x\lambda}\, w_{1,y})_{,xy}\Big] + \frac{1}{2}(K_{11}\, w^2_{1,x} \\
&\quad + K_{12}\, w^2_{1,y})_{,xx} + \frac{1}{2}(K_{12}\, w^2_{1,x} + K_{22}\, w^2_{1,y})_{,yy} + 2K_{66}(w_{1,x}\, w_{1,y})_{,xy} \\
&\quad - \frac{1}{2R}(C_{12}\, w^2_{1,x} + C_{22}\, w^2_{1,y}) + \frac{1}{2}(C_{11}\, w^2_{1,x} + C_{12}\, w^2_{1,y}) w^*_{0,xx} \\
&\quad + N_{x_1}\, w_{1,xx} + 2N_{xy_1}\, w_{1,xy} + N_{y_1}\, w_{1,yy}
\end{aligned}
\tag{28c}
$$

with boundary conditions

$$\left.\begin{aligned} N_{x_2} + \frac{1}{2} C_{11} w_{1,x}^2 + \frac{1}{2} C_{12} w_{1,y}^2 &= 0 \\ N_{xy_2} + C_{66} w_{1,x} w_{1,y} = 0 \quad &\text{or} \quad v_2 = 0 \\ w_2 &= 0 \\ M_{x_2} + \frac{1}{2} K_{11} w_{1,x}^2 + \frac{1}{2} K_{12} w_{1,y}^2 = 0 \quad &\text{or} \quad w_{2,x} = 0 \end{aligned}\right\} \tag{29}$$

Equations (28) and (29) can be converted into a set of ordinary simultaneous differential equations and boundary conditions by the following substitutions

$$\left.\begin{aligned} u_2 &= U_{20}(x) + U_{21}(x) \cos \frac{ny}{R} + U_{22}(x) \cos \frac{2ny}{R} \\ v_2 &= V_{21}(x) \sin \frac{ny}{R} + V_{22}(x) \sin \frac{2ny}{R} \\ w_2 &= W_{20}(x) + W_{21}(x) \cos \frac{ny}{R} + W_{22}(x) \cos \frac{2ny}{R} \end{aligned}\right\} \tag{30}$$

Since the differential equations of (28) are linear, solutions corresponding to each set of U_{2i}, V_{2i}, and W_{2i} $(i = 0,1,2)$ can be superposed. However, if the particular solution for U_{21}, V_{21}, and W_{21} is sought by algebraic means from equations (28) and (29), certain difficulties are encountered. If equations (28) and a set of boundary conditions from equation (29) are cast in finite-difference form after

substitution of (30), the resulting simultaneous algebraic equations can be written in matrix notation as

$$A_{21}Z_{21} = a\lambda_{cr}c_1 D_{21} \tag{31}$$

where Z_{21} is a column vector whose components are U_{21}, V_{21}, W_{21}, and M_{21} evaluated at each difference station and D_{21} is a column vector containing elements corresponding to the terms multiplied by a on the right-hand side of equations (28) and (29). Because the trigonometric function associated with U_{21}, V_{21}, and W_{21} has the argument ny/R, the determinant of A_{21} has a form identical to that used in determining the buckling load λ_{cr}. Hence,

$$\det A_{21} = 0 \tag{32}$$

which demonstrates that the particular solution resulting from (31) is a secular term which must be removed from the perturbation. A condition for removal of the secular term is the requirement that

$$A_{21}Z_{21} = a\lambda_{cr} D_{21} = 0 \tag{33}$$

If Z_{21} is identified as the eigenvector Z_1 corresponding to the solution of equations (23) and (24), then the desired condition for removal of the secular terms is

$$A_1Z_1 = A_{21}Z_{21} = 0 = a\lambda_{cr} D_{21}$$

or

$$Z_1^T A_{21} Z_1 = a\lambda_{cr}c_1 Z_1^T D_{21} = 0 \tag{34}$$

where Z_1^T is the transpose of Z_1. Since $Z_1^T D_{21}$ is finite and λ_{cr} and c_1 must be finite for buckling to occur, it follows that

$$a = 0 \tag{35}$$

Thus the only admissible solution corresponding to the functions U_{21}, V_{21}, and W_{21} is the solution to the homogeneous system

$$A_{21}Z_{21} = 0$$

Hence, the general solution to equations (28) and (29) with $a = 0$ becomes

$$\left.\begin{aligned} u_2 &= U_{20}(x) + c_2U_1(x) \cos \frac{ny}{R} + U_{22}(x) \cos \frac{2ny}{R} \\ v_2 &= c_2V_1 (x) \sin \frac{ny}{R} + V_{22}(x) \sin \frac{2ny}{R} \\ w_2 &= W_{20}(x) + c_2W_1(x) \cos \frac{ny}{R} + W_{22}(x) \cos \frac{2ny}{R} \end{aligned}\right\} \tag{36}$$

where c_2 is an arbitrary constant and U_1, V_1, and W_1 are the normalized components of the buckling eigenvector (see eq. (27)).

Third Perturbation

If $a = 0$, the equations corresponding to the third power of ξ can be written as follows

ξ^3:

$$
\left.
\begin{aligned}
N_{x_3,x} + N_{xy_3,y} &= - b\lambda_{cr}\left[C_{11}(w^*_{0,x\lambda}\, w_{1,x})_{,x} + C_{66}\, w^*_{0,x\lambda}\, w_{1,yy}\right] \\
&\quad - \left[C_{11}(w_{1,x}\, w_{2,x})_{,x} + C_{12}(w_{1,y}\, w_{2,y})_{,x} + C_{66}(w_{1,x}\, w_{2,y} + w_{1,y}\, w_{2,x})_{,y}\right] \\
N_{xy_3,x} + N_{y_3,y} &= - b\lambda_{cr}\left[C_{66}(w^*_{0,x\lambda}\, w_{1,y})_{,x} + C_{12}\, w^*_{0,x\lambda}\, w_{1,xy}\right] \\
&\quad - \left[C_{66}(w_{1,x}\, w_{2,y} + w_{1,y}\, w_{2,x})_{,x} + C_{12}(w_{1,x}\, w_{2,x})_{,y} + C_{22}(w_{1,y}\, w_{2,y})_{,y}\right] \\
- M_{x_3,xx} - 2M_{xy_3,xy} - M_{y_3,yy} &+ \frac{N_{y_3}}{R} - N^*_{x_0}\, w_{3,xx} - N_{x_3}\, w^*_{0,xx} - N^*_{y_0}\, w_{3,yy} \\
&= b\lambda_{cr}\Big[N^*_{x_0,\lambda}\, w_{1,xx} + N_{x_1}\, w^*_{0,xx\lambda} + N^*_{y_0,\lambda}\, w_{1,yy} + C_{11}\, w^*_{0,xx}\, w^*_{0,x\lambda}\, w_{1,x} - \frac{C_{12}}{R}\, w^*_{0,x\lambda}\, w_{1,x} \\
&\quad + K_{11}(w^*_{0,x\lambda}\, w_{1,x})_{,xx} + 2K_{66}(w^*_{0,x\lambda}\, w_{1,y})_{,xy} + K_{12}(w^*_{0,x\lambda}\, w_{1,x})_{,yy}\Big] + K_{11}(w_{1,x}\, w_{2,x})_{,xx} \\
&\quad + K_{12}\left[(w_{1,y}\, w_{2,y})_{,xx} + (w_{1,x}\, w_{2,x})_{,yy}\right] + K_{22}(w_{1,y}\, w_{2,y})_{,yy} + 2K_{66}(w_{1,x}\, w_{2,y} \\
&\quad + w_{1,y}\, w_{2,x})_{,xy} + (C_{11}\, w_{1,x}\, w_{2,x} + C_{12}\, w_{1,y}\, w_{2,y})w^*_{0,xx} - \frac{1}{R}(C_{12}\, w_{1,x}\, w_{2,x}
\end{aligned}
\right\} \quad (37)
$$

$$
\left.
\begin{aligned}
&+ C_{22}\, w_{1,y}\, w_{2,y}) + \frac{w_{1,xx}}{2}(C_{11}\, w_{1,x}^2 + C_{12}\, w_{1,y}^2) + \frac{w_{1,yy}}{2}(C_{12}\, w_{1,x}^2 \\
&+ C_{22}\, w_{1,y}^2) + 2C_{66}\, w_{1,x}\, w_{1,y}\, w_{1,xy} + N_{x_1}\, w_{2,xx} + N_{x_2}\, w_{1,xx} \\
&+ N_{y_1}\, w_{2,yy} + N_{y_2}\, w_{1,yy} + 2N_{xy_1}\, w_{2,xy} + 2N_{xy_2}\, w_{1,xy}
\end{aligned}
\right\}
$$

with boundary conditions

$$
\left.
\begin{aligned}
&N_{x_3} + C_{11}\, w_{1,x}\, w_{2,x} + C_{12}\, w_{1,y}\, w_{2,y} + b\lambda_{cr} C_{11}\, w^*_{0,x\lambda}\, w_{1,x} = 0 \\
&N_{xy_3} + C_{66}(w_{1,x}\, w_{2,y} + w_{1,y}\, w_{2,x}) + b\lambda_{cr} C_{66}\, w^*_{0,x\lambda}\, w_{1,y} = 0 \quad \text{or} \quad v_3 = 0 \\
&w_3 = 0 \\
&M_{x_3} + K_{11}\, w_{1,x}\, w_{2,x} + K_{12}\, w_{1,y}\, w_{2,y} + b\lambda_{cr} K_{11}\, w^*_{0,x\lambda}\, w_{1,x} = 0 \quad \text{or} \quad w_{3,x} = 0
\end{aligned}
\right\} \qquad (38)
$$

Equations (37) and (38) can be converted into a set of ordinary simultaneous differential equations and boundary conditions by the following substitutions:

$$\left.\begin{aligned} u_3 &= U_{30}(x) + U_{31}(x)\cos\frac{ny}{R} + U_{32}(x)\cos\frac{2ny}{R} + U_{33}(x)\cos\frac{3ny}{R} \\ v_3 &= V_{33}(x)\sin\frac{ny}{R} + V_{32}(x)\sin\frac{2ny}{R} + V_{33}\sin\frac{3ny}{R} \\ w_3 &= W_{30}(x) + W_{31}(x)\cos\frac{ny}{R} + W_{32}(x)\cos\frac{2ny}{R} + W_{33}(x)\cos\frac{3ny}{R} \end{aligned}\right\} \quad (39)$$

Paralleling the second perturbation, U_{31}, V_{31}, and W_{31} can be shown to be secular terms which must be eliminated. The resulting algebraic equation in this case can be written as:

$$A_{31}Z_{31} = b\lambda_{cr}c_1 D_{31} + c_1^3 E_{31} \quad (40)$$

where D_{31} is a column vector corresponding to the terms multiplied by b on the right-hand sides of (37) and (38) and E_{31} is a column matrix generated from the terms that are independent of b. In contrast to equation (31), the additional term multiplied by c_1^3 occurs in (40) because, when the general solutions (eqs. (27) and (36)) are substituted into the right-hand sides of (37) and (38), terms such as $\cos ny/R \cos 2ny/R$ result which can be expanded as

$$\cos\frac{ny}{R}\cos\frac{2ny}{R} = \frac{1}{2}\left(\cos\frac{3ny}{R} + \cos\frac{ny}{R}\right)$$

thereby yielding additional secular terms that are independent of b. The condition for removal of the secular terms that is the analogue of equation (34) can be written as

$$Z_1^T A_{31} Z_1 = b\lambda_{cr} c_1 Z_1^T D_{31} + c_1^3 Z_1^T E_{31} = 0 \tag{41}$$

which has the solution

$$b = \frac{-c_1^2 Z_1^T E_{31}}{\lambda_{cr} Z_1^T D_{31}} \tag{42}$$

Equation (42) together with consideration of the equilibrium equations and boundary conditions corresponding to the first, second and third perturbations can be shown to imply the following proportionalities:

$$\left.\begin{aligned} &w_1,\ N_{x_1},\ N_{xy_1},\ N_{y_1} \propto b^{1/2} \\ &w_2,\ N_{x_2},\ N_{xy_2},\ N_{y_2} \propto b \\ &w_3,\ N_{x_3},\ N_{xy_3},\ N_{y_3} \propto b^{3/2} \end{aligned}\right\} \tag{43}$$

It is interesting to note that the counterpart of equation (42) was found by Stein in a study of the postbuckling behavior of plates. (See equation (19) of reference 25.)

The proportionalities indicated in equations (43) have also been found in existing applications of the Koiter theory. For example, Fitch and Cohen in references 23 and 24 have obtained an explicit expression for b from energy considerations. In terms of the present notation, the results of references 23 and 24 can be expressed as:

$$b = -\frac{\int\int_{\text{surface}} \bar{A}\, dx\, dy + 2\int\int_{\text{surface}} \bar{B}\, dx\, dy}{\lambda_{cr}\int\int_{\text{surface}} \bar{C}\, dx\, dy} \tag{44}$$

where

$$\bar{A} = N_{x_2}\, w_{1,x}^2 + N_{y_2}\, w_{1,y}^2 + 2N_{xy_2}\, w_{1,x}\, w_{1,y} + \frac{1}{2} C_{11}\, w_{1,x}^4 + C_{12}\, w_{1,x}^2\, w_{1,y}^2$$

$$+ \frac{1}{2} C_{22}\, w_{1,y}^4 + 2C_{66}\, w_{1,x}^2\, w_{1,y}^2$$

$$\bar{B} = N_{x_1}\, w_{1,x}\, w_{2,x} + N_{y_1}\, w_{1,y}\, w_{2,y} + N_{xy_1}(w_{1,x} w_{2,y} + w_{1,y}\, w_{2,x})$$

$$\bar{C} = N^*_{x_0,\lambda}\, w_{1,x}^2 + N^*_{y_0,\lambda}\, w_{1,y}^2 + 2(N_{x_1}\, w^*_{0,x\lambda}\, w_{1,x} + N_{xy_1}\, w^*_{0,x\lambda}\, w_{1,y})$$

Using the proportionalities indicated in equation (43), it can be seen that equation (44) becomes independent of b and hence equation (44) must be the counterpart of (42). The general theory of references 23 and 24 can be specialized to a "classical" buckling theory by taking pre-buckling deformations consistent with a membrane state of stress. The index b has been obtained under these assumptions by Budiansky in references 20 to 22. For the cylinder, the use of classical buckling theory requires derivatives of w^*_0 to vanish. Inspection of equation (44) with this assumption reveals again that the equation is independent of b.

Determination of b

To determine b explicitly, the perturbation parameter ξ must be defined appropriately. If the parameter ξ is considered to be a scalar measure of the growth of the displacements in the shell just after buckling, then ξ must be related to the magnitude of these displacements. The displacement vector $\vec{D}$ is defined to be the following:

$$\vec{D} = (u - u_0^*)\vec{i} + v\vec{j} + (w - w_0^*)\vec{k} \tag{45}$$

so that to the second approximation using (11) with $a = 0$

$$\vec{D} = \left[u_1\xi + (b\lambda_{cr}u_{0,\lambda}^* + u_2)\xi^2\right]\vec{i} + (v_1\xi + v_2\xi^2)\vec{j} + \left[w_1\xi + (b\lambda_{cr}w_{0,\lambda}^* + w_2)\xi^2\right]\vec{k} \tag{46}$$

The parameter ξ in the present theory is taken to be such that the square of the perturbation parameter is equal to the square of the magnitude of the vector $\vec{D}$, $(\vec{D} \cdot \vec{D})$, averaged over the cylinder surface and nondimensionalized by the square of the cylinder thickness t. Hence

$$\xi^2 = \frac{\int\int_{\text{surface}} \vec{D} \cdot \vec{D}\, dx\, dy}{2\pi RAt^2} \tag{47}$$

Using equation (46)

$$2\pi RAt^2\xi^2 = \xi^2 \int\int_{\text{surface}} (u_1^2 + v_1^2 + w_1^2)\, dx\, dy + O(\xi^3) \tag{48}$$

Using the general solution for the first perturbation (eq. (27)) and expressing c_1 in terms of b from equation (42), b can be written as

$$b = \frac{-2\pi RAt^2 Z_1^T E_{31}}{\lambda_{cr} Z_1^T D_{31} \iint_{\text{surface}} \left(U_1^2 \cos^2 \frac{ny}{R} + V_1^2 \sin^2 \frac{ny}{R} + W_1^2 \cos^2 \frac{ny}{R} \right) dx\, dy} \tag{49}$$

Thus, to within $O(\xi^2)$, the expression for b becomes

$$b = \frac{-2At^2 Z_1^T E_{31}}{\lambda_{cr} Z_1^T D_{31} \int_0^A (U_1^2 + V_1^2 + W_1^2) dx} \tag{50}$$

VIII. NUMERICAL SOLUTION OF POSTBUCKLING EQUATIONS

The solution for the state of axisymmetric prestress at buckling has already been presented in closed form (eqs. (18) and (19)). The solution to the equilibrium equations and boundary conditions resulting from the first and second perturbations (eqs. (23), (24), (28), and (29)) were found for simply supported and clamped shells by using numerical methods. Following the finite-difference technique suggested by references 38 and 39, the system of ordinary differential equations resulting from substitution of the general solutions (eqs. (27) and (36)) are cast into a set of simultaneous second-order differential equations and boundary conditions involving the fundamental displacement variables U, V, and W and an auxiliary variable $\bar{M}_x$. By employing central differences, the equations are converted into simultaneous algebraic equations which are then solved on a digital computer by matrix methods. Because the resulting algebraic equations contain banded matrices, it is expedient to employ Gaussian elimination in the solution.

General Solution

In formulating the postbuckling solution, it is convenient to consider the left-hand sides of the equilibrium equations in general. When the general solutions for the first and second perturbations are substituted into the equilibrium equations and the definition of the moment resultant $\bar{M}_x$ is introduced, the following set of second-order differential equations and boundary conditions are obtained:

$$\left.\begin{aligned}
&\Lambda_{11}U'' + \Lambda_{12}U + \Lambda_{13}V' + \Lambda_{14}W'' + \Lambda_{15}W' + \Lambda_{16}W + \Lambda_{17}M' = D_1 \\
&\Lambda_{21}U' + \Lambda_{22}V'' + \Lambda_{23}V + \Lambda_{24}W'' + \Lambda_{25}W' + \Lambda_{26}W = D_2 \\
&\Lambda_{31}U' + \Lambda_{32}V'' + \Lambda_{33}V + \Lambda_{34}W'' + \Lambda_{35}W' + \Lambda_{36}W - M'' = D_3 \\
&\Lambda_{41}U' + \Lambda_{42}V + \Lambda_{43}W'' + \Lambda_{44}W' + \Lambda_{45}W + M = D_4
\end{aligned}\right\} \tag{51}$$

where

$$\Lambda_{11} = C_{11} - \frac{K_{11}^2}{D_{11}}$$

$$\Lambda_{12} = -C_{66}\left(\frac{mn}{R}\right)^2$$

$$\Lambda_{13} = \left(C_{12} + C_{66} - \frac{K_{12}K_{11}}{D_{11}}\right)\frac{mn}{R}$$

$$\Lambda_{14} = \left(C_{11} - \frac{K_{11}^2}{D_{11}}\right)w_{0,x}^*$$

$$\Lambda_{15} = \left(C_{11} - \frac{K_{11}^2}{D_{11}}\right)w_{0,xx}^* + \left(C_{12} - \frac{K_{12}K_{11}}{D_{11}}\right)\frac{1}{R} + \left(K_{12} + 2K_{66} - \frac{K_{11}D_{12}}{D_{11}}\right)\left(\frac{mn}{R}\right)^2$$

$$\Lambda_{16} = -C_{66}w_{0,x}^*\left(\frac{mn}{R}\right)^2$$

$$\Lambda_{17} = \frac{K_{11}}{D_{11}}$$

$$\Lambda_{21} = -(C_{12} + C_{66})\frac{mn}{R}$$

$$\Lambda_{22} = C_{66}$$

$$\Lambda_{23} = -C_{22}\left(\frac{mn}{R}\right)^2$$

$$\Lambda_{24} = (K_{12} + 2K_{66})\,\frac{mn}{R}$$

$$\Lambda_{25} = -(C_{12} + C_{66})w_{0,x}^{*}\,\frac{mn}{R}$$

$$\Lambda_{26} = -C_{66}w_{0,xx}^{*}\,\frac{mn}{R} - \frac{C_{22}mn}{R^2} - K_{22}\left(\frac{mn}{R}\right)^3$$

$$\Lambda_{31} = \frac{C_{12}}{R} + (K_{12} + 2K_{66})\left(\frac{mn}{R}\right)^2 - C_{11}w_{0,xx}^{*}$$

$$\Lambda_{32} = -2K_{66}\,\frac{mn}{R}$$

$$\Lambda_{33} = \frac{C_{22}mn}{R^2} + K_{22}\left(\frac{mn}{R}\right)^3 - C_{12}w_{0,xx}^{*}\,\frac{mn}{R}$$

$$\Lambda_{34} = \lambda_{cr} - \frac{K_{12}}{R} - (4D_{66} + D_{12})\left(\frac{mn}{R}\right)^2 + K_{11}w_{0,xx}^{*}$$

$$\Lambda_{35} = \left[\frac{C_{12}}{R} + (K_{12} + 2K_{66})\left(\frac{mn}{R}\right)^2\right]w_{0,x}^{*} - C_{11}w_{0,x}^{*}w_{0,xx}^{*}$$

$$\Lambda_{36} = \left\{\left[\frac{C_{12}K_{11}}{C_{11}} + 2(K_{66} - K_{12})\right]\left(\frac{mn}{R}\right)^2 - \frac{C_{12}}{R}\right\}w_{0,xx}^{*} + \frac{1}{R}\left(C_{22} - \frac{C_{12}^2}{R}\right)\left(\frac{mn}{R}\right)^2 w_0^{*}$$

$$+ D_{22}\left(\frac{mn}{R}\right)^4 + \frac{2K_{22}}{R}\left(\frac{mn}{R}\right)^2 + \frac{C_{22}}{R^2} - \frac{C_{12}}{C_{11}}\left(\frac{mn}{R}\right)^2 \lambda_{cr}$$

$$\Lambda_{41} = -K_{11}$$

$$\Lambda_{42} = -K_{12}\frac{mn}{R}$$

$$\Lambda_{43} = D_{11}$$

$$\Lambda_{44} = -K_{11}w^{*}_{0,x}$$

$$\Lambda_{45} = -\left[D_{12}\left(\frac{mn}{R}\right)^2 + \frac{K_{12}}{R}\right]$$

with

$$m = 0 \longrightarrow U_{20},\ V_{20},\ W_{20},\ M_{20}$$
$$m = 1 \longrightarrow U_{1},\ V_{1},\ W_{1},\ M_{1}$$
$$m = 2 \longrightarrow U_{22},\ V_{22},\ W_{22},\ M_{22}$$

and D_i $(i = 1 \text{ to } 4)$ the corresponding loading terms.

If the central difference formulae

$$\left.\begin{aligned} f_i' &= \frac{f_{i+1} - f_{i-1}}{2\Delta} \\ f_i'' &= \frac{f_{i+1} - 2f_i + f_{i-1}}{\Delta^2} \end{aligned}\right\} \tag{52}$$

are employed, equations (51) can be written at the ith station as

$$A_iZ_{i-1} + B_iZ_i + C_iZ_{i+1} = D_i \qquad (i = 1,2,\ldots,N) \tag{53}$$

with

$$A_i = \begin{bmatrix} \Lambda_{11} & -\frac{\Delta}{2}\Lambda_{13} & \Lambda_{14} & -\frac{\Delta}{2}\Lambda_{15} & -\frac{\Delta}{2}\Lambda_{17} \\ -\frac{\Delta}{2}\Lambda_{21} & \Lambda_{22} & \Lambda_{24} & -\frac{\Delta}{2}\Lambda_{25} & 0 \\ -\frac{\Delta}{2}\Lambda_{31} & \Lambda_{32} & \Lambda_{34} & -\frac{\Delta}{2}\Lambda_{35} & -1 \\ -\frac{\Delta}{2}\Lambda_{41} & 0 & \Lambda_{43} & -\frac{\Delta}{2}\Lambda_{44} & 0 \end{bmatrix}$$

$$B_i = \begin{bmatrix} -2\Lambda_{11} + \Delta^2\Lambda_{12} & 0 & -2\Lambda_{14} + \Delta^2\Lambda_{16} & 0 \\ 0 & -2\Lambda_{22} + \Delta^2\Lambda_{23} & -2\Lambda_{24} + \Delta^2\Lambda_{26} & 0 \\ 0 & -2\Lambda_{32} + \Delta^2\Lambda_{33} & -2\Lambda_{34} + \Delta^2\Lambda_{36} & 2 \\ 0 & \Delta^2\Lambda_{42} & -2\Lambda_{43} + \Delta^2\Lambda_{45} & \Delta^2 \end{bmatrix}$$

$$C_i = \begin{bmatrix} \Lambda_{11} & \frac{\Delta}{2}\Lambda_{13} & \Lambda_{14} + \frac{\Delta}{2}\Lambda_{15} & \frac{\Delta}{2}\Lambda_{17} \\ \frac{\Delta}{2}\Lambda_{21} & \Lambda_{22} & \Lambda_{24} + \frac{\Delta}{2}\Lambda_{25} & 0 \\ \frac{\Delta}{2}\Lambda_{31} & \Lambda_{32} & \Lambda_{34} + \frac{\Delta}{2}\Lambda_{35} & -1 \\ \frac{\Delta}{2}\Lambda_{41} & 0 & \Lambda_{43} + \frac{\Delta}{2}\Lambda_{44} & 0 \end{bmatrix}$$

where Δ is the width of a finite-difference space and i is numbered so that $i = 1, N$ corresponds to the boundaries of the cylinder.

Boundary Conditions

For the present investigation, the so-called "classical" simple support and clamped boundary conditions were employed, that is, for simple support

$$\left.\begin{aligned} N_x &= -\lambda \\ v &= 0 \\ w &= 0 \\ M_x &= 0 \end{aligned}\right\} \tag{54}$$

at the boundaries, while for clamped support

$$\left.\begin{aligned} N_x &= -\lambda \\ v &= 0 \\ w &= 0 \\ w_{,x} &= 0 \end{aligned}\right\} \tag{55}$$

at the boundaries.

Using the results of the first and second perturbations (eqs. (27) and (36)) and the finite-difference approximations, the boundary conditions can be written as

$$\left.\begin{aligned} \bar{A}_1 Z_0 + \bar{B}_1 Z_1 + \bar{C}_1 Z_2 &= \bar{D}_1 \\ \bar{A}_N Z_{N-1} + \bar{B}_N Z_N + \bar{C}_N Z_{N+1} &= \bar{D}_N \end{aligned}\right\} \tag{56}$$

where for simple support

$$\bar{A}_1 = \begin{bmatrix} -C_{11}\frac{\Delta}{2} & 0 & -K_{11} - C_{11}w^*_{0,x}(1)\frac{\Delta}{2} & 0 \\ 0 & 0 & 0 & 0 \\ 0 & 0 & 0 & 0 \\ 0 & 0 & 0 & 0 \end{bmatrix}$$

$$\bar{B}_1 = \begin{bmatrix} 0 & \frac{mn}{R}C_{12}\Delta^2 & \frac{C_{12}}{R}\Delta^2 + 2K_{11} + K_{12}\Delta^2\left(\frac{mn}{R}\right)^2 & 0 \\ 0 & 1 & 0 & 0 \\ 0 & 0 & 1 & 0 \\ 0 & 0 & 0 & 1 \end{bmatrix}$$

$$\bar{C}_1 = \begin{bmatrix} C_{11}\frac{\Delta}{2} & 0 & -K_{11} + C_{11}w^*_{0,x}(1)\frac{\Delta}{2} & 0 \\ 0 & 0 & 0 & 0 \\ 0 & 0 & 0 & 0 \\ 0 & 0 & 0 & 0 \end{bmatrix}$$

and $\bar{A}_N$, $\bar{B}_N$, and $\bar{C}_N$ are given by similar expressions differing only in that $w^*_{0,x}$ is evaluated at station N rather than station 1.

For clamped support, the last row of equations (56) is modified so that

$$\left.\begin{aligned}
\bar{A}_1(4,j) &= \begin{bmatrix} 0 & 0 & -\frac{\Delta}{2} & 0 \end{bmatrix} = \bar{A}_N(4,j) \\
\bar{B}_1(4,j) &= \begin{bmatrix} 0 & 0 & 0 & 0 \end{bmatrix} = \bar{B}_N(4,j) \\
\bar{C}_1(4,j) &= \begin{bmatrix} 0 & 0 & \frac{\Delta}{2} & 0 \end{bmatrix} = \bar{C}_N(4,j)
\end{aligned}\right\} \tag{57}$$

The contribution by points exterior to the boundary (denoted by the subscripts 0 and N+1) introduced by the finite-difference scheme is eliminated by writing the equilibrium equation at the boundary (see, for example, ref. 38), thereby obtaining two simultaneous equations in three unknowns at each boundary. If the exterior points are algebraically eliminated, the equilibrium equations and boundary conditions take the following form:

$$\begin{bmatrix}
\hat{B}_1 & \hat{C}_1 & & & & & & \\
A_2 & B_2 & C_2 & & & & & \\
 & A_3 & B_3 & C_3 & & & & \\
 & \cdots & \cdots & \cdots & \cdots & \cdots & \cdots & \\
 & & & A_{N-2} & B_{N-2} & C_{N-2} & & \\
 & & & & A_{N-1} & B_{N-1} & C_{N-1} & \\
 & & & & & \hat{A}_N & \hat{B}_N &
\end{bmatrix}
\begin{bmatrix} Z_1 \\ Z_2 \\ Z_3 \\ \cdots \\ Z_{N-2} \\ Z_{N-1} \\ Z_N \end{bmatrix}
=
\begin{bmatrix} \hat{D}_1 \\ D_2 \\ D_3 \\ \cdots \\ D_{N-2} \\ D_{N-1} \\ \hat{D}_N \end{bmatrix} \tag{58}$$

and

$$\bar{Z}_{11}(i) = \begin{bmatrix} \bar{U}_1(i) \\ \bar{V}_1(i) \\ \bar{W}_1(i) \\ \bar{M}_1(i) \end{bmatrix} \quad \text{where } i \text{ denotes the ith station } i = (1,2,\ldots,N)$$

Since A_{11} is a banded matrix, it is convenient to triangularize A_{11} by Gaussian elimination so that equation (59) becomes

$$\hat{A}_{11}\bar{Z}_{11} = 0 \tag{60}$$

where

$$\hat{A}_{11} = \begin{bmatrix} R_1 & C_1 & & & \\ & R_2 & C_2 & & \\ \cdot & \cdot & \cdot & \cdot & \cdot \\ & & & R_{N-1} & C_{N-1} \\ & & & & R_N \end{bmatrix} \tag{61}$$

and

$$R_1 = \hat{B}_1$$

$$R_i = B_i - A_i P_{i-1} \qquad i = 2,3,\ldots,N$$

with

$$P_1 = \hat{B}_1^{-1}\hat{C}_1$$

$$P_i = R_i^{-1}C_i \qquad i = 2,3,\ldots,N$$

where

$$\hat{B}_1 = \bar{B}_1 - \bar{A}_1 A_1^{-1} B_1$$

$$\hat{C}_1 = \bar{C}_1 - \bar{A}_1 A_1^{-1} C_1$$

$$\hat{D}_1 = \bar{D}_1 - \bar{A}_1 A_1^{-1} D_1$$

$$\hat{A}_N = \bar{A}_N - \bar{C}_N C_N^{-1} A_N$$

$$\hat{B}_N = \bar{B}_N - \bar{C}_N C_N^{-1} B_N$$

$$\hat{D}_N = \bar{D}_N - \bar{C}_N C_N^{-1} D_N$$

Solutions to equations (58) for each of the perturbations are discussed in the following sections.

Solution for First Perturbation

For the first perturbation, the right-hand side of equation (58) becomes a null vector so that the equation becomes

$$A_{11} \bar{Z}_{11} = 0 \tag{59}$$

where

$$A_{11} = \begin{bmatrix} \hat{B}_1 & \hat{C}_1 & & & & & & \\ A_2 & B_2 & C_2 & & & & & \\ & A_3 & B_3 & C_3 & & & & \\ \cdots & \cdots & \cdots & \cdots & \cdots & & & \\ & & & & A_{N-2} & B_{N-2} & C_{N-2} & \\ & & & & & A_{N-1} & B_{N-1} & C_{N-1} \\ & & & & & & \hat{A}_N & \hat{B}_N \end{bmatrix} \quad \text{with} \quad m = 1$$

A condition for solution of equation (60) is that

$$\det \hat{A}_{11} = 0$$

so that

$$\det(R_1 R_2 \ldots R_N) = 0$$

Using Potters' method (ref. 42) applied to a general eigenvalue problem, it can be shown that $\det R_N = 0$ is a sufficient condition for solution. This determinant, however, contains spurious poles which can be removed conveniently by the method outlined in reference 40 using the condition

$$\frac{\det R_1}{\left|\det R_1\right|} \frac{\det R_2}{\left|\det R_2\right|} \cdot \cdot \cdot \det R_N = 0 \tag{62}$$

For the first perturbation solution, λ_{cr} must be such that equation (62) is satisfied. For the present study, the buckling load was determined from a computer program developed in reference 41 by using the techniques of reference 38, and equation (62) was used to verify the accuracy of the present equations. The buckling solution of reference 41 differs from the present solution for the zeroth and first perturbation only in that deformations prior to buckling are found from a numerical rather than closed-form solution, and that provision is made to investigate various values of n and the applied load in order to find the buckling load λ_{cr} by determinant plotting (see also ref. 38). Once the buckling load has been determined, its corresponding eigenvector can be found by a method suggested by reference 38.

If

$$R_N = \begin{bmatrix} a_{11} & a_{12} & a_{13} & a_{14} \\ a_{21} & a_{22} & a_{23} & a_{24} \\ a_{31} & a_{32} & a_{33} & a_{34} \\ a_{41} & a_{42} & a_{43} & a_{44} \end{bmatrix}$$

it can be shown that the components of the eigenvector at the boundary are given by

$$\left.\begin{aligned} \overline{U}_1(N) &= \det \begin{bmatrix} a_{12} & a_{13} & a_{14} \\ a_{22} & a_{23} & a_{24} \\ a_{42} & a_{43} & a_{44} \end{bmatrix} \\ \overline{V}_1(N) &= -\det \begin{bmatrix} a_{11} & a_{13} & a_{14} \\ a_{21} & a_{23} & a_{24} \\ a_{41} & a_{43} & a_{44} \end{bmatrix} \\ \overline{W}_1(N) &= \det \begin{bmatrix} a_{11} & a_{12} & a_{14} \\ a_{21} & a_{22} & a_{24} \\ a_{41} & a_{42} & a_{44} \end{bmatrix} \\ \overline{M}_1(N) &= -\det \begin{bmatrix} a_{11} & a_{12} & a_{13} \\ a_{21} & a_{22} & a_{23} \\ a_{41} & a_{42} & a_{43} \end{bmatrix} \end{aligned}\right\} \qquad (63)$$

With the components of the vector $\bar{Z}_{11}(N)$ known, the eigenvectors at other stations are found from the recurrence relation

$$\bar{Z}_{11}(i) = -P_i\bar{Z}_{11}(i + 1) \qquad i = 1,2,\ldots,N-1 \tag{64}$$

After obtaining $\bar{Z}_{11}$ at all stations, the resulting vector was normalized for the present computations so that

$$Z_{11} = \frac{\bar{Z}_{11}}{\left|\dfrac{\bar{W}_1(i)_{max}}{t}\right|} \tag{65}$$

with

$$Z_{11}(i) = \begin{Bmatrix} U_1(i) \\ V_1(i) \\ W_1(i) \\ M_1(i) \end{Bmatrix} \qquad i = 1,2,\ldots,N$$

This normalization was used as a convenience to compare results from conventional Koiter theory (e.g., eq. (44)) with the present theory.

Solution for Second Perturbation

For the second perturbation, the equilibrium equations can be written as

$$A_{2m}Z_{2m} = D_{2m} \qquad m = 0,2 \tag{66}$$

with

$$A_{2m} = \begin{bmatrix} \hat{B}_1 & \hat{C}_1 & & & & & & \\ A_2 & B_2 & C_2 & & & & & \\ & A_3 & B_3 & C_3 & & & & \\ \cdot & \cdot & \cdot & \cdot & \cdot & \cdot & \cdot & \cdot \\ & & & & A_{N-2} & B_{N-2} & C_{N-2} & \\ & & & & & A_{N-1} & B_{N-1} & C_{N-1} \\ & & & & & & \hat{A}_N & \hat{B}_N \end{bmatrix}$$

$$Z_{2m}(i) = \begin{bmatrix} U_{2m}(i) \\ V_{2m}(i) \\ W_{2m}(i) \\ M_{2m}(i) \end{bmatrix} \qquad \text{and} \qquad D_{2m}(i) = \Delta^2 \begin{bmatrix} d_{21}(i) \\ d_{22}(i) \\ d_{23}(i) \\ d_{24}(i) \end{bmatrix}$$

where m takes on the value 0 to evaluate the axisymmetric part of the general solution (eq. (36)), for example, W_{20}, and m has the value 2 for the asymmetric part, for example, W_{22}. In equation (66), the components of the vector D_{2m} can be written at the ith station as

$$\left.\begin{aligned}
d_{21}(i) &= -\frac{1}{2} C_{11} W_1' W_1'' + \frac{m-1}{2}\left(\frac{n}{R}\right)^2 C_{12} W_1 W_1' + \frac{m}{2}\left(\frac{n}{R}\right)^2 C_{66} W_1 W_1' \\
d_{22}(i) &= \frac{m}{2}\left[\frac{n}{2R}(C_{12} + C_{66})(W_1')^2 - \frac{1}{2}\left(\frac{n}{R}\right)^3 C_{22} W_1^2 + \frac{n}{2R} C_{66} W_1 W_1''\right] \\
d_{23}(i) &= \frac{K_{11}}{2}\left[(W_1'')^2 + W_1' W_1'''\right] - \left(\frac{m-1}{2} K_{12} + mK_{66}\right)\left(\frac{n}{R}\right)^2 W_1 W_1'' \\
&\quad + \left[\left(\frac{1-2m}{2} K_{12} - mK_{66}\right)\left(\frac{n}{R}\right)^2 + \frac{1}{4}\left(C_{11} w_{0,xx}^* - \frac{C_{12}}{R}\right)\right](W_1')^2 \\
&\quad + \left[\frac{m}{2}\left(\frac{n}{R}\right)^2 K_{22} + \frac{m-1}{4}\left(\frac{C_{22}}{R} - C_{12} w_{0,xx}^*\right)\right]\left(\frac{n}{R}\right)^2 W_1^2 \\
&\quad + \frac{1}{2} \bar{N}_{x_1} W_1'' + (m-1)\frac{n}{R} \bar{N}_{xy_1} W_1' - \frac{1}{2}\left(\frac{n}{R}\right)^2 \bar{N}_{y_1} W_1 \\
d_{24}(i) &= 0
\end{aligned}\right\} \quad (67)$$

where the bar over the stress resultants indicates the part of the stress resultant that is independent of y (viz., $N_{x_1} = \overline{N}_{x_1} \cos \frac{ny}{R}$).

Following the development used to eliminate exterior points in the general solution (see section entitled :Boundary Conditions)

$$\left.\begin{aligned} \hat{D}_{2m}(1) &= \overline{D}_{2m}(1) - \overline{A}_1 A_1^{-1} D_{2m}(1) \\ \hat{D}_{2m}(N) &= \overline{D}_{2m}(N) - \overline{C}_N C_N^{-1} D_{2m}(N) \end{aligned}\right\} \tag{68}$$

where $\overline{A}_1$, A_1, $\overline{C}_1$, and C_1 are evaluated for $m = 0$ or $m = 2$. For simple support boundary conditions

$$\overline{D}_{2m} = -\Delta^2 \begin{Bmatrix} \frac{1}{4} C_{11}\left[W_1'(i)\right]^2 \\ 0 \\ 0 \\ \frac{1}{4} K_{11}\left[W_1'(i)\right]^2 \end{Bmatrix}, \quad i = 1,N \tag{69}$$

and for clamped boundary conditions, $\overline{D}_{2m}$ becomes a null vector. It should also be noted that rigid body displacements will occur in U_{20} if $N_{x_{20}}$ is prescribed at both ends of the cylinder. To suppress these deformations, the boundary conditions of equations (68) and (69) were modified so that the axial displacement was fixed at one end (i.e., $U_{20}(N) = 0$).

Thus, the solution for displacements resulting from the second perturbation requires solutions to two sets of simultaneous algebraic equations having the form

$$\begin{bmatrix} \hat{B}_1 & \hat{C}_1 & & & & & & \\ A_2 & B_2 & C_2 & & & & & \\ & A_3 & B_3 & C_3 & & & & \\ \cdot & \cdot & \cdot & \cdot & \cdot & \cdot & \cdot & \cdot \\ & & & A_{N-2} & B_{N-2} & C_{N-2} & & \\ & & & & A_{N-1} & B_{N-1} & C_{N-1} & \\ & & & & & \hat{A}_N & \hat{B}_N & \end{bmatrix} \begin{bmatrix} Z_{2m}(1) \\ Z_{2m}(2) \\ Z_{2m}(3) \\ \cdot\ \cdot\ \cdot \\ Z_{2m}(N-2) \\ Z_{2m}(N-1) \\ Z_{2m}(N) \end{bmatrix} = \begin{bmatrix} \hat{D}_{2m}(1) \\ D_{2m}(2) \\ D_{2m}(3) \\ \cdot\ \cdot\ \cdot \\ D_{2m}(N-2) \\ D_{2m}(N-1) \\ \hat{D}_{2m}(N) \end{bmatrix} \tag{70}$$

with $m = 0,2$.

To solve these equations, Gaussian elimination (sometimes referred to as Potters' method, ref. 42) was employed on a digital computer.

Evaluation of b

As mentioned in the derivation of the governing equations, the determination of b requires identification of the secular terms occurring in the general solution of the third perturbation. To accomplish this, the general solutions of equations (39) are substituted into the equilibrium equations, and terms whose coefficients are either $\cos \frac{ny}{R}$ or $\sin \frac{ny}{R}$ are collected. The resulting equilibrium equations associated only with secular terms can be written as

$$A_{11}Z_{31} = b\lambda_{cr}c_1D_{31} + c_1^3E_{31} \tag{71}$$

in which

$$D_{31} = \Delta^2 \begin{bmatrix} d_{31}(i) \\ d_{32}(i) \\ d_{33}(i) \\ 0 \end{bmatrix} \qquad i = 1,2,\ldots,N$$

with

$$d_{31}(i) = -C_{11}(w^*_{0,x\lambda}W_1'' + w^*_{0,xx\lambda}W_1'') + \left(\frac{n}{R}\right)^2 C_{66}w^*_{0,x\lambda}W_1$$

$$d_{32}(i) = \frac{n}{R} C_{66}w^*_{0,xx\lambda}W_1 + \frac{n}{R}(C_{12} + C_{66})w^*_{0,x\lambda}W_1'$$

$$\begin{aligned} d_{33}(i) = {} & -W_1'' + \bar{N}_{x_1}w^*_{0,xx\lambda} - \left(\frac{n}{R}\right)^2 N^*_{y_{0,\lambda}}W_1 \\ & + C_{11}w^*_{0,xx}w^*_{0,x\lambda}W_1' - \frac{C_{12}}{R} w^*_{0,x\lambda}W_1' \\ & + K_{11}(w^*_{0,x\lambda}W_1'''' + 2w^*_{0,xx\lambda}W_1'' + w^*_{0,xxx\lambda}W_1') \\ & - 2\left(\frac{n}{R}\right)^2 K_{66}w^*_{0,xx\lambda}W_1 - \left(\frac{n}{R}\right)^2(2K_{66} + K_{12})w^*_{0,x\lambda}W_1' \end{aligned}$$

and

$$E_{31} = \Delta^2\begin{bmatrix} e_{31}(i) \\ e_{32}(i) \\ e_{33}(i) \\ 0 \end{bmatrix} \qquad i = 1,2,\ldots,N$$

with

$$\begin{aligned} e_{31}(i) = {} & -C_{11}\left[W_1''\left(W_{20}' + \frac{1}{2} W_{22}'\right) + W_1'\left(W_{20}'' + \frac{1}{2} W_{22}''\right)\right] \\ & + \left(\frac{n}{R}\right)^2 C_{12}(W_1'W_{22} + W_1W_{22}') \\ & + \left(\frac{n}{R}\right)^2 C_{66}\left(3W_1'W_{22} + \frac{3}{2} W_1W_{22}' + W_1W_{20}'\right) \end{aligned}$$

$$\begin{aligned} e_{32}(i) = {} & \frac{n}{R}(C_{12} + C_{66})W_1'\left(W_{20}' + \frac{1}{2} W_{22}'\right) \\ & + \frac{n}{R} C_{66}\left[W_1''W_{22} + W_1\left(W_{20}'' - \frac{1}{2} W_{22}''\right)\right] \\ & + \left(\frac{n}{R}\right)^3 C_{22}W_1W_{22} \end{aligned}$$

$$
\begin{aligned}
e_{33}(i) = \bar{K}_{33} + \bar{C}_{33} + w^*_{0,xx}\Big[C_{11}W_1'\Big(W_{20}' + \tfrac{1}{2}\,W_{22}'\Big) - \Big(\tfrac{n}{R}\Big)^2\, C_{12}W_1W_{22}\Big] \\
+ \bar{N}_{x_1}\Big(W_{20}'' + \tfrac{1}{2}\,W_{22}''\Big) + \Big(\bar{N}_{x_{20}} + \tfrac{1}{2}\,\bar{N}_{x_{22}}\Big)W_1'' \\
- 2\Big(\tfrac{n}{R}\Big)^2\,\bar{N}_{y_1}W_{22} - \Big(\tfrac{n}{R}\Big)^2\,W_1\Big(\bar{N}_{y_{20}} + \tfrac{1}{2}\,\bar{N}_{y_{22}}\Big) \\
+ 2\,\tfrac{n}{R}\,\bar{N}_{xy_1}W_{22}' + \tfrac{n}{R}\,\bar{N}_{xy_{22}}W_1'
\end{aligned}
$$

where

$$
\begin{aligned}
\bar{K}_{33} = K_{11}\Big[W_1''''\Big(W_{20}' + \tfrac{1}{2}\,W_{22}'\Big) + W_1''(2W_{20}'' + W_{22}'') + W_1'\Big(W_{20}''' + \tfrac{1}{2}\,W_{22}'''\Big)\Big] \\
-\Big(\tfrac{n}{R}\Big)^2\,K_{12}\Big[W_1''W_{22} + W_1'\Big(W_{20}' + \tfrac{13}{2}\,W_{22}'\Big) + W_1W_{22}''\Big] + 9\Big(\tfrac{n}{R}\Big)^3\,K_{22}W_1W_{22} \\
-\Big(\tfrac{n}{R}\Big)^2\,K_{66}\Big[6W_1''W_{22} + W_1'(2W_{20}' + 9W_{22}') + W_1(2W_{20}'' + 3W_{22}'')\Big]
\end{aligned}
$$

$$
\begin{aligned}
\bar{C}_{33} = \frac{1}{R}\Big[\Big(\tfrac{n}{R}\Big)^2\,C_{22}W_1W_{22} - C_{12}W_1'\Big(W_{20}' + \tfrac{1}{2}\,W_{22}'\Big)\Big] \\
+ W_1''\Big[\tfrac{3}{8}\,C_{11}(W_1')^2 + \tfrac{1}{8}\Big(\tfrac{n}{R}\Big)^2\,C_{12}W_1^2\Big] \\
- \Big(\tfrac{n}{R}\Big)^2\,W_1\Big[\tfrac{3}{8}\,C_{12}(W_1')^2 + \tfrac{1}{8}\Big(\tfrac{n}{R}\Big)^2\,C_{22}W_1^2\Big] \\
+ \tfrac{1}{2}\Big(\tfrac{n}{R}\Big)^2\,C_{66}(W_1')^2\,W_1
\end{aligned}
$$

Following the procedure for development of boundary conditions

$$
\left.
\begin{aligned}
\hat{D}_{31}(1) &= \bar{D}_{31}(1) - \bar{A}_1A_1^{-1}D_{31}(1) \\
\hat{D}_{31}(N) &= \bar{D}_{31}(N) - \bar{C}_1C_1^{-1}D_{31}(N)
\end{aligned}
\right\} \qquad (72a)
$$

and

$$\hat{E}_{31}(1) = \bar{E}_{31}(1) - \bar{A}_1 A_1^{-1} E_{31}(1)$$

$$\hat{E}_{31}(N) = \bar{E}_{31}(N) - \bar{C}_1 C_1^{-1} E_{31}(N) \tag{72b}$$

where $\bar{A}_1$, A_1, $\bar{C}_1$, and C_1 are evaluated for $m = 1$.

For simple support boundary conditions

$$\bar{D}_{31}(i) = -\Delta^2 \begin{bmatrix} C_{11} w^*_{0,x\lambda}(i) W_1'(i) \\ 0 \\ 0 \\ K_{11} w^*_{0,x\lambda}(i) W_1'(i) \end{bmatrix} \qquad i = 1,N \tag{73a}$$

$$\bar{E}_{31}(i) = -\Delta^2 \begin{bmatrix} C_{11} W_1'(i) \left[W_{20}'(i) + \frac{1}{2} W_{22}'(i) \right] \\ 0 \\ 0 \\ K_{11} W_1'(i) \left[W_{20}'(i) + \frac{1}{2} W_{22}'(i) \right] \end{bmatrix} \qquad i = 1,N \tag{73b}$$

For clamped boundary conditions, $\bar{D}_{31}$ and $\bar{E}_{31}$ become null vectors. Thus the vectors D_{31} and E_{31} can be written as

$$D_{31} = \begin{bmatrix} \hat{D}_{31}(1) \\ D_{31}(2) \\ \vdots \\ D_{31}(N-1) \\ \hat{D}_{31}(N) \end{bmatrix} \quad \text{and} \quad E_{31} = \begin{bmatrix} \hat{E}_{31}(1) \\ E_{31}(2) \\ \vdots \\ E_{31}(N-1) \\ \hat{E}_{31}(N) \end{bmatrix} \tag{74}$$

Finally, using the equation for b (eq. (50)) previously developed

$$b = \frac{-2t^2 A Z_{11}^T E_{31}}{\lambda_{cr} Z_{11}^T D_{31} \int_0^A (U_1^2 + V_1^2 + W_1^2)dx} \tag{75}$$

Program SICK

The numerical computations to determine the sensitivity index b were performed on a CDC 6600 series computer using a Fortran program entitled SICK (Sensitivity Index for Cylinders ex Koiter). A listing of this program is contained in appendix A. In the program, four key subroutines were employed: MATRIX, PØTTER, DIF, and SIMP. MATRIX is a CDC general purpose program which permits addition, subtraction, multiplication and inversion of matrices. PØTTER is a Langley Research Center program which solves banded matrix equations with a three-vector bandwidth by Gaussian elimination (Potters' method, ref. 42). DIF is a Langley program which numerically differentiates a function using a 10-point Gauss quadrature method. SIMP is an elementary program which integrates a function by Simpson's rule.

The numerical results were found to converge with about 40 finite-difference elements. The results presented herein were obtained with 60 elements. In the numerical approach employed, a major consideration was computer storage required to solve the equations resulting from the second perturbation (eqs. (70)) using the subroutine PØTTER. The choice of 60 elements was largely dictated by the fact that it led to a requirement of 70,000 octal storage units by program SICK. This storage was the

maximum obtainable on the Langley remote terminal system. Running times for a typical problem were quite excellent with the solution requiring about 25 seconds' computing time.

IX. INVESTIGATION OF RELATIVE IMPERFECTION SENSITIVITY OF FIBER-REINFORCED CYLINDERS

The imperfection sensitivity of certain fiber-reinforced cylinders was investigated with the Koiter index b determined from both the present theory (eq. (75)) as well as the theory of references 23 and 24. To employ the latter theory, equation (44) was employed together with the normalization described in equation (65). Three types of cylinders were considered: glass-epoxy, boron-epoxy, and aluminum reinforced with an overlay of boron-epoxy. The cylinders considered had a fixed radius-thickness ratio R/t of 100 and a length-radius ratio A/R of 0.7. The helical wrap angle of the cylinders was varied in an attempt to identify configurations of minimum imperfection sensitivity.

The investigation of the sensitivity index was limited to a few specific configurations because of the tedious and expensive nature of the calculations. It was found that buckling loads using the theory of reference 41 could be extracted by computer with only moderate difficulty. However, many additional computations were required in certain instances to obtain a buckling mode shape sufficiently accurate to pursue post-buckling calculations.

The elastic constants for the single fiber-reinforced layer in each cylinder were estimated by the procedure summarized in an appendix of reference 1. In this procedure elastic constants along principal axes of unidirectionally reinforced material were obtained from the theoretical study by Hashin and Rosen (ref. 33). The upper bound of the random fiber array model described therein was employed in the present study.

Elastic constants for the helically wrapped layers with filaments oriented at $\pm\alpha$ from the cylinder axis were estimated using transformation equations of orthotropic elasticity together with the concept of effective stiffness of cross-plied laminates (refs. 35, 36). This technique has been shown to give predictions in reasonable agreement with experiments to determine elastic constants of glass-epoxy (ref. 1) or boron-epoxy (ref. 4) cylinders. Constituent material properties and layer properties are summarized in table I.

Glass-Epoxy Cylinders

The cylinders investigated were composed of a single helically wrapped layer ($\pm\alpha$). The constituent properties and fiber volume fraction v_f selected for the investigation are typical of well-made filament-wound cylinders. Buckling predictions for cylinders whose wrap angle varies from 0 to 90° are shown in figure 3. The predictions are based on boundary conditions of simple support in which

$$N_{x_1} = 0$$

$$v_1 = 0$$

$$w_1 = 0$$

$$M_{x_1} = 0$$

The solid curves of figure 3 labeled "consistent theory" were obtained from reference 41 from a theory which considers nonlinear effects of change in shape of the cylinder due to load prior to buckling. The dash-dot curves of figure 3 labeled "classical theory" were obtained from the theory of reference 2 which assumes a membrane state of stress in the

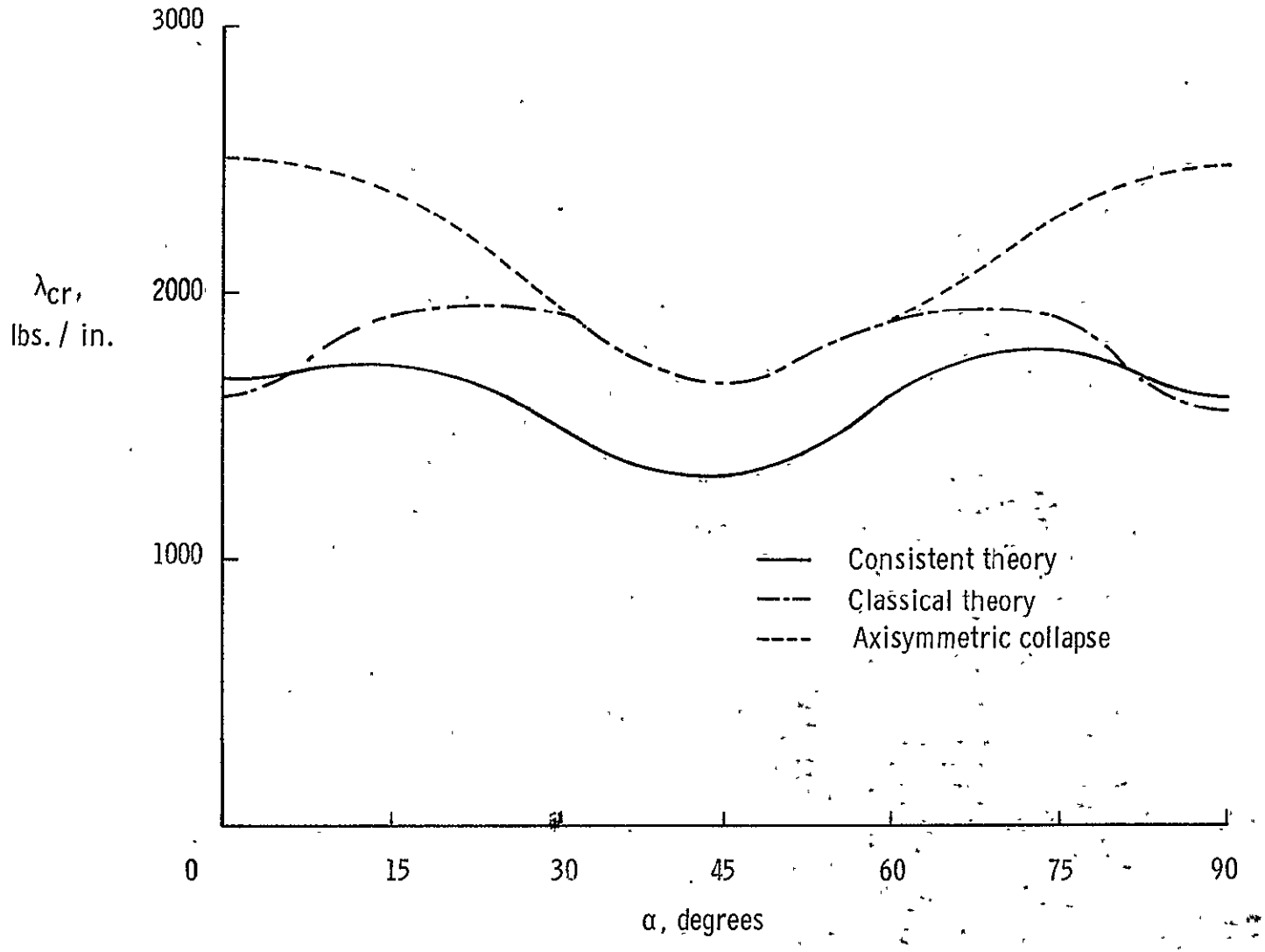

Figure 3.- Buckling loads for glass-epoxy cylinders ($R/t = 100$, $A/R = 0.7$, $v_f = 0.65$).

cylinder prior to buckling and ignores changes in shape due to loading. The dashed curve labeled "axisymmetric collapse" can be obtained from either classical theory with n equal to zero (ref. 2) or by a limiting solution of equations governing axisymmetric deformations prior to buckling (e.g., eq. (17)).

From figure 3 it can be seen that on the basis of classical theory, cylinders with helical wrap angles from 30 to 60° are expected to collapse axisymmetrically. Consistent theory predictions, however, do not suggest this mode, but rather gives loads based on asymmetric modes which are substantially lower than axisymmetric collapse predictions. The relative position of axisymmetric collapse predictions to consistent theory buckling predictions is extremely important in the present considerations of imperfection sensitivity, because the sensitivity index b is undefined when axisymmetric collapse is the predicted mode of failure. Thus, because consistent theory predictions are less than axisymmetric collapse predictions for all values of the helical wrap angle, the sensitivity index can be defined everywhere.

Substantial differences between consistent theory and classical theory predictions are indicated in figure 3. The differences are functions of the helical wrap angle and are greatest for α equal to 45°. At this angle, consistent theory predictions are about 80 percent of classical theory. For isotropic cylinders with the same radius-thickness ratio, length-radius ratio and boundary conditions, consistent theory predictions are also about 80 percent of classical theory (ref. 43). The results suggest that prebuckling deformations in

filamentary shells possessing high shear stiffness are an important consideration for accurate buckling predictions.

Imperfection sensitivity indices for the simply supported glass-epoxy cylinders are shown in figure 4. Calculations of the index b were made using the present theory (solid curve), as well as the theory of references 23 and 24 (dashed curve). The results for the sensitivity index b have been normalized by the index b_{iso} for an isotropic cylinder having the same R/t and A/R as the present cylinders. The values of b_{iso} obtained from the theory of references 23 and 24 agreed well with unpublished data (ref. 44) by J. W. Hutchinson. In plotting results on figure 4, computed data have been linked by straight line segments to indicate the points at which discrete calculations were made.

The results shown in figure 4 indicate similar trends in relative imperfection sensitivity predictions based on the two theories considered. The differences in magnitude of the imperfection sensitivity indices are attributed to differences in definition of the perturbation parameter ξ. In figure 4, the normalized sensitivity index b/b_{iso} takes on its smallest values for helical wrap angles from 30 to 60°. Thus, both theories suggest that glass-epoxy cylinders with these wrap angles are desirable configurations since they have a relatively low index. Because of the high index values for α equal to 75°, this configuration is presumed to be undesirable.

The results of a recent imperfection study by Khot (ref. 14) using a classical approach which ignores load-induced deformations prior to buckling but considers an initial imperfection of specified shape, should

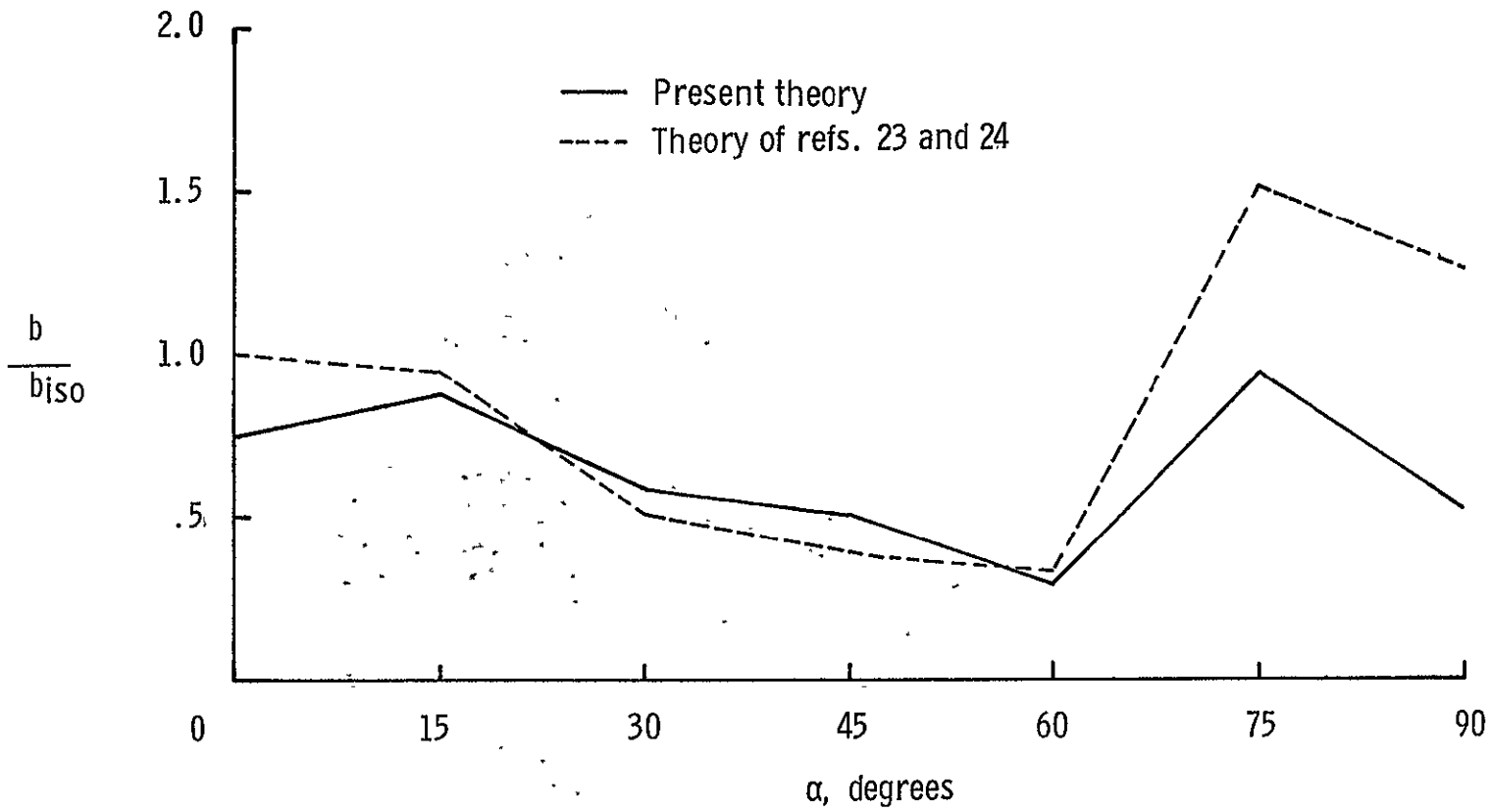

Figure 4.- Imperfection sensitivity indices for glass-epoxy cylinders.

also be noted. For three-layer glass-epoxy cylinders possessing 0, $-\alpha$, $+\alpha$, or 90, $-\alpha$, $+\alpha$, degree configurations, Khot found that maximum compressive buckling loads for small amplitude imperfections occur for shells where α is 45°. This result coupled with the present results suggests that the use of wrap angles near 45° in glass filament-wound cylinders may improve their buckling strength due to reduced sensitivity to initial imperfections.

Boron-Epoxy Cylinders

Buckling predictions for single layer, simply supported, boron-epoxy cylinders are presented in figure 5. In contrast to the glass-epoxy cylinders, consistent theory predictions for boron-epoxy cylinders indicate that axisymmetric collapse will occur for some wrap angles. As mentioned previously, the Koiter sensitivity index is undefined for these wrap angles. Note from figure 5 that consistent theory and classical theory predictions do not yield identical wrap angles for axisymmetric collapse. For consistent theory, collapse is predicted for wrap angles from 15 to 35° whereas for classical theory, collapse is predicted from 30 to 60°.

As was the case in glass-epoxy cylinders, agreement between consistent and classical theory for boron-epoxy cylinders is a function of the helical wrap angle. Maximum differences between the two theories occur for wrap angles of 45 and 75°. For these wrap angles, consistent theory yields predictions which are roughly 85 percent of classical theory. Both classical and consistent theory buckling loads are

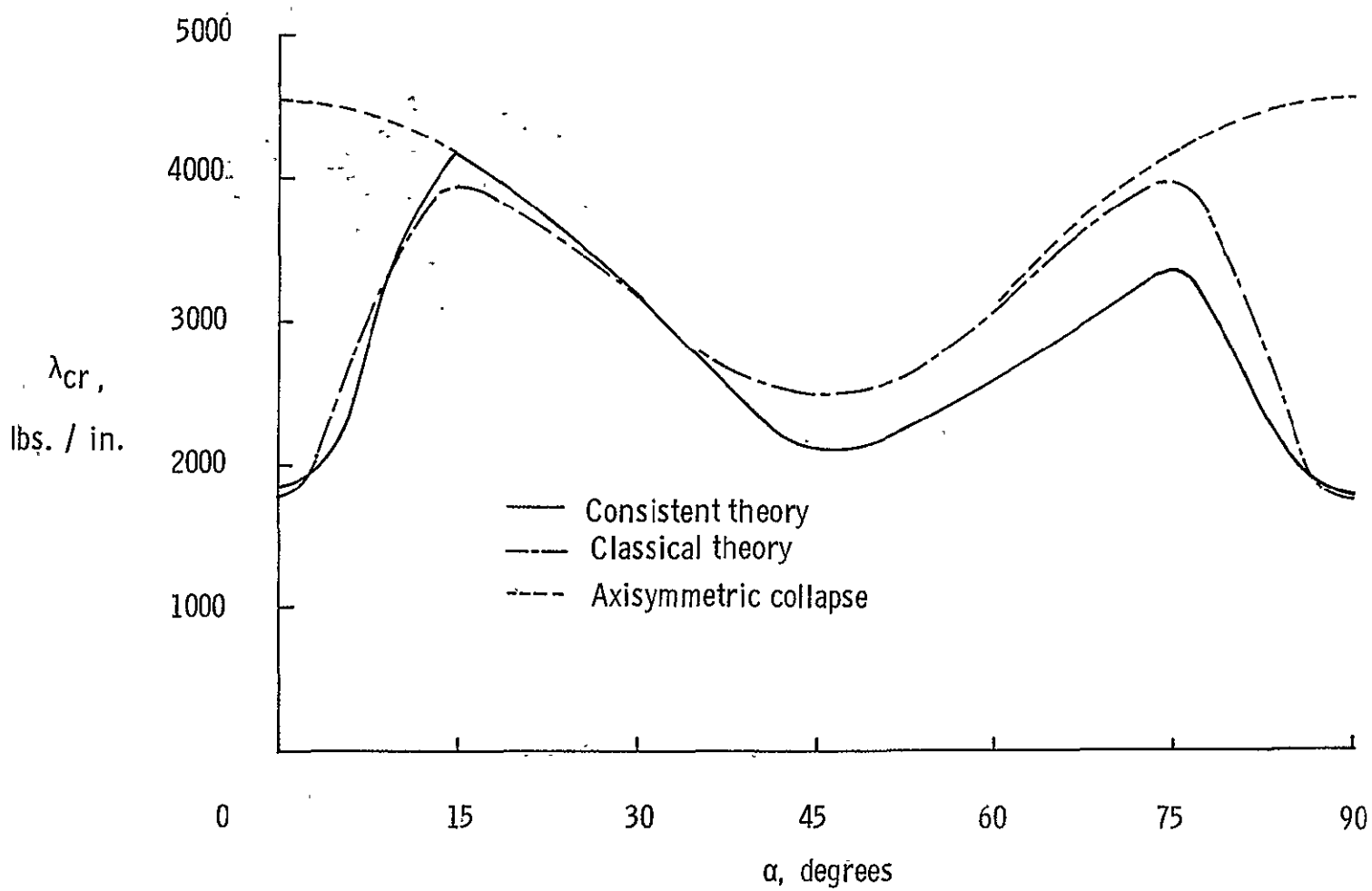

Figure 5.- Buckling loads for boron-epoxy cylinders ($R/t = 100$, $A/R = 0.7$, $v_f = 0.50$)

relatively high for cylinders with a wrap angle of 15°. The magnitude of load is believed to be a consequence of the high axial extensional and axial bending stiffness of boron filaments in this configuration, coupled with unusually large values of the product of Poisson's ratios $\mu_x\mu_y$ (see table I). Since most of the structural stiffnesses of the shell are proportional to $1/(1 - \mu_x\mu_y)$, large values of $\mu_x\mu_y$ result in increased stiffness.

Imperfection sensitivity indices for boron-epoxy cylinders are presented in figure 6. Again, agreement in trend between the present theory and the theory in references 23 and 24 is good. Because of axisymmetric collapse, the sensitivity index is undefined for helical wrap angles where $15 \leqq \alpha \leqq 35$. Note from the figure that values of sensitivity indices adjacent to the zone of axisymmetric collapse may be quite different. For α equal to 10°, the sensitivity index (as well as the buckling load) is relatively high. On the other hand, for α equal to 40°, both the sensitivity index and the buckling load are low. These results demonstrate that cylinders which buckle near axisymmetric collapse loads are not necessarily desirable from the standpoint of reduced imperfection sensitivity.

A comparison of the magnitude of the sensitivity index for glass-epoxy cylinders (fig. 4) with boron-epoxy cylinders (fig. 6) in regions of minimum imperfection sensitivity reveals that boron-epoxy shells are less sensitive. Thus, shells with wrap angles around 45° would appear to be an attractive configuration in boron-epoxy cylinders. Khot's imperfection study (ref. 14) indicated that the 45° wraps in 0, $-\alpha$, $+\alpha$,

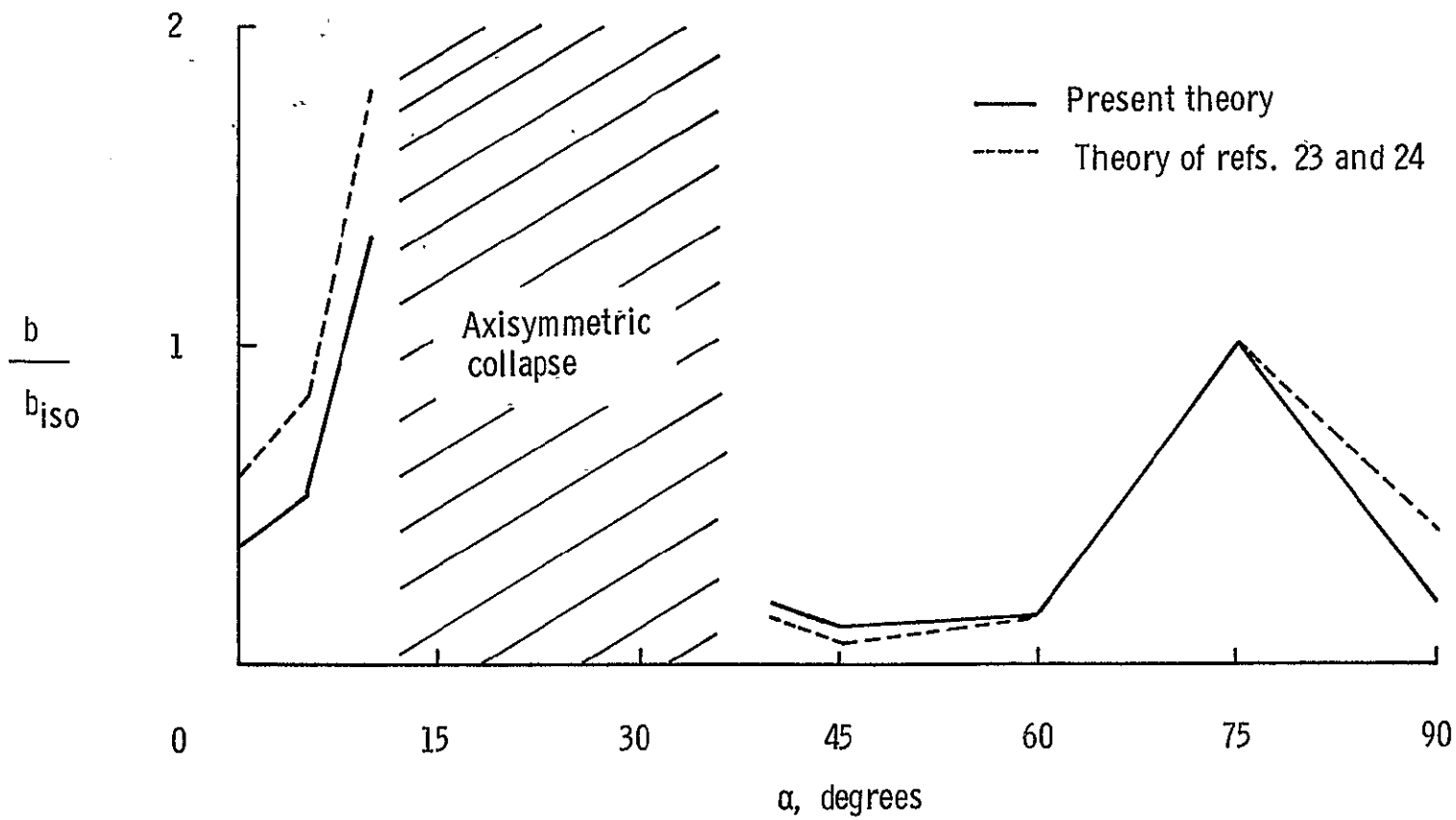

Figure 6.- Imperfection sensitivity indices for boron-epoxy cylinders.

and 90, $-\alpha$, $+\alpha$, configurations gave higher buckling loads for small amplitude imperfections. He also concluded that boron-epoxy cylinders were less sensitive to initial imperfections than glass-epoxy cylinders.

Boron-Aluminum Cylinders

In the studies of glass-epoxy and boron-epoxy cylinders, it was concluded that cylinders with wrap angles of 45° had reduced imperfection sensitivity. A shortcoming of this wrap angle in the simple configuration investigated ($\pm \alpha$) is its relatively low buckling load compared to other angles, especially in the case of boron-epoxy cylinders (see fig. 5). It seemed desirable to investigate more complex configurations, perhaps with other materials, which might possess both reduced imperfection sensitivity while still retaining relatively large buckling strengths.

An interesting concept in fiber-reinforced structures now being pursued by the NASA is that of employing a metal substrate and overlaying on it boron-epoxy tapes. This concept of selective reinforcement is attractive in that it reduces practical attachment problems and costs in using expensive filamentary material, yet at the same time provides good possibilities for structural weight savings. A recent study of tubular columns (ref. 45) in which metal tubes were overlayed with axially oriented boron filaments has produced some spectacular results for compressive buckling.

Because of current interest in the selective reinforcement concept, boron-aluminum cylinders were investigated. The cylinders were composed of two layers of equal thickness, one of aluminum, the other of boron-

epoxy with filaments at $\pm\alpha$. Based on total thickness, the cylinders had the same radius-thickness ratios as the glass and boron cylinders already mentioned. The boron-epoxy layer was located on the outer surface of the aluminum. Preliminary calculations using classical buckling theory indicated that substantial differences in buckling load occurred depending on whether the boron layer was located on the inner or outer surface of the aluminum. The highest buckling loads were developed for the configuration chosen. This effect of layer sequence is the counterpart of the stiffener eccentricity effects discussed in references 9 and 38.

Buckling predictions for the boron-aluminum cylinders are presented in figure 7. Although classical theory predictions suggest axisymmetric collapse for $30 \leqq \alpha \leqq 45$, consistent theory predictions yield only asymmetric modes so that the imperfection sensitivity index exists everywhere. Note from figure 7 that substantial differences exist between consistent and classical theory predictions. The largest differences occur for α equal to zero where the consistent theory prediction is about 73 percent of the classical prediction. The maximum load carried by the boron-aluminum cylinders occurs for a wrap angle of 60°. The reason why cylinders with this wrap angle perform so well is not obvious, since the effects of prebuckling deformations and eccentricity in multilayered shells have not been thoroughly investigated. The only unique feature of the 60° wrap is its large value of μ_y (see table I).

Imperfection sensitivity indices for boron-aluminum cylinders are presented in figure 8. Again, reasonable agreement in trends occur for

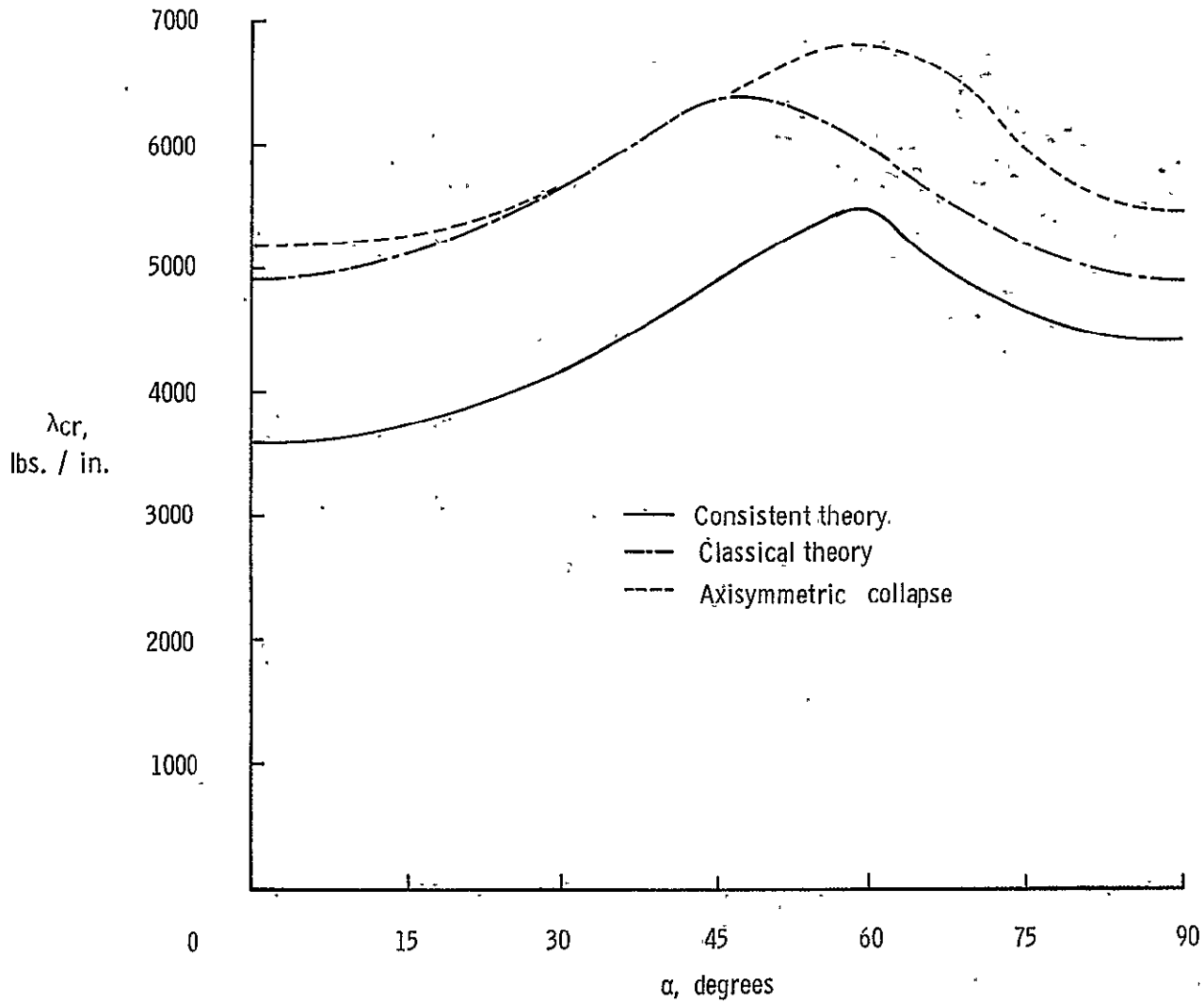

Figure 7.- Buckling loads for boron-aluminum cylinders ($R/t = 100$, $A/R = 0.7$, $v_f = 0.50$).

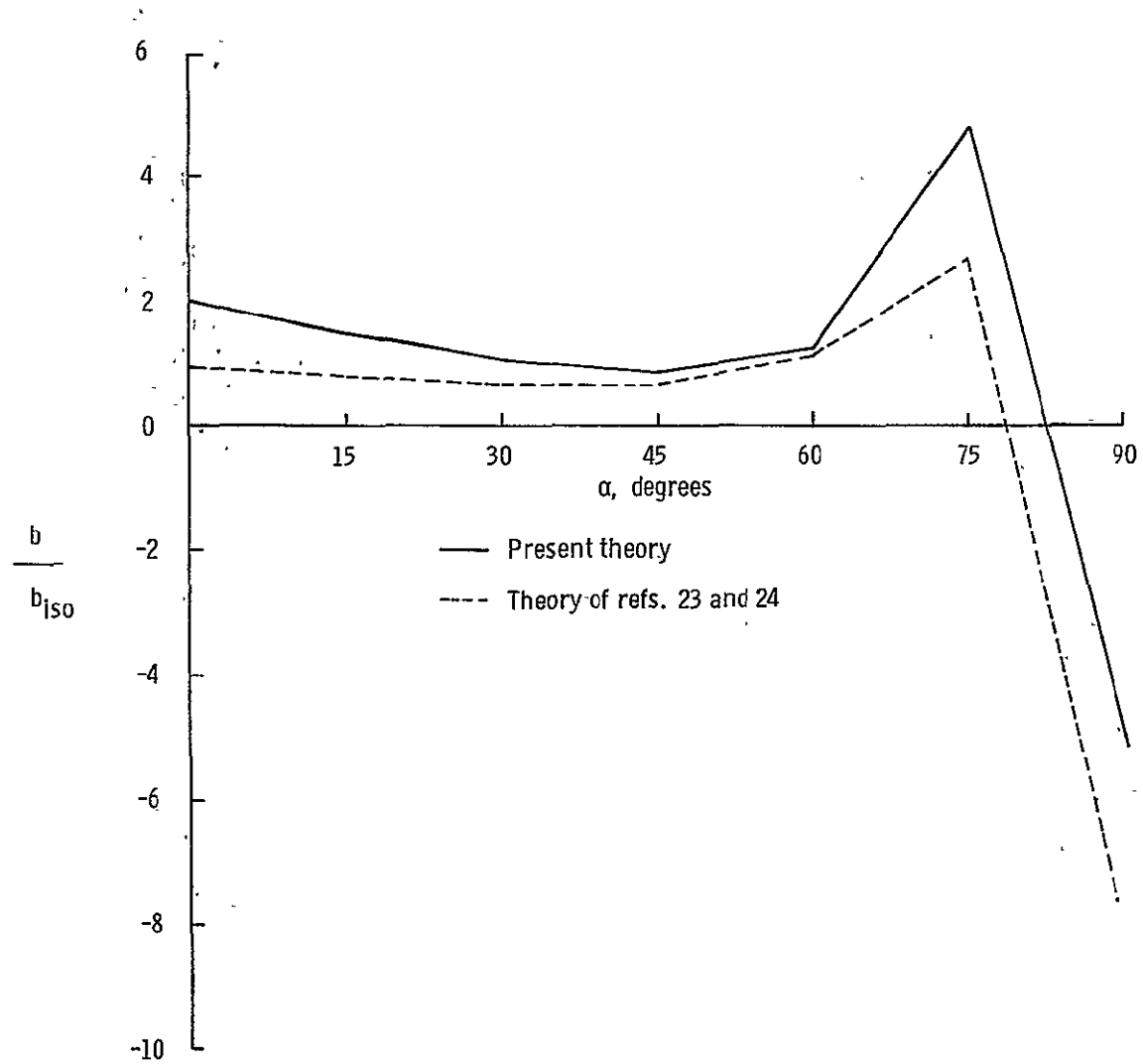

Figure 8.- Imperfection sensitivity indices for boron-aluminum cylinders.

the two versions of the Koiter theory. An interesting and encouraging result is the negative values of the normalized imperfection sensitivity index which occur for α equal to 90°. Negative values indicate a positive slope of the load-shortening curve for the cylinder in the postbuckling region. While this result is somewhat unexpected, it may be explained by observing that for α equal to 90°, the cylinder behaves as a ring-stiffened shell with very closely spaced, stiff (boron-epoxy) rings located on the outer aluminum surface. There is some evidence in the literature that ring-stiffened shells have unusual postbuckling behavior. In postbuckling studies, both Thielemann (ref. 10) and Shang (ref. 12) have found relatively large minimum postbuckling loads for ring-stiffened cylinders, thereby suggesting that they possess little imperfection sensitivity.

Relatively small imperfection sensitivity is also indicated for the 45° configuration. The magnitude of the normalized index, however, is much closer to unity than that for boron and glass cylinders with the same wrap angle. Thus imperfect boron-aluminum shells in this configuration would be expected to perform about the same as imperfect isotropic shells.

A somewhat frustrating law appears to evolve from the present investigation. As the compressive-load carrying capability of fiber-reinforced cylinders is improved by varying the filament orientation, the structure's sensitivity to imperfections becomes larger. An attractive fiber-reinforced cylinder configuration has been identified, however. Because of a positive slope in its postbuckling load-shortening

curve and its reasonably good load-carrying ability, the 90° or circumferentially wrapped boron-aluminum cylinder appears to be the most desirable of the configurations investigated herein. Whether its performance will be superior to configurations with greater potential load-carrying capability but greater imperfection sensitivity can only be determined by experiment.

X. EXPERIMENTAL INVESTIGATION

Test Specimens

To investigate the buckling behavior of fiber-reinforced cylindrical shells, compression tests were conducted on 12 filament-wound, glass-epoxy cylinders. The test specimens had an inside diameter of 30 inches, were 30 inches long, and had a nominal thickness of 0.072 inch. The cylinders were wrapped in helical layers composed of two half layers, with filaments oriented at angles $+\alpha$ or $-\alpha$ measured from the cylinder axis. The variables in the test program were the helical wrap angle α and the cylinder wall configuration.

Six of the cylinders had walls composed entirely of five helically wrapped layers in the sequence $\pm\alpha$, $\pm\alpha$, $\pm\alpha$, $\pm\alpha$, $\pm\alpha$. The walls of the other six cylinders were composed of four helical layers and four circumferentially wrapped layers in the sequence $\pm\alpha$, 90, $\pm\alpha$, 90, $\pm\alpha$, 90, $\pm\alpha$, 90, where the last circumferential wrap (+90) formed the external surface of the cylinder. Photomicrographs of the two cylinder wall configurations are shown in figure 9. For cylinders containing circumferential wraps, the helical layers at $\pm\alpha$ can be seen to be roughly twice the thickness of the circumferentially wrapped layers.

Table II contains material data for the cylinder constituents. The properties shown for glass fibers are typical of those usually employed for type E glass filament. Values of modulus and density shown for the ERL-2256 epoxy resin were obtained from compression tests of four 3-inch-diameter, solid resin cylinders about 6 inches long. The cylinders were cured with the same curing cycle as the test specimens, that is, 250° F for 2 hours. The solid cylinders were instrumented with both Tuckerman

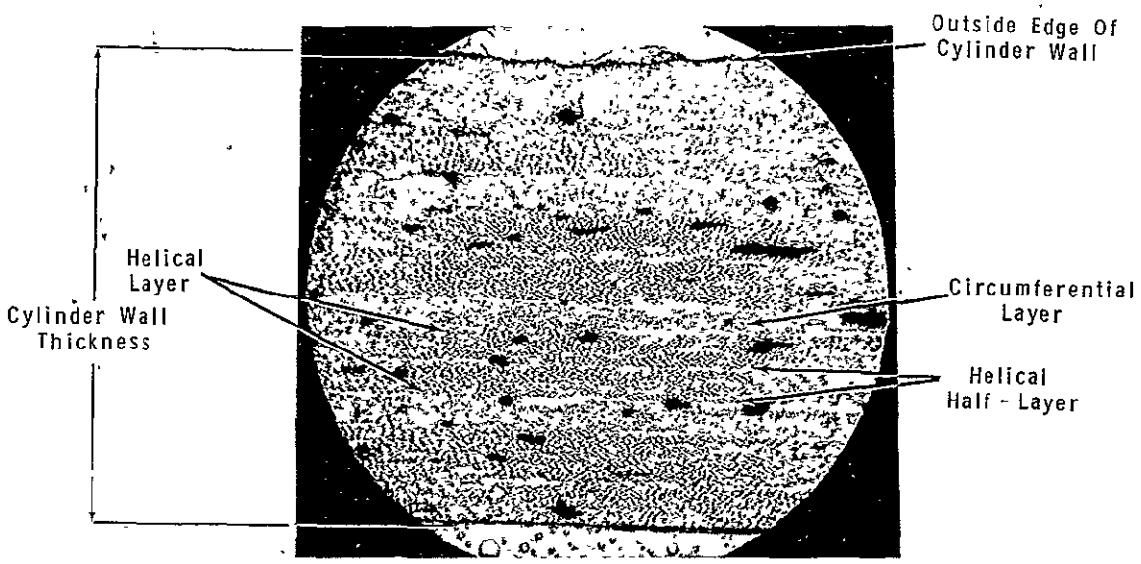

(a) Cylinder 2

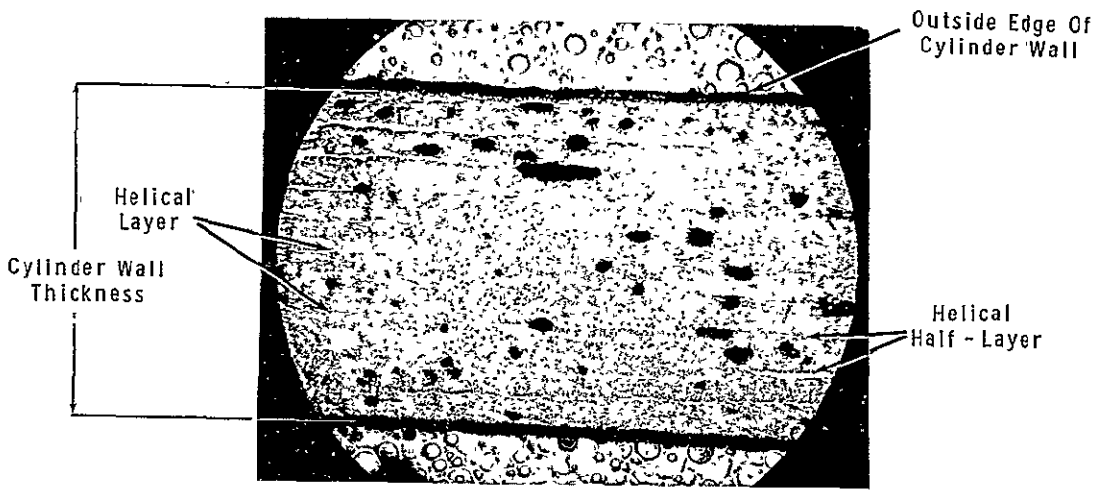

(b) Cylinder 12

Figure 9.- Photomicrographs of wall of test cylinders.

optical strain gages and differential transformer gages. The four cylinders were tested in compression at a loading rate of 20,000 pounds per minute. A typical stress-strain curve generated on an X-Y plotter by the transformer gages is reproduced in figure 10. All cylinders appeared to be capable of straining indefinitely at maximum load so that the tests were terminated when about 6 percent compressive strain had been experienced by the cylinder. No apparent damage could be observed at the conclusion of the test. Based on the test results, ERL-2256 appears to have a proportional limit of about 10 ksi in compression.

The dimensions and helical wrap angles of the glass-epoxy test specimens are presented in table III. The values of total wall thickness t shown are the average of several measurements taken at random locations. The scatter in individual measurements was ± 4 percent of the value tabulated and is attributed to the irregular outer surface of the specimens. It should also be noted that the outer surface of each specimen was reinforced at each end with circumferentially wrapped layers about 1-1.3 inches wide with thickness equal to that of the shell. The purpose of this reinforcement was to prevent local crippling due to the end loads.

The fiber volume fraction v_f, the resin volume fraction v_r, and the void volume fraction v_v, expressed as percentages, are also presented in table III. The fiber volume fractions were determined by elevated temperature exposures of two or three coupons cut from the wall of each specimen. The coupons were subjected to a temperature of 1100° F for a period of 3 hours to permit virtually all of the resin in the

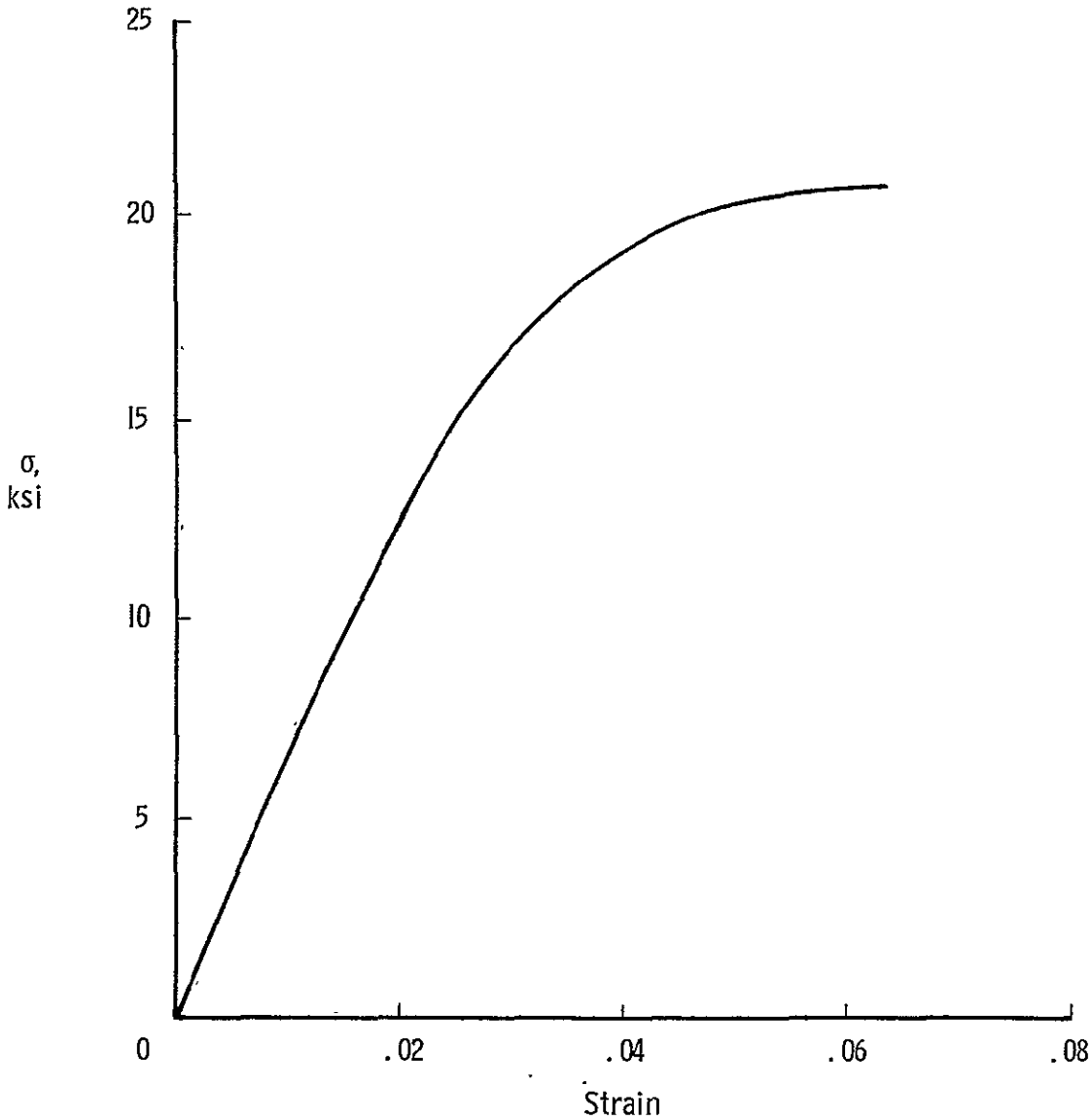

Figure 10.- Stress-strain curve for 3-inch-diameter ERL-2256 epoxy block loaded in compression.

coupon to decompose. The remaining glass was weighed and the equivalent fiber volume fraction was calculated using the values of density presented in table II. Prior to heating, the volume of each coupon was determined using Archimedes' principle. The resin and void contents were then calculated using the glass volume fraction together with the total volume and the density of resin quoted in table II. Although widely used, this method of determining void content is not extremely accurate, so that the true void content probably can be determined only to the nearest half a percent. It should be noted that the volume fractions of table III together with studies of photomicrographs of specimen walls suggest that the quality of the test specimens was only fair. Well-made glass-epoxy, filament-wound cylinders usually possess fiber volume fractions of about 65 percent while those of the present specimens are about 51 percent.

Test Procedure

Each of the 12 cylinders was instrumented with 16 wire-resistance strain gages with a gage length of 6 inches. The gages were bonded in back-to-back pairs on the surfaces of the cylinder and oriented in the axial and circumferential directions at the middle of the cylinder about 90° apart. The purpose of the axial gages was to measure initial strains from which the axial extensional modulus could be calculated, and to detect any bending deformations which might suggest buckling of the cylinder wall. The circumferential gages were present to measure strains from which Poisson's ratio $\bar{\mu}_x$, associated with loading in the axial direction, could be determined. Additional instrumentation consisted of

two linear differential transformers which were used to track the relative motion of the testing machine platens.

For testing purposes, a 3/8-inch plywood bulkhead was inserted at each end of the cylinder to ensure that the ends of the specimen would remain circular. The cylinders were tested flat-ended in compression in the Langley Research Center's 1,200 kip-capacity testing machine. The loading head of the testing machine was carefully alined to promote uniform loading of the cylinders by checking strain distributions in the axial strain gages under small loads. The buckling test consisted of a single load cycle to failure at a loading rate of 5,000 pounds per minute. During the test, data were recorded at a virtually continuous rate on the Langley Central Digital Data Recording System.

Test Results

Elastic constants.- The data obtained during the tests were reduced by computer and presented in the form of load-strain or load-displacement curves for each specimen. A sample plot of data for cylinder 10 is shown in figure 11. Data from the axial and circumferential gages have been plotted so that back-to-back pairs of gages have the same origin. For convenience, only the magnitudes of strain have been plotted. The average slope of the axial strain data was linear over a wide range of the loading history, and values of slopes determined from individual pairs of gages were in good agreement. The average of the linear slopes of the axial gages expressed as a Young's Modulus is presented in table III as $\overline{E}_x$. Values of $\overline{E}_x$ deduced from the transformer measurements of overall

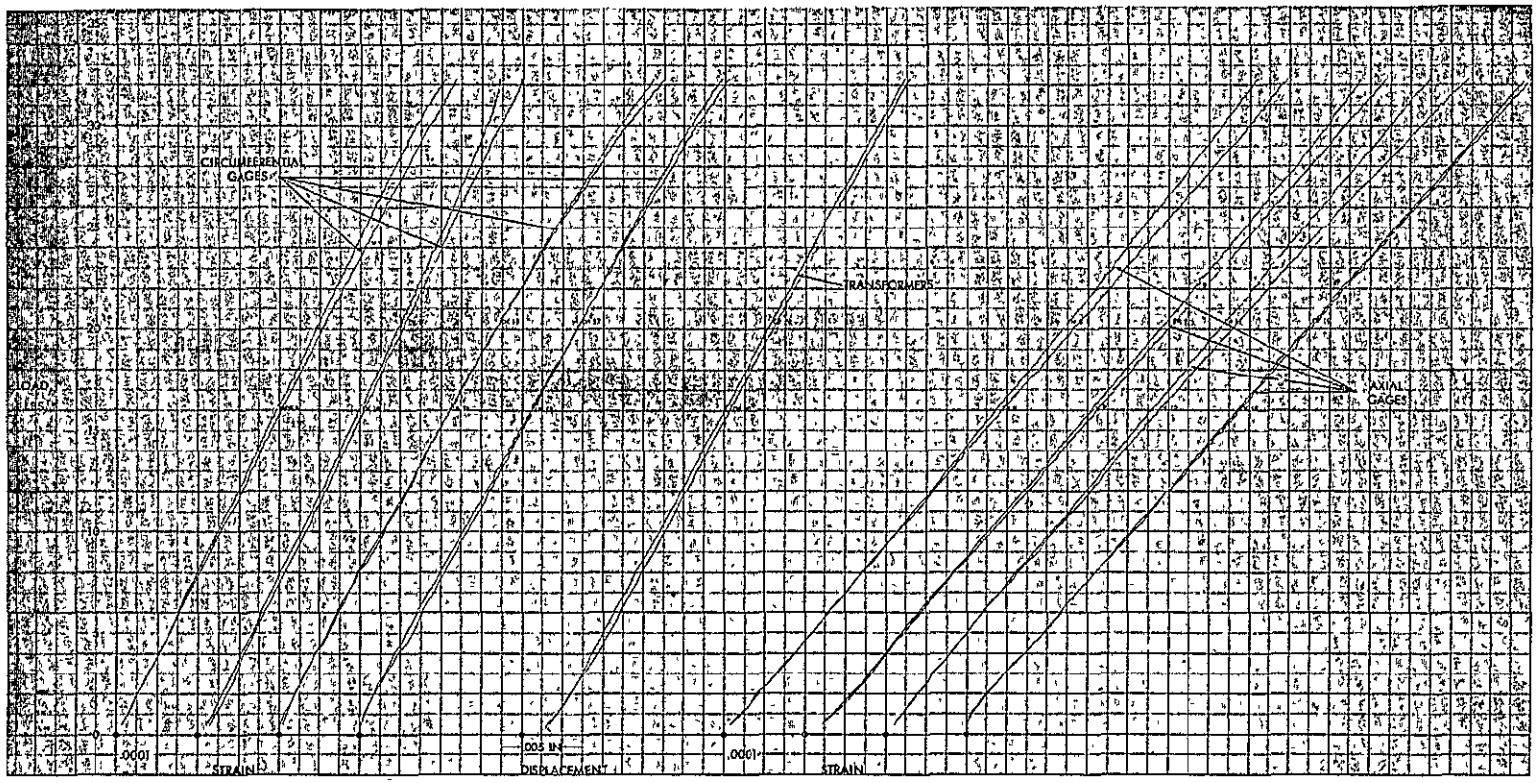

Figure 11.- Sample plot of cylinder test data.

shortening after corrections for the cylinder end reinforcement were in reasonable agreement with the axial strain-gage data.

Data from the circumferential gages were somewhat more nonlinear, and in some cases, substantial differences in individual gage slopes existed. The initial slopes of the circumferential gages were used to determine Poisson's ratio of each cylinder by dividing $\overline{E}_x$ by the average of the circumferential slopes. The Poisson's ratio associated with circumferential strain induced by axial load $\overline{\mu}_x$ is also shown in table III. The underlined values in the table are values in which large variations in individual circumferential gage slopes were present.

The test data for elastic constants are compared in figures 12 to 15 with theoretical predictions for total extensional stiffness of the cylinder wall based on references 33 and 35. It can be seen that theory and experiment are in good agreement for the extensional modulus of the cylinder wall and in fair agreement for Poisson's ratios in spite of the scatter in data. The results suggest that the techniques employed herein for predicting elastic constants yield good engineering estimates of structural stiffnesses.

Buckling.- Failure of most of the test specimens was accompanied by a loud report and the appearance of two tiers of large, diamond-shaped buckles uniformly distributed around the cylinder. As suggested in the load-strain curves of figure 11 which are plotted up to maximum load, no strain reversal was apparent prior to failure. The maximum load carried by the cylinder λ_{exp} is presented in table III. A photograph of a buckled cylinder is presented as figure 16. An observation associated

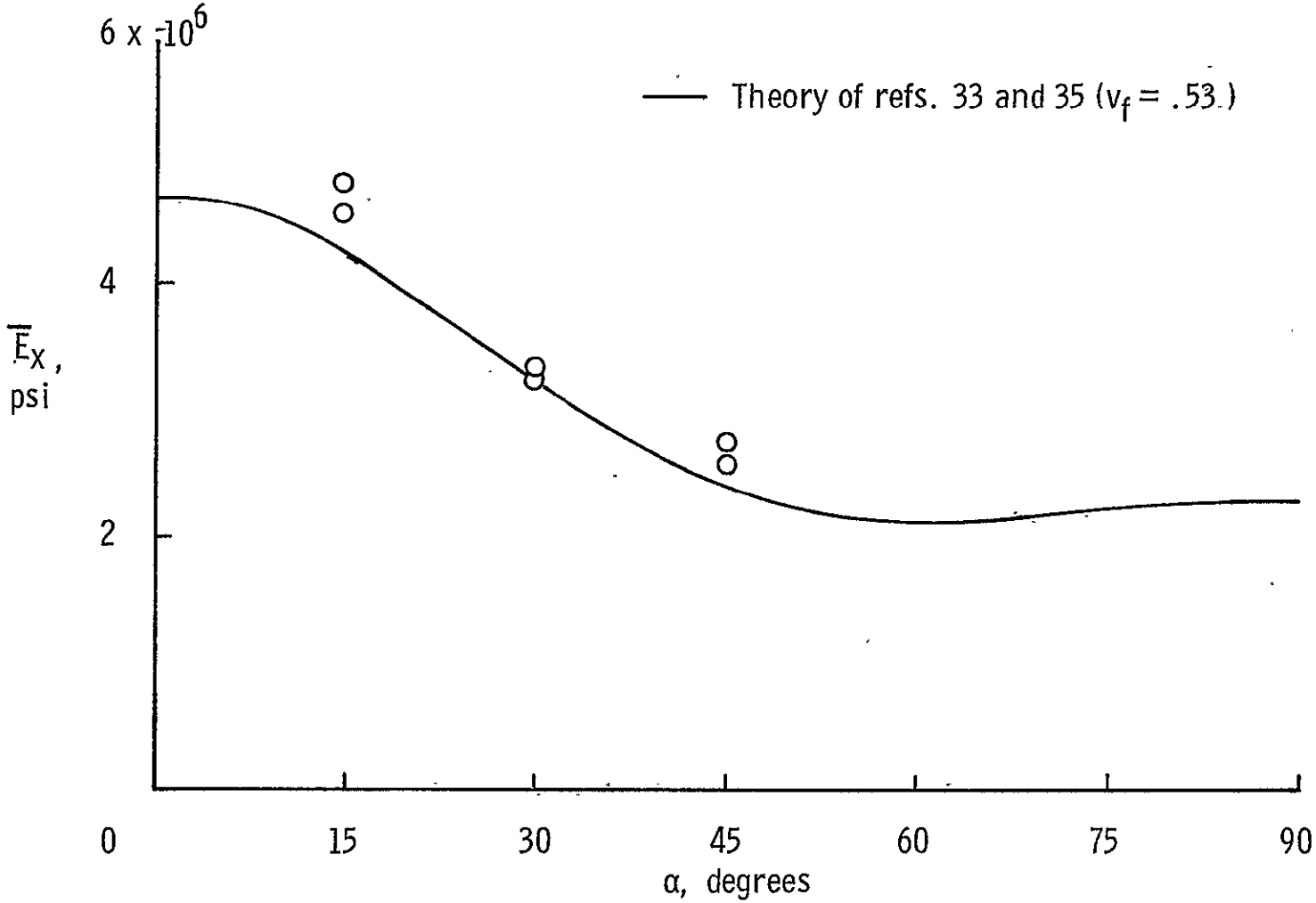

Figure 12.- Extensional moduli for test cylinders with alternating helical and circumferential wraps (cylinders 1 to 6).

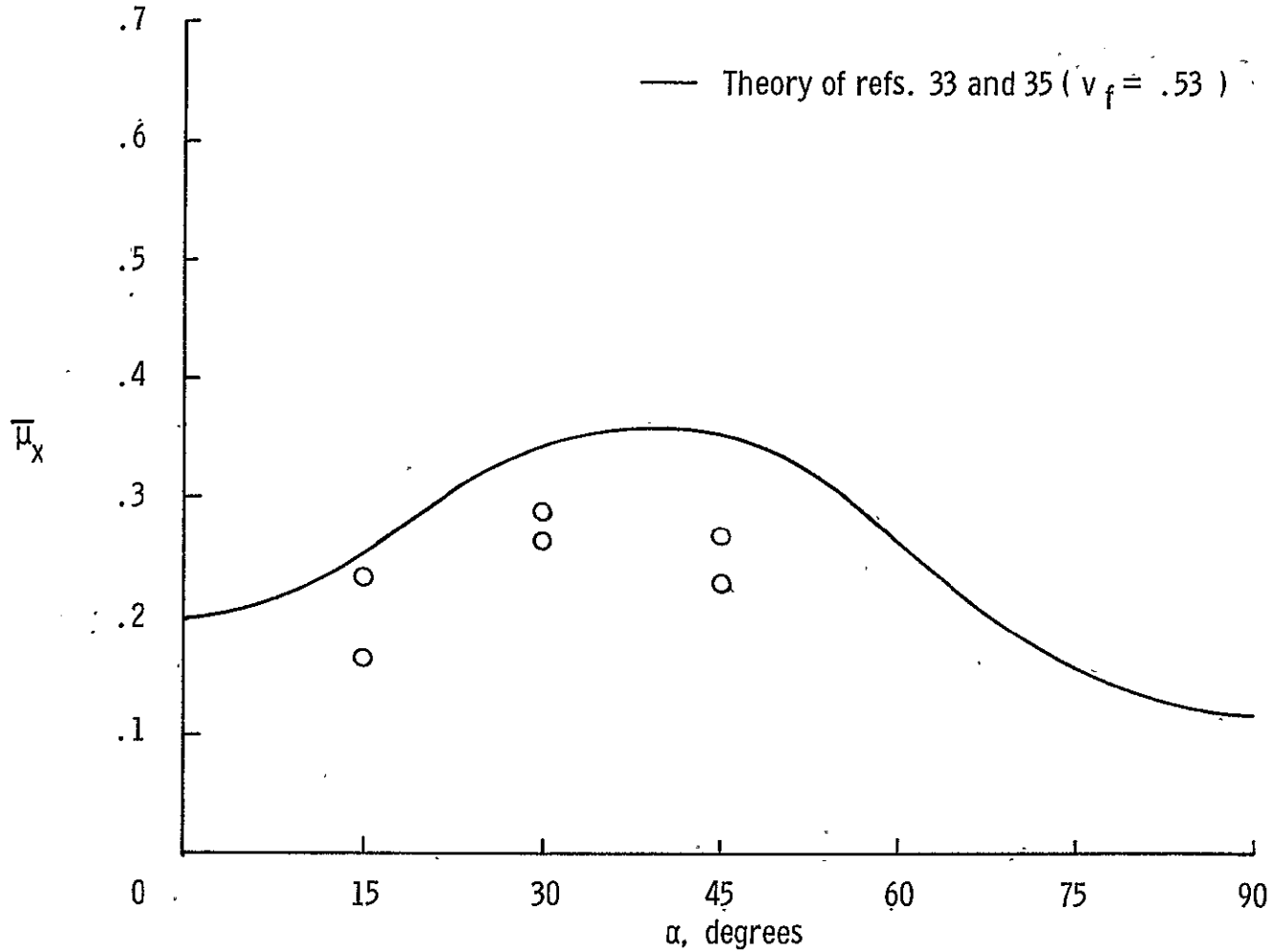

Figure 13.- Poisson's ratio associated with radial expansion induced by axial loading of test cylinders with alternating helical and circumferential wraps (cylinders 1 to 6).

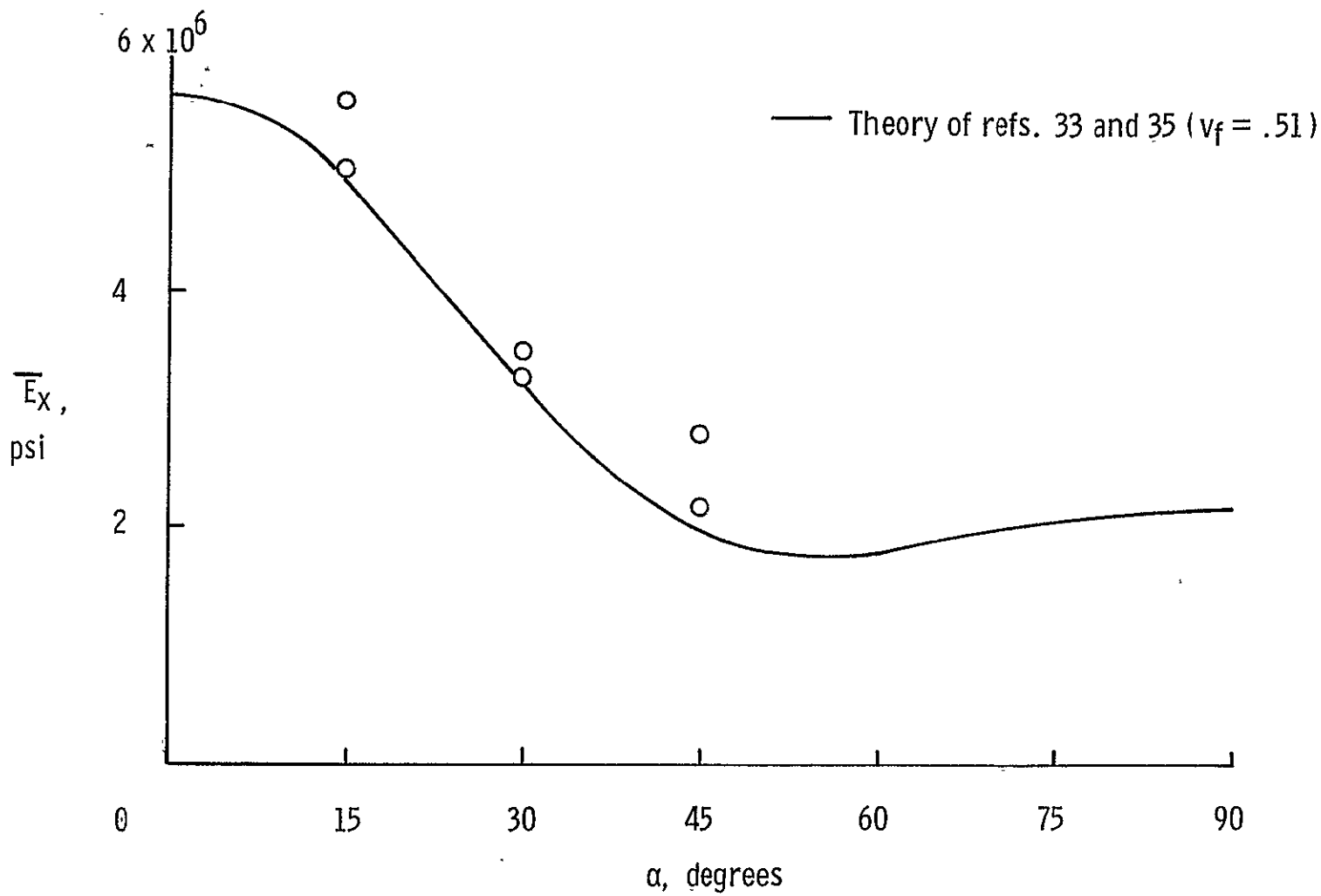

Figure 14.- Extensional moduli for test cylinders with helical wraps (cylinders 7 to 12).

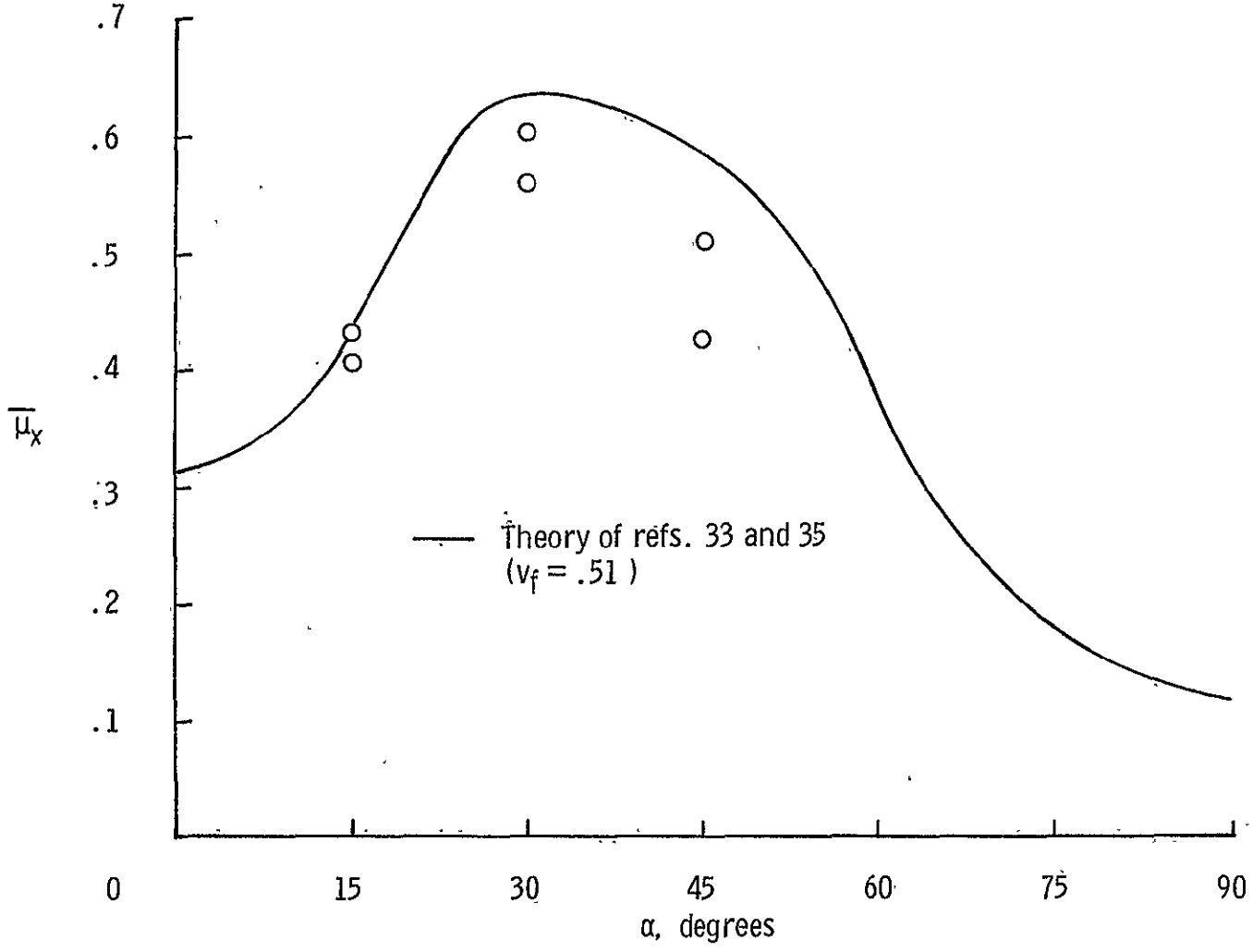

Figure 15.- Poisson's ratio associated with radial expansion induced by axial loading of test cylinders with helical wraps (cylinders 7 to 12).

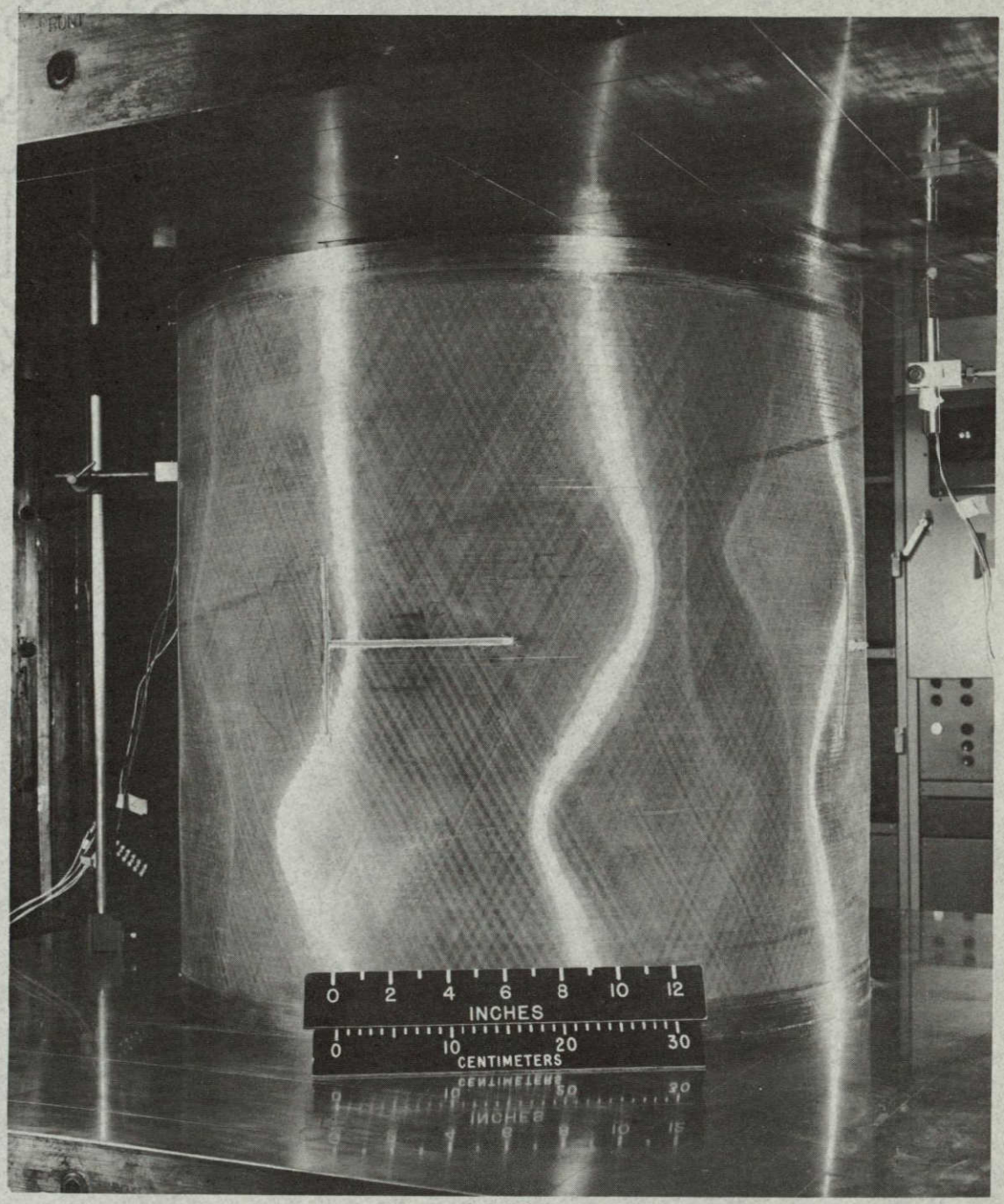

Figure 16.- Buckled test cylinder.

with the two specimens having 30° helical and circumferential wraps (cylinders 3 and 4) should be noted. On both these specimens, buckles appeared only on roughly one-half of the shell surface. As a matter of routine, before unloading, the specimens were prepared for photography by removing instrumentation wiring. In both cylinders, during this time period, a uniform buckle pattern suddenly developed, replacing the original, nonuniform pattern with no large changes in load or platen shortening. Since all specimens were tested with the same procedure, it appears that nonuniform buckle patterns might be an intrinsic characteristic of that wrap configuration. The particular configuration (±30, 90) happens to possess two-dimensional isotropy with regard to bending and extensional stiffness (but not complete isotropy due to lack of symmetry about the shell midsurface). It seems, experimentally, that less isotropic wrap configurations possess more uniform postbuckling patterns.

Comparison of Theory and Experiment

The experimentally obtained buckling loads for the test cylinders with alternating helical and circumferential wraps are compared with theoretical predictions in figure 17 and table III. The theoretical loads λ_{cr} were based on the simple support boundary conditions previously mentioned. The computations were performed using the consistent theory taking into account nonlinear prebuckling deformations (ref. 41). A few calculations using the clamped boundary conditions

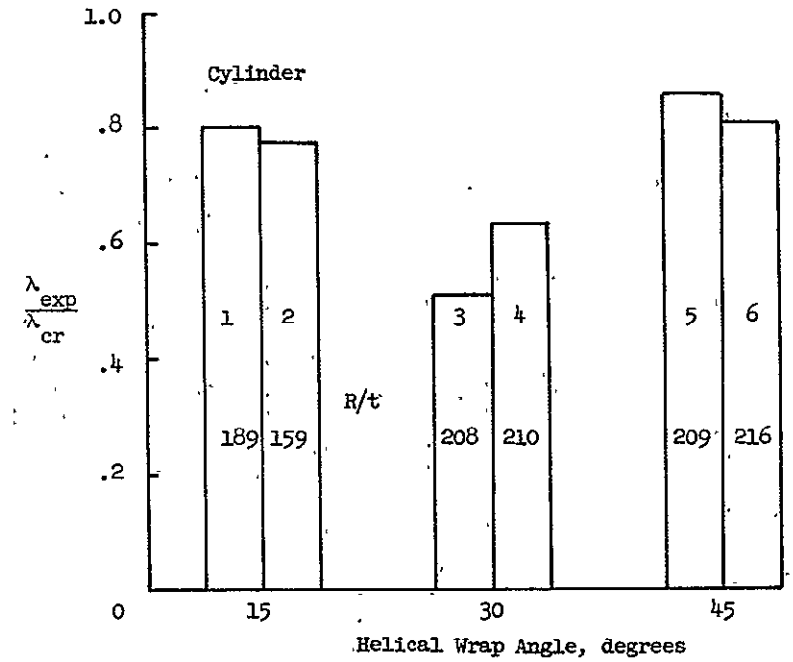

Figure 17.- Comparison of theoretical and experimental buckling loads for test cylinders with alternating helical and circumferential wraps.

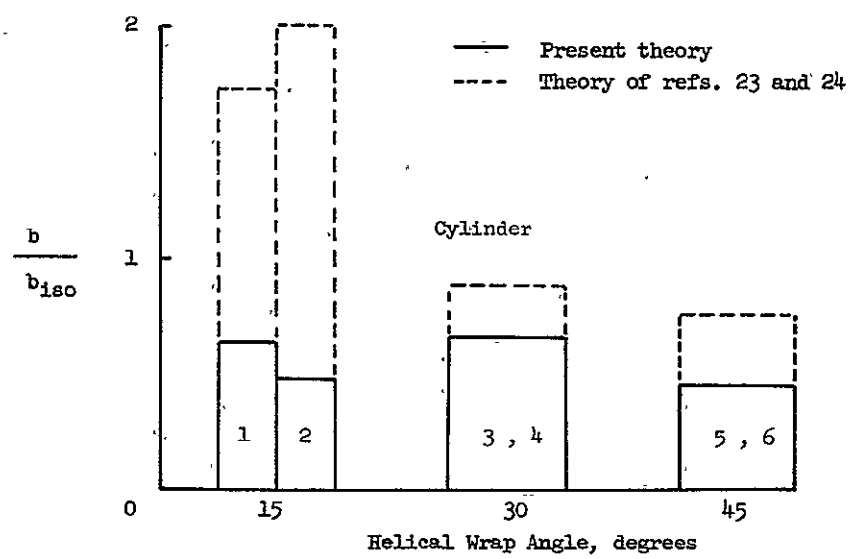

Figure 18.- Imperfection sensitivity indices for test cylinders with helical and circumferential wraps.

$$N_{x_1} = 0$$

$$v_1 = 0$$

$$w_1 = 0$$

$$w_{1,x} = 0$$

suggested that differences between clamped and simple support calculations were small because of the length of the test specimens.

The trends shown in figure 17 indicate that the greatest difference between theory and experiment occurs for a wrap angle of 30° in cylinders 3 and 4. As mentioned previously, these cylinders possess two-dimensional isotropy with respect to bending and extensional stiffness, and behaved somewhat differently at buckling than the other, less isotropic cylinders in the test program. If the data in figure 17 for wrap angles of 30° and 45° are compared, it is evident that, for cylinders with nearly identical radius-thickness ratios, agreement between theory and experiment is much better for the less isotropic configuration (that is, 45°). Moreover, from table III it can be seen that analytically, the 30° configurations were expected to carry more load than the 45° configurations, whereas experimentally the reverse was true. Presumably, the reason for this unusual phenomenon is associated with the 45° configuration being less imperfection-sensitive than the nearly isotropic configuration. Thus, the present tests offer experimental evidence that certain filament orientations can enhance the buckling strength of a cylinder due to their decreased imperfection sensitivity. Direct comparisons between the 15° and 30° configurations are complicated due to the differences in radius-thickness ratios.

Imperfection sensitivity indices for cylinders 1 to 6 are presented in figure 18. The indices have been normalized by the index b_{iso} for isotropic cylinders of the same geometry. Results are shown for both the present theory and the theory of references 23 and 24. Agreement between the two theories is fair except for a wrap angle of 15°. The large value obtained for the sensitivity index at this angle from the referenced theory is not presently understood.

The trend of data from the present theory, however, is quite encouraging in that maximum values of the sensitivity index occur at 30°. Thus the Koiter theory predicts that cylinders 3 and 4 should be most imperfection sensitive. This result is in agreement with the experimental data, if it is hypothesized that the more sensitive buckling of a structure is to geometric imperfections, the lower is its value of $\lambda_{exp}/\lambda_{cr}$. It was expected that the sensitivity index for wrap angles of 30° would be about the same as an isotropic cylinder so that $b/b_{iso} \approx 1$. The lower value of the normalized index shown in figure 18 is believed to be a consequence of the antisymmetry of the wall of the cylinder.

The experimentally obtained buckling loads for the test cylinders with helical wraps are compared with theoretical predictions for simply supported cylinders in figure 19 and table III. From figure 19, the only obvious trend in the data is the lack of reduction in values of $\lambda_{exp}/\lambda_{cr}$ as R/t is increased from 160 to 225. In isotropic cylinders, of course, some reduction would have been expected even in this relatively small change of R/t.

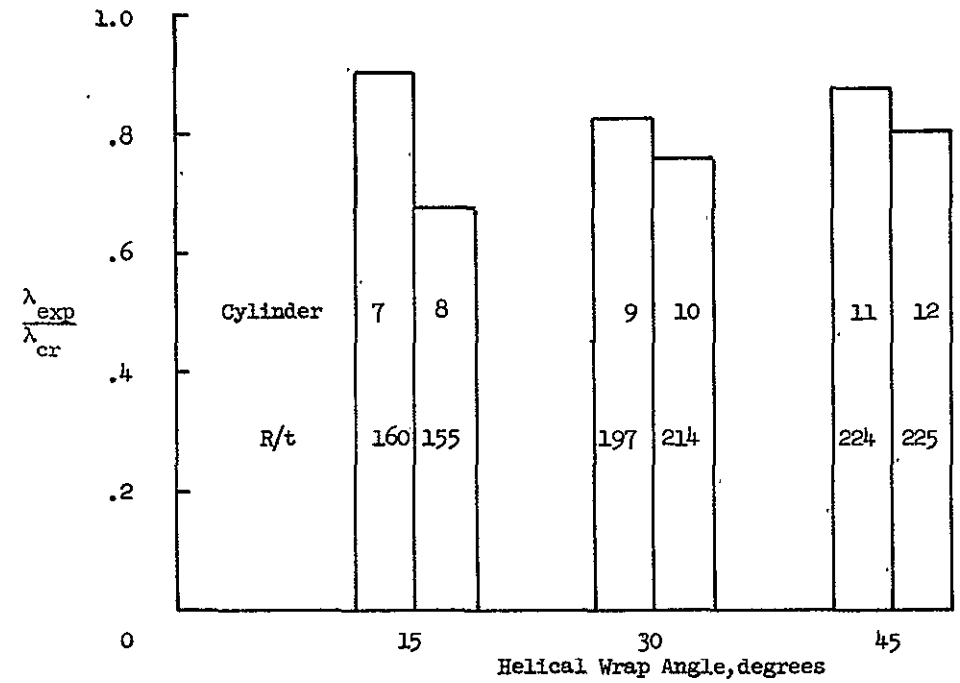

Figure 19.- Comparison of theoretical and experimental buckling loads for test cylinders with helical wraps.

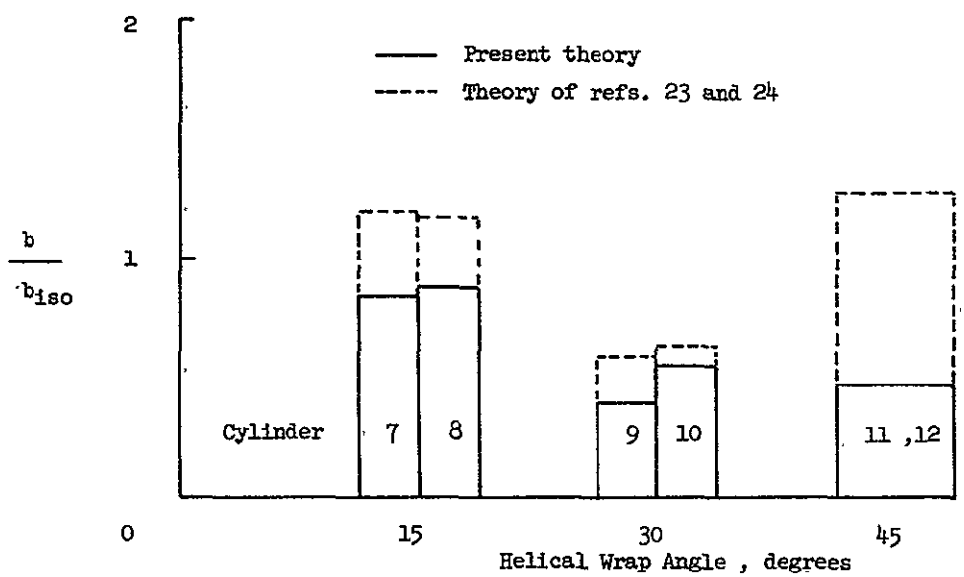

Figure 20.- Imperfection sensitivity indices for test cylinders with helical wraps.

For the 15° configuration, the data for cylinders 7 and 8 are inconsistent. From table III it can be seen that even though cylinder 7 was thinner than cylinder 8, it carried more load. Volume fractions and thicknesses were carefully reinvestigated, but no reasons were apparent to explain the discrepancies in the data.

Imperfection sensitivity indices for cylinders 7 to 12 are presented in figure 20. Agreement between the two theories presented is fair except for large disagreement for a helical wrap angle of 45°. This anamoly was unexpected, since the agreement for this wrap angle for glass-epoxy cylinders with $R/t = 100$ was much better (see fig. 4). In figure 20, variations in R/t make comparisons between wrap angles difficult. However, the trend of the indices for the present theory suggests that cylinders with wrap angles of 30° and 45° should perform better than isotropic cylinders of the same radius-thickness ratio. The high values of $\lambda_{exp}/\lambda_{cr}$ shown in figure 19, especially for the largest R/t (cylinders 11 and 12), tend to support this prediction. The sensitivity indices for cylinders with the lowest radius-thickness ratio suggest that their buckling behavior should be about the same as isotropic cylinders. The values of $\lambda_{exp}/\lambda_{cr}$ for cylinders 7 and 8, and the scatter in data seem to support this prediction also. Thus the trends in buckling data suggested by the sensivitity indices of the present theory are in fair agreement with experimental buckling data.

XI. CONCLUDING REMARKS

A theory has been developed to assess the sensitivity of buckling of axially compressed, fiber-reinforced cylindrical shells to small geometric imperfections in the shell wall. Following the work of Koiter (ref. 19), an index of imperfection sensitivity is obtained by investigating the character of the initial postbuckling region for a geometrically perfect cylindrical shell. The theory presented herein differs from existing applications of Koiter theory in that it is developed by using techniques of perturbation theory. The theory represents an extension to cylindrical shells of the plate postbuckling theory derived by Stein (ref. 25). Using Donnell-von Karman strain-displacement relations, the postbuckling equations are obtained for a multilayered, orthotropic cylinder in which the principal axes of orthotropy in each layer are alined with the longitudinal and circumferential coordinates of the shell. The imperfection sensitivity index is identified by suppressing secular terms in the perturbation and employing a suitable definition of the perturbation parameter. The governing equations were solved by finite difference techniques and by exploiting Gaussian elimination. A computer program to solve the large systems of simultaneous equations resulting was developed for the CDC 6600 series computer.

The results of an investigation of the imperfection sensitivity index for fiber-reinforced shells have been presented. Glass-epoxy, boron-epoxy, and boron-aluminum shells having various helical wrap angles were studied in order to identify wrapping configurations of minimum imperfection sensitivity. In conducting the investigation, both the

present theory and an extension of existing theory to multilayered, orthotropic shells were employed. Agreement between predicted sensitivity indices based on the two theories was reasonably good. Computed results for buckling in this investigation suggest that substantial differences (up to 27 percent) can exist between classical and consistent theory predictions for buckling, depending on the wrapping configuration. The differences are attributed to the neglect of load-induced prebuckling deformations in classical theory.

The studies of helically wrapped cylinders indicated that 45° was a desirable wrap angle in both glass-epoxy and boron-epoxy cylinders. For wraps with small imperfection sensitivity, boron-epoxy shells appeared to be more desirable than glass-epoxy shells. The most desirable shell configuration uncovered in the investigation was that of an aluminum shell overwrapped with a circumferentially wound boron-epoxy layer. This configuration was found to possess a positive postbuckling slope and appears to behave much like a ring-stiffened cylinder.

The results of an experimental program to investigate the buckling behavior of fiber-reinforced, glass-epoxy cylinders have been presented. Compressive buckling tests were conducted on twelve 30-inch-diameter filament-wound cylinders with various wrap angles. Elastic constants derived from data prior to buckling were compared with analytical predictions. The agreement between theory and experiment suggests that the approximations employed to estimate structural stiffnesses of the cylinder wall are valid. Cylinder buckling loads varied from 50 to 90 percent of consistent theory predictions, depending on wrap angle. Comparisons of calculated sensitivity indices with the cylinder buckling data show

that the indices are in fair agreement with the experimental data trends. Both the theoretical and experimental results reported herein demonstrate that certain fiber orientations can enhance the buckling strength of geometrically similar cylinders. These configurations appear to possess reduced sensitivity to geometric imperfections present in the cylinder wall prior to loading. The present results suggest the desirability of further experimental investigations into the buckling behavior of configurations such as the circumferentially wrapped boron-aluminum cylinder.

XII. ACKNOWLEDGMENTS

The author wishes to express his thanks to the National Aeronautics and Space Administration for permitting him to use its facilities to perform this research. He also wishes to thank Drs. Manuel Stein and Paul A. Cooper of NASA for their council and encouragement, and Dr. Daniel Frederick, Professor of Engineering Mechanics, Virginia Polytechnic Institute, for his continuing efforts to provide his students with a sound education in the fundamentals of Engineering Mechanics. Finally, he wishes to thank his wife, Jo-Ann, for without her patience, consideration, and cooperation, this research might never have been accomplished.

XIII. REFERENCES

1. Card, M. F.: Experiments to Determine Elastic Constants for Filament-Wound Cylinders. NASA TN D-3110, 1965.

2. Card, M. F.: Experiments to Determine the Compressive Strength of Filament-Wound Cylinders. NASA TN D-3522, 1966.

3. Davis, J. G., Jr.; and Zender, G. W.: Compressive Behaviour of Plates Fabricated From Glass Filaments and Epoxy Resin. NASA TN D-3918, 1967.

4. Herring, H. W.; Baucom, R. M.; and Pride, R. A.: Research on Boron Filaments and Boron Reinforced Composites. Paper presented at 1966 SAMPE Symposium on Composite Materials, San Diego, Nov. 9-11, 1966.

5. Dow, N.; and Rosen, B. W.: Evaluations of Filament-Reinforced Composites for Aerospace Structural Applications. NASA CR-207, 1965.

6. Horton, W. H.; and Durham, S. C.: Imperfections, A Main Contributor to Scatter in Experimental Values of Buckling Load. Int. J. Solids Structures, vol. 1, 1965, pp. 59-72.

7. Almroth, B. O.; Holmes, A. M. C.; and Brush, D. O.: An Experimental Study of the Buckling of Cylinders Under Axial Compression. Soc. for Experimental Stress Analysis, Paper No. 878, May 1964.

8. Tennyson, R. C.: An Experimental Investigation of the Buckling of Circular Cylindrical Shells in Axial Compression Using the Photoelastic Technique. University of Toronto, UTIAS Rept. No. 102, November 1964.

9. Card, M. F.; and Jones, R. M.: Experimental and Theoretical Results for Buckling of Eccentrically Stiffened Cylinders. NASA TN D-3639, 1966.

10. Thielemann, W. F.: New Developments in the Nonlinear Theories of the Buckling of Thin Cylindrical Shells. Aeroanutics and Astronautics, Proc. Durand Cent. Conf. Stanford Univ., 1959. Pergamon Press, 1960.

11. Almroth, B. O.: Postbuckling Behavior of Orthotropic Cylinders Under Axial Compression. AIAA J., vol. 2, no. 10, October 1964.

12. Shang, Jeng-Chong: Nonlinear Elastic Buckling of Imperfect Orthotropic Cylinders. Ph.D. Dissertation, Illinois Institute of Technology, 1967.

13. Khot, N. S.: On the Effects of Fiber Orientation and Nonhomogeneity on Buckling and Postbuckling Equilibrium Behavior of Fiber-Reinforced Cylindrical Shells Under Uniform Axial Compression. AFFDL-TR-68-19. Air Force Flight Dynamics Laboratory, May 1968.

14. Khot, N. S.: On the Influence of Initial Geometric Imperfections on the Buckling and Postbuckling Behavior of Fiber-Reinforced Cylindrical Shells Under Uniform Axial Compression. AFFDL-TR-68-136, Air Force Flight Dynamics Laboratory, October 1968.

15. Burns, A. B.; and Almroth, B. O.: Structural Optimization of Axially Compressed Ring-Stringer-Stiffened Cylinders. J. Spacecraft and Rockets, vol. 3, no. 1, January 1966.

16. Hutchinson, J. W.; and Amazigo, J. C.: Imperfection-Sensitivity of Eccentrically Stiffened Cylindrical Shells. AIAA J., vol. 5, no. 3, March 1967.

17. Hutchinson, J. W.; and Frauenthal, J. C.: Elastic Postbuckling Behavior of Stiffened and Barreled Cylindrical Shells. Harvard U. Rept. SM-27, August 1968.

18. (a) Brush, D. O.: Imperfection Sensitivity of Stringer-Stiffened Cylinders. AIAA J., vol. 6, no. 12, December 1968.

(b) Brush, D. O.: Initial Postbuckling Behavior of Stiffened Cylindrical Shells. Rept. 6-77-67-52, Lockheed Missiles and Space Co., November 1967.

19. Koiter, W. T.: On the Stability of Elastic Equilibrium. Thesis, Delft, H. J. Paris, Amsterdam, 1945.

20. Budiansky, B.; and Hutchinson, J. W.: Dynamic Buckling of Imperfection-Sensitive Structures. Proceedings of the XI International Congress of Applied Mechanics, Springer-Verlag, Berlin, 1964, pp. 636-651.

21. Budiansky, B.; and Hutchinson, J. W.: A Survey of Some Buckling Problems. AIAA J., vol. 4, no. 9, September 1966.

22. Budiansky, B.: Post-Buckling Behavior of Cylinders in Torsion. Harvard U. Rept. No. SM-17, 1967. IUTAM Symposium, Copenhagen, 1967. Theory of Thin Shells, F. L. Niordson, ed., Springer-Verlag, N. Y., 1969.

23. Cohen, G. A.: Effect of a Nonlinear Prebuckling State on the Post-Buckling Behavior and Imperfection Sensitivity of Elastic Structures. AIAA J., vol. 6, no. 8, August 1968.

24. Fitch, J. R.: The Buckling and Post-Buckling Behavior of Spherical Caps Under Concentrated Load. Int. J. Solids and Structures, vol. 4, no. 4, April 1968.

25. Stein, M.: Loads and Deformations of Buckled Rectangular Plates. NASA TR R-40, 1959.

26. Donnell, L. H.; and Wan, C. C.: Effect of Imperfections on Buckling of Thin Cylinders and Columns Under Axial Compression. J. Appl. Mech., vol. 17, no. 1, 1950.

27. Babcock, C. D.; and Sechler, E. E.: The Effect of Initial Imperfections on the Buckling Stress of Cylindrical Shells. Collected Papers on Instability of Shell Structures, NASA TN D-1510.

28. Dow, D. A.; and Peterson, J. P.: Test of a Large-Diameter Ring-Stiffened Cylinder Subjected to Hydrostatic Pressure. NASA TN D-3647, 1966.

29. Minorsky, N.: Introduction to Non-Linear Mechanics. J. W. Edwards, Ann Arbor, 1947.

30. Bogoliubov, N. M.; and Mitropolsky, Y. A.: Asymptotic Methods in the Theory of Non-Linear Oscillations. Hindustan Publ. Corp. (India). Distr. by Gordon and Breach Science Publishers, Inc., New York, 1961.

31. Ambartsumyan, S. A.: Theory of Anisotropic Shells. NASA TT F-118, 1964.

32. Tsai, S. W.: Structural Behavior of Composite Materials. NASA CR-75, 1964.

33. Hashin, Z.; and Rosen, B. W.: The Elastic Moduli of Fiber-Reinforced Materials. Trans. ASME, Ser. E: J. Appl. Mech., vol. 31, no. 2, June 1964, pp. 223-232.

34. Eckvall, J. C.: Structural Behavior of Monofilament Composites. Paper presented at AIAA Sixth Struct. and Matls. Conf., Palm Springs, Cal., April 5-7, 1965.

35. Greszczuk, L. B.: Elastic Constants and Analysis Methods for Filament Wound Shell Structures. Rept. No. SM-45849, Missile and Space Systems Div., Douglas Aircraft Co., Inc., January 1965.

36. Dietz, Albert G. H., ed.: Engineering Laminates. John Wiley and Sons, Inc., 1949.

37. Forest Products Laboratory: Stress-Strain Relations in Wood and Plywood Considered as Orthotropic Materials. Rept. No. 1503, U.S. Dept. of Agriculture, 1962.

38. Block, D. L.: Influence of Discrete Ring Stiffeners and Prebuckling Deformations on the Buckling of Eccentrically Stiffened Orthotropic Cylinders. NASA TN D-4283, 1968.

39. Budiansky, B.; and Radkowski, P. P.: Numerical Analysis of Unsymmetrical Bending of Shells of Revolution. AIAA J., vol. 1, no. 8, August 1963.

40. Blum, R. E.; and Fulton, R. E.: A Modification of Potters' Method for Solving Eigenvalue Problems Involving Tridiagonal Matrices. AIAA J., vol. 4, no. 12, December 1966.

41. Chang, L. K.; and Card, M. F.: Buckling of Thermally Stressed Stiffened Orthotropic Cylinders. (Proposed NASA TN.)

42. Potters, M. L.: A Matrix Method for the Solution of a Linear Second Order Difference Equation in Two Variables. MR 19, Math Centrum (Amsterdam), 1955. (Reviewed by J. M. Hedgepeth in Appl. Mech. Rev., vol. 9, no. 3, March 1956, p. 93.

43. Almroth, B. O.: Influence of Edge Conditions on the Stability of Axially Compressed Cylindrical Shells. NASA CR-161, February 1965.

44. Hutchinson, J. W.: Private Communication to R. W. Leonard, November 5, 1968.

45. Zender, G. W.; and Dexter, H. B.: Compressive Properties and Column Efficiency of Metals Reinforced on the Surface With Bonded Filaments. NASA TN D-4878, 1968.

XIV. VITA

Mr. Card graduated from Port Colborne High School, Ontario, Canada, in 1954. He attended Massachusetts Institute of Technology and received the degree of Bachelor of Science in Aeronautical Engineering. Since 1958, he has been employed as an Aerospace Engineer in the Structures Research Division of the National Aeronautics and Space Administration, Langley Research Center. He began graduate study at Virginia Polytechnic Institute in 1960 and received a Master of Science degree in Engineering Mechanics in 1964. He is the author or co-author of several NASA Technical Notes in the field of stability and strength of plate and shell structures. He has attended the Evening College of William and Mary and completed several courses in the liberal arts. He is a member of Sigma Xi, Phi Kappa Phi, and AIAA. He is married and has three children, David, Christopher, and Elisabeth.

Michael F Card

XV. APPENDIX A

In this section program SICK is described in detail. A flow diagram for the program is presented as figure 21. The input data required are as follows:

R	radius of cylindrical shell to reference surface
A	length of cylindrical shell
DELBAR	distance from inner surface of shell to reference surface (for the present calculations $t/2$)
BC	boundary condition code BC = 1 simple support ($N_{x_1} = v_1 = w_1 = M_{x_1} = 0$) BC = 3 clamped ($N_{x_1} = v_1 = w_1 = W_{1,x} = 0$)
NXB	applied axial compression load at buckling, λ_{cr}
N	number of full waves in circumferential buckle pattern, n
EX(I)	elastic modulus for shell layer in axial direction, E_x^i
EY(I)	elastic modulus for shell layer in circumferential direction, E_y^i
NUX(I)	Poisson's ratio of shell layer associated with load applied in axial direction, μ_x^i
NUY(I)	Poisson's ratio of shell layer associated with load applied in circumferential direction, μ_y^i
GXY(I)	shear modulus of shell layer, G_{xy}^i
H(I)	thickness of shell layer
LAYER	total number of layers in shell wall
ST	code to detect stiffening ST = 0 cylinder is unstiffened ST = 1 cylinder is stiffened
NSTAT	number of finite difference stations, N

NØRM	code to specify normalization	NØRM = 0 $\lvert\vec{Z}_1\rvert$ is normalizing factor NØRM = 1 W_{max}/t is normalizing factor

IPRINT code to specify type of output printed
IPRINT = 0 gives minimum output
IPRINT = 1 gives maximum output

If ST = 1 the following additional input is required:

ER modulus of ring

AR area of ring

IR moment of inertia of ring about its centroid

ZR distance from reference surface to ring centroid (+ only if ring is external)

GRJR torsional stiffness of ring

RS ring spacing

ES modulus of stringer

AS area of stringer

IS moment of inertia of stringer about its centroid

ZS distance from reference surface to stiffener centroid (+ only if stringer is external)

GSJS torsional stiffness of stringer

BS stringer spacing

Some conversions between the program notation and the notation of the paper which may not be self-evident are:

WOX $w^*_{0,x}$

WOXX $w^*_{0,xx}$

WOXL $w^*_{0,x\lambda}$

WOL $w^*_{0,\lambda}$

MØDRES modified residual resulting from taking determinant of left-hand side of buckling equations (see left-hand side of equation (62))

A listing of the program together with a sample case for the circumferentially overwrapped boron-aluminum cylinder follows.

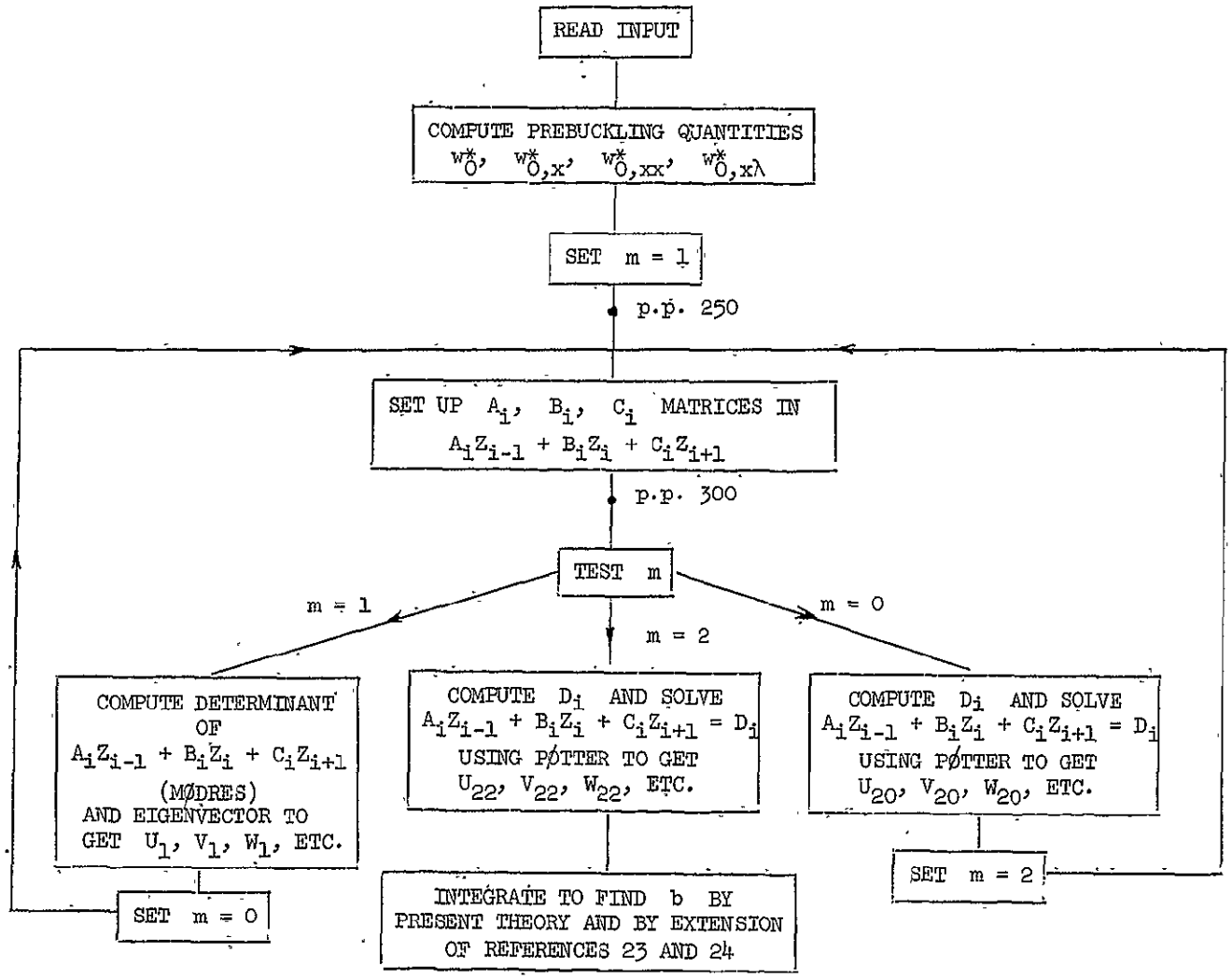

Figure 21.- Flow diagram for program SICK.

```
C     PROGRAM SICK (SENSITIVITY INDEX FOR CYLINDERS EX KOITER)
      PROGRAM SICK (INPUT,OUTPUT)
   10 FORMAT(///* IMPERFECTION SENSITIVITY OF AXIALLY COMPRESSED CYLINDE
     1R*/                                                              *
     1 CARD-SYKES  A2338  RDF367  OCTOBER,1968)
   11 FORMAT(//*  LAYER*,6X*EX*,9X*EY*,9X*NUX*,8X*NUY*,8X*GXY*,9X*H*)
   12 FORMAT(I5,3X,6E11.3)
   13 FORMAT(//13X*11*,17X*12*,17X*22*,17X*66*/)
   14 FORMAT(1X*B*,I3,E16.8,3(3XE16.8))
   15 FORMAT(1X*C*,4(3XE16.8))
   16 FORMAT(1X*D*,4(3XE16.8))
   17 FORMAT(1X*K*,4(3XE16.8))
   18 FORMAT(*1*,4X*STATION*,9X*WO*,17X*WOX*,17X*WOXX*,16X*WOXL*,
     116X*WOL*)
   19 FORMAT(I8,4E20.8)
   20 FORMAT(////* MODRES=*E16.8)
   21 FORMAT(//5X*W1 VALUES*/)
   22 FORMAT(I5,E20.8)
      DIMENSION WO( 61),WOX( 61),WOXX( 61),WOXL( 61),EX(20),EY(20),NUX(2
     10),NUY(20),GXY(20),H(20),B11(20),B12(20),B22(20),S(20),SS(20),SSS(
     220),B66(20), NYOL( 61), WOL( 61)
      DIMENSION AA( 61,4,4),B( 61,4,4),C( 61,4,4),AB(2,4,4),BB(2,4,4),
     1CB(2,4,4),DUMA(4,4),DUMB(4,4),DUMC(4,4),DUMAB(4,4),DUMBB(4,4),
     2DUMCB(4,4),B1(4,4),C1(4,4),AN(4,4),BN(4,4),P( 61,4,4),R1( 61,4,4),
     3PIM1(4,4),RI(4,4),PI(4,4),U1( 61),V1( 61),W1( 61),M1( 61),Z1( 61,4
     44),Z(4),PD(4,4), Z1SQ(1), ZD(4)
      DIMENSION X( 61),U1X( 61),V1X( 61),W1X( 61),W1XX( 61),WO2L( 61),
     1W13X( 61),WO3L( 61),NX1( 61),NY1( 61),NXY1( 61),D( 61,4),
     2SMAT( 61,4,4),DMAT( 61,4),PP( 61,4,4),QQ( 61,4),Z20( 61,4),
     3Z22( 61,4),U20( 61),V20( 61),W20( 61),M20( 61),U22( 61),V22( 61),
     4W22( 61),M22( 61),W20X( 61),U20X( 61),U22X( 61),V22X( 61),W22X( 61
     5),W20XX( 61),W22XX( 61),NX20( 61),NY20( 61),NX22( 61),NY22( 61),
     6NXY22( 61), DB(4), DUMD(4), W20XXX( 61), W22XXX( 61)
      DIMENSION DP3( 61,4),EP3( 61,4),DUMDE(244),Z1T(244),FOFX( 61),
     1XTE(1),XTD(1) ,Z1V(244), DPB3(2,4), EPB3(2,4)
      REAL M1,NYOL
      REAL IR,IS,NUX,NUY,K11,K12,K22,K66,NXB
      REAL NX1, NY1, NXY1, M20,   M22, NX20, NY20, NX22, NY22, NXY22
      INTEGER BC,ST
      REAL M, LAM11, LAM12, LAM13, LAM17, LAM21, LAM22, LAM23, LAM24,
     1        LAM32, LAM41, LAM42, LAM43, LAM45, LAM14, LAM15, LAM16,
     2        LAM25, LAM26, LAM31, LAM33, LAM34, LAM35, LAM36, LAM44,
```

```
    3         MODRES
      INTEGER SUBTRAC , TRANSPO
      NAMELIST/INPUT/R,A,DELBAR,BC,NXB,N,EX,EY,NUX,NUY,GXY,H,LAYER,ST,NS
     1TAT,NORM, IPRINT
      NAMELIST/STIFF/ER,AR,IR,ZR,GRJR,RS,ES,AS,IS,ZS,GSJS,BS
 1000 READ INPUT
      PRINT INPUT
      PRINT 10
      PRINT 11
      DO 50 L=1,LAYER
   50 PRINT 12, L, EX(L), EY(L), NUX(L), NUY(L), GXY(L), H(L)

CALCULATE B VALUES

      TEST3=0.
      DO 60 L=1,LAYER
      B11(L)=EX(L)/(1.-NUX(L)*NUY(L))
      B12(L)=NUY(L)*B11(L)
      B22(L)=EY(L)/(1.-NUX(L)*NUY(L))
   60 B66(L)=GXY(L)

CALCULATE C, K, AND D VALUES

      L=LAYER
      CALL SUM(1,L,B11,H,C11)
      CALL SUM(1,L,B12,H,C12)
      CALL SUM(1,L,B22,H,C22)
      CALL SUM(1,L,B66,H,C66)
      S(1)=H(1)
      S1=S(I)**2-2.*DELBAR*S(1)
      K11=.5*B11(1)*S1
      K12=.5*B12(1)*S1
      K22=.5*B22(1)*S1
      K66=.5*B66(1)*S1
      S2=S(1)**3-3.*DELBAR*S(1)**2+3.*DELBAR**2*S(1)
      D11=B11(1)*S2/3.
      D12=B12(1)*S2/3.
      D22=B22(1)*S2/3.
      D66=B66(1)*S2/3.
      IF(LAYER.EQ.1) GO TO 80
      DO 70 I=2,LAYER
      S(I)=S(I-1)+H(I)
      SS(I)=S(I)**2-S(I-1)**2-2.*DELBAR*(S(I)-S(I-1))
```

```
   70 SSS(I)=S(I)**3-S(I-1)**3-3.*DELBAR*(S(I)**2-S(I-1)**2)+3.*DELBAR**
     12*(S(I)-S(I-1))
      CALL SUM(2,L,B11,SS,ANS)
      K11=K11+.5*ANS
      CALL SUM(2,L,B12,SS,ANS)
      K12=K12+.5*ANS
      CALL SUM(2,L,B22,SS,ANS)
      K22=K22+.5*ANS
      CALL SUM(2,L,B66,SS,ANS)
      K66=K66+.5*ANS
      CALL SUM(2,L,B11,SSS,ANS)
      D11=D11+ANS/3.
      CALL SUM(2,L,B12,SSS,ANS)
      D12=D12+ANS/3.
      CALL SUM(2,L,B22,SSS,ANS)
      D22=D22+ANS/3.
      CALL SUM(2,L,B66,SSS,ANS)
      D66=D66+ANS/3.
   80 IF(ST-1)51,51,52
   52 READ STIFF
      PRINT STIFF
      D11=D11+ES*IS/BS+ES*AS*ZS**2/BS
      D22=D22+ER*IR/RS+ER*AR*ZR**2/RS
      K11=K11+ES*AS*ZS/BS
      K22=K22+ER*AR*ZR/RS
      C11=C11+ES*AS/BS
      C22=C22+ER*AR/RS
   51 PRINT 13
      DO 53 L=1,LAYER
   53 PRINT 14, L, B11(L), B12(L), B22(L), B66(L)
      PRINT 15, C11, C12, C22, C66
      PRINT 16, D11, D12, D22, D66
      PRINT 17, K11, K12, K22, K66
C     PREBUCKLING QUANTITIES
      RG1=(C11*C22-C12**2)/(D11*C11-K11**2)
      RG2=(K11*C12-K12*C11)/(D11*C11-K11**2)
      RG3=(R*C11)/(2.*D11*C11-2.*K11**2)
      RGB=(SQRT(RG1)-RG2-NXB*RG3)/(2.*R)
      RGG=(SQRT(RG1)+RG2+NXB*RG3)/(2.*R)
      BETA=SQRT(RGB)
      GAMA=SQRT(RGG)
      BETAL=-C11/(8.*BETA*(D11*C11-K11**2))
      GAMAL=C11/(8.*GAMA*(D11*C11-K11**2))
```

```
      P1=(R*C12)/(C11*C22-C12**2)
      SS=SINH(BETA*A/2.)*SIN(GAMA*A/2.)
      SC=SINH(BETA*A/2.)*COS(GAMA*A/2.)
      CC=COSH(BETA*A/2.)*COS(GAMA*A/2.)
      CS=COSH(BETA*A/2.)*SIN(GAMA*A/2.)
      SHCH=SINH(BETA*A/2.)*COSH(BETA*A/2.)
      SNCN=SIN(GAMA*A/2.)*COS(GAMA*A/2.)
      GO TO(1,2,2),BC
    1 G1=NXB*P1*(BETA**2-GAMA**2)-(K11*NXB)/(D11*C11-K11**2)
      G2=2.*NXB*P1*BETA*GAMA
      DBAR=D11*C11-K11**2
      G1L=P1*(BETA**2-GAMA**2+2.*NXB*(BETA*BETAL-GAMA*GAMAL))-K11/DBAR
      G2L=P1*(2.*NXB*(BETA*GAMAL+GAMA*BETAL)+2.*BETA*GAMA)
      G12=G1*CC-G2*SS
      G21=G1*SS+G2*CC
      G=2.*BETA*GAMA*(SS**2+CC**2)
      F1=G12/G
      F2=-G21/G
      PRINT 999, BETA, GAMA, F1, F2
  999 FORMAT(//* BETA=*E16.8,5X*GAMA=*E16.8,5X*F1=*E16.8,5X*F2=*E16.8)
      FOL=2.*G12*(BETA*GAMAL+GAMA*BETAL)*(SS**2+CC**2)/G**2+2.*G12*GAMA*
     1BETA*A*(BETAL*SHCH-GAMAL*SNCN)/G**2
      F1L=G1L*CC/G-G2L*SS/G+A*SC*(G1*BETAL-G2*GAMAL)/(2.*G)-A*CS*(G1*GAM
     1AL+G2*BETAL)/(2.*G)-FOL
      F2L=-G1L*SS/G-G2L*CC/G+A*CS*(G2*GAMAL-G1*BETAL)/(2.*G)-A*SC*(G1*GA
     1MAL+G2*BETAL)/(2.*G)+FOL*G21/G12
      GO TO 3
    2 G=BETA*SNCN+GAMA*SHCH
      F1=NXB*P1*(BETA*SC-GAMA*CS)/G
      F2=-NXB*P1*(BETA*CS+GAMA*SC)/G
      G12=F1*G
      G21=-F2*G
      FOL=NXB*P1*G12*(BETAL*SIN(GAMA*A)+A*BETA*GAMAL*COS(GAMA*A)+GAMAL*(
     1EXP(BETA*A)-EXP(-BETA*A))/2.+A*GAMA*BETAL*(EXP(BETA*A)+EXP(-BETA*A
     2))/2.)/(2.*G**2)
      F1L=P1*G12/G+NXB*P1*(BETAL*SC-GAMAL*CS)/G+A*NXB*P1*CC*(BETA*BETAL-
     1G
     1AMA*GAMAL)/(2.*G)-A*NXB*P1*SS*(BETA*GAMAL+GAMA*BETAL)/(2.*G)-FOL
      F2L=-P1*G21/G-NXB*P1*(BETAL*CS+GAMAL*SC)/G-A*NXB*P1*SS*(BETA*BETAL
     1-
     1GAMA*GAMAL)/(2.*G)-A*NXB*P1*CC*(BETA*GAMAL+GAMA*BETAL)/(2.*G)+FOL*
     2G21/G12
    3 PRINT 18
```

```
      DO 4 I=1,NSTAT
      J=I-1
      IF(I-1)5,5,6
    5 XB=-A/2.
      GO TO 7
    6 X=FLOAT(J)*A/FLOAT(NSTAT-1)
      XB=X-A/2.
    7 SXSX=SINH(BETA*XB)*SIN(GAMA*XB)
      CXCX=COSH(BETA*XB)*COS(GAMA*XB)
      SXCX=SINH(BETA*XB)*COS(GAMA*XB)
      CXSX=COSH(BETA*XB)*SIN(GAMA*XB)
      WO(I)=F1*SXSX+F2*CXCX+P1*NXB
      WOX(I)=(F1*BETA-F2*GAMA)*CXSX+(F1*GAMA+F2*BETA)*SXCX
      WOXX(I)=(F1*(BETA**2-GAMA**2)-2.*GAMA*BETA*F2)*SXSX+(2.*GAMA*BETA*
     1F1+(BETA**2-GAMA**2)*F2)*CXCX
      F1LL=F1L*(BETA*CXSX+GAMA*SXCX)+F2L*(BETA*SXCX-GAMA*CXSX)
      B1LL=BETAL*(F1*CXSX+F2*SXCX+XB*(F1*BETA-F2*GAMA)*SXSX+XB*(F1*GAMA+
     1F2*BETA)*CXCX)
      G1LL=GAMAL*(F1*SXCX-F2*CXSX+XB*(F1*BETA-F2*GAMA)*CXCX-XB*(F1*GAMA+
     1F2*BETA)*SXSX)
      WOXL(I)=F1LL+B1LL+G1LL
      WOL(I)=F1L*SXSX+F2L*CXCX+XB*(F1*BETAL-F2*GAMAL)*CXSX+XB*(F1*GAMAL
     1+F2*BETAL)*SXCX+P1
      IF(IPRINT.EQ.0) GO TO 4
      PRINT 502, I, WO(I), WOX(I), WOXX(I), WOXL(I), WOL(I)
    4 CONTINUE
      T=0.
      DO 55 L=1,LAYER
   55 T=H(L)+T
      M=1.
C     FORM L.H.S. OF EQUILIBRIUM EQUATIONS   A*Z(I-1)+B*Z(I)+C*Z(I+1)
  250 CONTINUE
      DEL=A/FLOAT(NSTAT-1)
      LAM11=C11-K11**2/D11
      LAM12=-C66*(M*N/R)**2
      LAM13=(C12+C66-K12*K11/D11)*M*N/R
      LAM17=K11/D11
      LAM21=-(C12+C66)*M*N/R
      LAM22=C66
      LAM23=-C22*(M*N/R)**2
      LAM24=(K12+2.*K66)*M*N/R
      LAM32=-2.*K66*M*N/R
      LAM41=-K11
```

```
      LAM42=-K12*M*N/R
      LAM43=D11
      LAM45=-(D12*(M*N/R)**2+K12/R)
      NEND=NSTAT+1
      IF(ST.NE.0)  GO TO 99
      GSJS=0.
      GRJR=0.
      BS=1.
      RS=1.
   99 DO 100 I=1,NSTAT
      LAM14=(C11-K11**2/D11)*WOX(I)
      LAM15=(C11-K11**2/D11)*WOXX(I)+(C12-K12*K11/D11)/R+(K12+2.*K66-K11
     1*D12/D11)*(M*N/R)**2
      LAM16=-C66*WOX(I)*(M*N/R)**2
      LAM25=-(C12+C66)*WOX(I)*M*N/R
      LAM26=-C66*WOXX(I)*M*N/R-C22*M*N/R**2-K22*(M*N/R)**3
      LAM31=C12/R+(K12+2.*K66)*(M*N/R)**2-C11*WOXX(I)
      LAM33=C22*M*N/R**2+K22*(M*N/R)**3-C12*WOXX(I)*M*N/R
      LAM34=NXB-K12/R-(4.*D66+GSJS/BS+GRJR/RS+D12)*(M*N/R)**2+K11*WOXX(I
     1)
      LAM35=(C12/R+(K12+2.*K66)*(M*N/R)**2)*WOX(I)-C11*WOX(I)*WOXX(I)
      LAM36=((C12*K11/C11+2.*(K66-K12))*(M*N/R)**2-C12/R)*WOXX(I)+1./R*(
     1C
     122-C12**2/C11)*(M*N/R)**2*WO(I)  +D22*(M*N/R)**4+2.*K22/R*(M*N/R)**
     22+C22/R**2-C12*(M*N/R)**2*NXB/C11
      LAM44=-K11*WOX(I)
      AA(I,1,1)=LAM11
      AA(I,1,2)=-DEL*LAM13/2.
      AA(I,1,3)=LAM14-DEL*LAM15/2.
      AA(I,1,4)=-DEL*LAM17/2.
      AA(I,2,1)=-DEL*LAM21/2.
      AA(I,2,2)=LAM22
      AA(I,2,3)=LAM24-DEL*LAM25/2.
      AA(I,2,4)=0.
      AA(I,3,1)=-DEL*LAM31/2.
      AA(I,3,2)=LAM32
      AA(I,3,3)=LAM34-DEL*LAM35/2.
      AA(I,3,4)=-1.
      AA(I,4,1)=-DEL*LAM41/2.
      AA(I,4,2)=0.
      AA(I,4,3)=LAM43-DEL*LAM44/2.
      AA(I,4,4)=0.
      B(I,1,1)=-2.*LAM11+DEL**2*LAM12
```

```
      B(I,1,2)=0.
      B(I,1,3)=-2.*LAM14+DEL**2*LAM16
      B(I,1,4)=0.
      B(I,2,1)=0.
      B(I,2,2)=-2.*LAM22+DEL**2*LAM23
      B(I,2,3)=-2.*LAM24+DEL**2*LAM26
      B(I,2,4)=0.
      B(I,3,1)=0.
      B(I,3,2)=-2.*LAM32+DEL**2*LAM33
      B(I,3,3)=-2.*LAM34+DEL**2*LAM36
      B(I,3,4)=2.
      B(I,4,1)=0.
      B(I,4,2)=LAM42*DEL**2
      B(I,4,3)=-2.*LAM43+DEL**2*LAM45
      B(I,4,4)=DEL**2
      C(I,1,1)=LAM11
      C(I,1,2)=DEL*LAM13/2.
      C(I,1,3)=LAM14+DEL*LAM15/2.
      C(I,1,4)=DEL*LAM17/2.
      C(I,2,1)=DEL*LAM21/2.
      C(I,2,2)=LAM22
      C(I,2,3)=LAM24+DEL*LAM25/2.
      C(I,2,4)=0.
      C(I,3,1)=DEL*LAM31/2.
      C(I,3,2)=LAM32
      C(I,3,3)=LAM34+DEL*LAM35/2.
      C(I,3,4)=-1.
      C(I,4,1)=DEL*LAM41/2.
      C(I,4,2)=0.
      C(I,4,3)=LAM43+DEL*LAM44/2.
  100 C(I,4,4)=0.
      GO TO(101,102,103),BC
  101 AB(1,1,1)=-C11*DEL/2.
      AB(1,1,2)=0.
      AB(1,1,3)=-K11-C11*DEL*WOX(1)/2.
      AB(1,1,4)=0.
      BB(1,1,1)=0.
      BB(1,1,2)=C12*M*N*DEL**2/R
      BB(1,1,3)=C12*DEL**2/R+2.*K11+K12*DEL**2*(M*N/R)**2
      BB(1,1,4)=0.
      BB(1,2,1)=0.
      BB(1,2,2)=1.0
      BB(1,2,3)=0.
```

```
      BB(1,2,4)=0.
      BB(1,3,1)=0.
      BB(1,3,2)=0.
      BB(1,3,3)=1.0
      BB(1,3,4)=0.
      BB(1,4,1)=0.
      BB(1,4,2)=0.
      BB(1,4,3)=0.
      BB(1,4,4)=1.0
      CB(1,1,1)=C11*DEL/2.
      CB(1,1,2)=0.
      CB(1,1,3)=-K11+C11*DEL*WOX(1)/2.
      CB(1,1,4)=0.
      DO 110 J=2,4
      DO 110 K=1,4
      AB(1,J,K)=0.
  110 CB(1,J,K)=0.
      DO 111 J=1,4
      DO 111 K=1,4
C  STATION 2 CORRESPONDS TO THE NSTAT BOUNDARY IN AB  BB  AND  CB
      AB(2,J,K)=AB(1,J,K)
      BB(2,J,K)=BB(1,J,K)
      CB(2,J,K)=CB(1,J,K)
      AB(2,1,3)=-K11-C11*DEL*WOX(NSTAT)/2.
  111 CB(2,1,3)=-K11+C11*DEL*WOX(NSTAT)/2.
      IF(M.GT.0.)GO TO 105
      DO 510 J=1,4
      AB(2,1,J)=0.
      BB(2,1,J)=0.
  510 CB(2,1,J)=0.
      BB(2,1,1)=1.
      GO TO 105
  102 DO 112 J=1,4
      DO 112 K=1,4
      AB(1,J,K)=0.
      BB(1,J,K)=0.
      CB(1,J,K)=0.
      AB(2     ,J,K)=0.
      BB(2     ,J,K)=0.
  112 CB(2     ,J,K)=0.
      AB(1,4,3)=-DEL/2.
      AB(2,4,3)=-DEL/2.
      BB(1,1,1)=1.
```

```
      BB(1,2,2)=1.
      BB(1,3,3)=1.
      BB(2     ,1,1)=1.
      BB(2     ,2,2)=1.
      BB(2     ,3,3)=1.
      CB(1,4,3)=DEL/2.
      CB(2,4,3)=DEL/2.
      GO TO 105
  103 DO 113 J=1,4
      DO 113 K=1,4
      AB(1,J,K)=0.
      BB(1,J,K)=0.
      CB(1,J,K)=0.
      AB(2     ,J,K)=0.
      BB(2     ,J,K)=0.
  113 CB(2     ,J,K)=0.
      AB(1,1,1)=-C11*DEL/2.
      AB(1,1,3)=-K11-C11*DEL*WOX(1)/2.
      BB(1,1,2)=C12*M*N*DEL**2/R
      BB(1,1,3)=C12*DEL**2/R+2.*K11+K12*DEL**2*(M*N/R)**2
      CB(1,1,1)=C11*DEL/2.
      CB(1,1,3)=-K11+C11*DEL*WOX(1)/2.
      AB(1,4,3)=-DEL/2.
      AB(2,1,1)=AB(1,1,1)
      AB(2,1,3)=-K11-C11*DEL*WOX(NSTAT)/2.
      BB(2,1,2)=BB(1,1,2)
      BB(2,1,3)=BB(1,1,3)
      CB(2,1,1)=CB(1,1,1)
      CB(2,1,3)=-K11+C11*DEL*WOX(NSTAT)/2.
      AB(2,4,3)=-DEL/2.
      BB(1,2,2)=1.
      BB(1,3,3)=1.
      BB(2     ,2,2)=1.
      BB(2     ,3,3)=1.
      CB(1,4,3)=DEL/2.
      CB(2,4,3)=DEL/2.
      IF(M.GT.0.)GO TO 105
      DO 511 J=1,4
      AB(2,1,J)=0.
      BB(2,1,J)=0.
  511 CB(2,1,J)=0.
      BB(2,1,1)=1.
      GO TO 105
```

```
C       FORM B1,C1,AN,BN AT BOUNDARIES
  105   DO 120 J=1,4
        DO 120 K=1,4
        DUMA(J,K)=AA(1,J,K)
        DUMB(J,K)=B(1,J,K)
        DUMC(J,K)=C(1,J,K)
        DUMAB(J,K)=AB(1,J,K)
        DUMBB(J,K)=BB(1,J,K)
  120   DUMCB(J,K)=CB(1,J,K)
        INVERT=10
        MULTIPL =20
        SUBTRAC =22
        CALL MATRIX(INVERT,4,4,0,DUMA,4,DETERM1)
C             -1
C       DUMA=A1
        CALL MATRIX(MULTIPL ,4,4,4,DUMAB,4,DUMA,4,DUMA,4)
C                   -1
C       DUMA=AB1 * A1
        CALL MATRIX(MULTIPL ,4,4,4,DUMA,4,DUMB,4,DUMB,4)
C                   -1
C       DUMB=AB1 * A1 * B1
        CALL MATRIX(SUBTRAC,4,4,0,DUMBB,4,DUMB,4,B1,4)
C                   -1
C       B1=BB1-AB1*A1 *B1
        CALL MATRIX(MULTIPL ,4,4,4,DUMA,4,DUMC,4,DUMC,4)
C                  -1
C       DUMC=AB1*A1 *C1
        CALL MATRIX(SUBTRAC ,4,4,0,DUMCB,4,DUMC,4,C1,4)
C                   -1
C       C1=CB1-AB1*A1 *C1
        DO 121 J=1,4
        DO 121 K=1,4
        DUMA(J,K)=AA(NSTAT,J,K)
        DUMB(J,K)=B(NSTAT,J,K)
        DUMC(J,K)=C(NSTAT,J,K)
        DUMAB(J,K)=AB(2    ,J,K)
        DUMBB(J,K)=BB(2    ,J,K)
  121   DUMCB(J,K)=CB(2    ,J,K)
        CALL MATRIX(INVERT,4,4,0,DUMC,4,DETERM1)
        CALL MATRIX(MULTIPL ,4,4,4,DUMCB,4,DUMC,4,DUMC,4)
        CALL MATRIX(MULTIPL ,4,4,4,DUMC,4,DUMA,4,DUMA,4)
        CALL MATRIX(SUBTRAC,4,4,0,DUMAB,4,DUMA,4,AN,4)
C                   -1
```

```
C       AN=ABN-CBN*CN **AN
        CALL MATRIX(MULTIPL ,4,4,4,DUMC,4,DUMB,4,DUMB,4)
        CALL MATRIX(SUBTRAC,4,4,0,DUMBB,4,DUMB,4,BN,4)
C                    -1
C       BN=BBN-CBN*CN **BN
        DO 122 J=1,4
        DO 122 K=1,4
        B(1,J,K)=B1(J,K)
        C(1,J,K)=C1(J,K)
        AA(NSTAT,J,K)=AN(J,K)
  122   B(NSTAT,J,K)=BN(J,K)
C       TEST M AND ROUTE TO 1ST OR 2ND PERTURBATION EQUATIONS
  300   MT=IFIX(M)
        IF (MT-1)210,211,212
  211   CONTINUE
        IF (TEST3.GT.0.)GO TO 407
C       TRIANGULATION OF A B AND C MATRICES FOR BUCKLING EQUATIONS
C       FIRST PERTURBATION
        CALL MATRIX(INVERT,4,4,0,B1,4,MODRES)
C       B1=(B1)INV
C       MODRES=DET(B1)
        CALL MATRIX(MULTIPL ,4,4,4,B1,4,C1,4,PIM1,4)
C                 -1
C       P(I-1)=B1*C1
        DO 130 J=1,4
        DO 130 K=1,4
        P(1,J,K)=PIM1(J,K)
  130   R1(1,J,K)=B(1,J,K)
        SCALE=ABS(MODRES)
        MODRES=MODRES/SCALE
        DO 135 I=2,NSTAT
        DO 136 J=1,4
        DO 136 K=1,4
        PIM1(J,K)=P(I-1,J,K)
        DUMA(J,K)=AA(I,J,K)
        DUMB(J,K)=B(I,J,K)
  136   DUMC(J,K)=C(I,J,K)
        CALL MATRIX(MULTIPL ,4,4,4,DUMA,4,PIM1,4,DUMA,4)
        CALL MATRIX(SUBTRAC ,4,4,0,DUMB,4,DUMA,4,RI,4)
C       R(I)=B-A*P(I-1)
        DO 137 J=1,4
        DO 137 K=1,4
  137   R1(I,J,K)=RI(J,K)
```

```
      CALL MATRIX(INVERT,4,4,0,RI,4,DETRI)
      CALL MATRIX(MULTIPL ,4,4,4,RI,4,DUMC,4,PI,4)
      DO 138 J=1,4
      DO 138 K=1,4
  138 P(I,J,K)=PI(J,K)
      SCALE=ABS(DETRI)
      IF(I.EQ.NSTAT)  SCALE=1.
      DETRI=DETRI/SCALE
  135 MODRES=MODRES*DETRI
      PRINT 20, MODRES
C     EIGENVECTOR CALCULATION
      DO 160 J=1,4
      DO 160 K=1,4
  160 DUMA(J,K)=R1(NSTAT,J,K)
      U1(NSTAT)=DUMA(1,2)*DUMA(2,3)*DUMA(4,4)+DUMA(1,3)*DUMA(2,4)*DUM
     1,2)+DUMA(1,4)*DUMA(2,2)*DUMA(4,3)-DUMA(4,2)*DUMA(2,3)*DUMA(1,4)
     2MA(4,3)*DUMA(2,4)*DUMA(1,2)-DUMA(4,4)*DUMA(2,2)*DUMA(1,3)
      V1(NSTAT)=DUMA(4,1)*DUMA(2,3)*DUMA(1,4)+DUMA(4,3)*DUMA(2,4)*DUM
     1,1)+DUMA(4,4)*DUMA(2,1)*DUMA(1,3)-DUMA(1,1)*DUMA(2,3)*DUMA(4,4)
     2MA(1,3)*DUMA(2,4)*DUMA(4,1)-DUMA(1,4)*DUMA(2,1)*DUMA(4,3)
      W1(NSTAT)=DUMA(1,1)*DUMA(2,2)*DUMA(4,4)+DUMA(1,2)*DUMA(2,4)*DUM
     1,1)+DUMA(1,4)*DUMA(2,1)*DUMA(4,2)-DUMA(4,1)*DUMA(2,2)*DUMA(1,4)
     2MA(4,2)*DUMA(2,4)*DUMA(1,1)-DUMA(4,4)*DUMA(2,1)*DUMA(1,2)
      M1(NSTAT)=DUMA(4,1)*DUMA(2,2)*DUMA(1,3)+DUMA(4,2)*DUMA(2,3)*DUM
     1,1)+DUMA(4,3)*DUMA(2,1)*DUMA(1,2)-DUMA(1,1)*DUMA(2,2)*DUMA(4,3)
     2MA(1,2)*DUMA(2,3)*DUMA(4,1)-DUMA(1,3)*DUMA(2,1)*DUMA(4,2)
      Z1(NSTAT,1)=U1(NSTAT)
      Z1(NSTAT,2)=V1(NSTAT)
      Z1(NSTAT,3)=W1(NSTAT)
      Z1(NSTAT,4)=M1(NSTAT)
      WMAX=W1(NSTAT)
      NS1=NSTAT-1
      DO 170 II=1,NS1
      I=NSTAT-II
      DO 171 J=1,4
      DO 171 K=1,4
      PD(J,K)=-P(I,J,K)
  171 Z(K)=Z1(I+1,K)
      CALL MATRIX(MULTIPL ,4,4,1,PD,4,Z,4,ZD,4)
      DO 172 K=1,4
  172 Z1(I,K)=ZD(K)
C     Z1(I)=-P(I)*ZI(I+1)
      U1(I)=Z1(I,1)
```

```
      V1(I)=Z1(I,2)
      W1(I)=Z1(I,3)
      IF(ABS(W1(I)).GT.WMAX)  WMAX=ABS(W1(I))
  170 M1(I)=Z1(I,4)
      PRINT 23
   23 FORMAT(*1*,4X*STATION*,9X*U1*,17X*V1*,17X*W1*)
      DO 173 I=1,NSTAT
      W1(I)=W1(I)/WMAX
   24 FORMAT(I8,3E20.8)
  173 PRINT 24,I, U1(I),V1(I),W1(I)
C     NORMALIZE Z VECTOR BY ITS MAGNITUDE
      PRINT 30
   30 FORMAT(///4X*STATION*,9X*U1*,17X*V1*,17X*W1*,17X*M1*)
      ZMAG2=0.
      DO 180 I=1,NSTAT
      W1(I)=WMAX*W1(I)
  180 ZMAG2=U1(I)**2+V1(I)**2+W1(I)**2+M1(I)**2+ZMAG2
      ZNORM=SQRT(ZMAG2)
      IF(NORM.GT.0) ZNORM=WMAX/T
      DO 181 I=1,NSTAT
      U1(I)=U1(I)/ZNORM
      V1(I)=V1(I)/ZNORM
      W1(I)=W1(I)/ZNORM
      M1(I)=M1(I)/ZNORM
      Z1(I,1)=U1(I)
      Z1(I,2)=V1(I)
      Z1(I,3)=W1(I)
      Z1(I,4)=M1(I)
      IF(IPRINT.EQ.0) GO TO 181
      PRINT 31, I, U1(I), V1(I), W1(I), M1(I)
   31 FORMAT(I8,4E20.8)
  181 CONTINUE
C     CALCULATE W1X,W1XX,W1XXX,WOXXL,WOXXXL
      DEL=A/FLOAT(NSTAT-1)
      X(1)=0
      DO 200 I=2,NSTAT
  200 X(I)=X(I-1)+DEL
      PRINT 921
  921 FORMAT(////4X*STATION*,9X*W1X*,17X*U1X*,17X*V1X*,16X*W1XX*)
      DO 201 I=1,NSTAT
      W1X(I)=DIF(I,1,NSTAT,X,W1)
      U1X(I)=DIF(I,1,NSTAT,X,U1)
      V1X(I)=DIF(I,1,NSTAT,X,V1)
```

```
      W1XX(I)=K11*(U1X(I)+WOX(I)*W1X(I))/D11+K12*(N*V1(I)/R+W1(I)/R)/
     1+D12*(N/R)**2*W1(I)/D11-M1(I)/D11
      WO2L(I)=DIF(I,1,NSTAT,X,WOXL)
      NYOL(I)=(C12*K11/C11-K12)*WO2L (I)+(C22-C12**2/C11)*WOL(I)/R-C1
     1C11
      IF(IPRINT.EQ.0) GO TO 201
      PRINT 922, I, W1X(I), U1X(I), V1X(I), W1XX(I)
  922 FORMAT(I8,4E20.8)
  201 CONTINUE
      PRINT 923
  923 FORMAT(////4X*STATION*,9X*NX1*,17X*NY1*,17X*NXY1*,17X*NYOL*)
      DO 202 I=1,NSTAT
      W13X(I)=DIF(I,1,NSTAT,X,W1XX)
      WO3L(I)=DIF(I,1,NSTAT,X,WO2L)
C     CALCULATE NX1,NY1,NXY1
      EPSX=U1X(I)+WOX(I)*W1X(I)
      EPSY=N*V1(I)/R+W1(I)/R
      EPSXY=-N*U1(I)/R+V1X(I)-WOX(I)*N*W1(I)/R
      NX1(I)=C11*EPSX+C12*EPSY-K11*W1XX(I)+(N/R)**2*W1(I)*K12
      NY1(I)=C12*EPSX+C22*EPSY-K12*W1XX(I)+(N/R)**2*W1(I)*K22
      NXY1(I)=C66*EPSXY+2.*K66*N*W1X(I)/R
      IF(IPRINT.EQ.0) GO TO 202
      PRINT 924, I, NX1(I), NY1(I), NXY1(I) ,NYOL(I)
  924 FORMAT(I8,4E20.8)
  202 CONTINUE
      M=0.
      GO TO 250
  210 CONTINUE
C     SECOND PERTURBATION TO OBTAIN U20,V20,W20
  225 DO 226 I=1,NSTAT
      D(I,1)=-C11*W1X(I)*W1XX(I)*DEL**2/2.-(DEL*N/R)**2*C12*W1(I)*W1X
     1/2.
      D(I,2)=0.
      DL2=DEL**2
      E1=DL2*K11*(W1XX(I)**2 +W1X(I)*W13X(I))/2.
      E2=DL2 *(N/R)**2*(K12/2.)*W1(I)*W1XX(I)
      E3=DL2*(K12*(N/R)**2/2.+(C11*WOXX(I)-C12/R)/4.)*W1X(I)**2
      E4=DL2*(N/R)**2/4.*(C12*WOXX(I)-C22/R)*W1(I)**2
      E5=DL2*NX1(I)*W1XX(I)/2.-N/R*NXY1(I)*W1X(I)*DL2-(N/R)**2*DL2/2.
     11(I)*W1(I)
      D(I,3)=E1+E2+E3+E4+E5
  226 D(I,4)=0.
      GO TO (220, 221, 221),BC
```

```
C     FORM D1 AND DN AT BOUNDARIES
  220 DB(1)=-DEL**2*C11*W1X(1)**2/4.
      DB(2)=0.
      DB(3)=0.
      DB(4)=-DEL**2*K11*W1X(1)**2/4.
      DO 700 J=1,4
      DO 700 K=1,4
      DUMA(J,K)=AA(1,J,K)
      DUMC(J,K)=C(NSTAT,J,K)
      DUMAB(J,K)=AB(1,J,K)
  700 DUMCB(J,K)=CB(2,J,K)
      CALL MATRIX(INVERT,4,4,0,DUMA,4,DETERMI)
      CALL MATRIX(INVERT,4,4,0,DUMC,4,DETERMI)
      CALL MATRIX(MULTIPL,4,4,4,DUMAB,4,DUMA,4,DUMA,4)
      CALL MATRIX(MULTIPL,4,4,4,DUMCB,4,DUMC,4,DUMC,4)
      DO 701 J=1,4
  701 DUMD(J)=D(1,J)
      CALL MATRIX(MULTIPL,4,4,1,DUMA,4,DUMD,4,DUMD,4)
      CALL MATRIX(SUBTRAC,4,1,0,DB,4,DUMD,4,DUMD,4)
      DO 702 J=1,4
  702 D(1,J)=DUMD(J)
      DB(1)=0.
      DB(2)=0.
      DB(3)=0.
      DB(4)=-DEL**2*K11*W1X(NSTAT)**2/4.
      DO 703 J=1,4
  703 DUMD(J)=D(NSTAT,J)
      CALL MATRIX(MULTIPL,4,4,1,DUMC,4,DUMD,4,DUMD,4)
      CALL MATRIX(SUBTRAC,4,1,0,DB,4,DUMD,4,DUMD,4)
      DO 704 J=1,4
  704 D(NSTAT,J)=DUMD(J)
      GO TO 227
  221 DO 223 J=1,4
      D(1,J)=0.
  223 D(NSTAT,J)=0.
C     CALCULATE Z20 BY GAUSSIAN ELIMINATION
  227 CALL POTTER (AA,B,C,D,NSTAT,4,SMAT,DMAT,PP,QQ,Z20, E1,4)
      M=2.
      GO TO 250
  212 DL2=DEL**2
C     SECOND PERTURBATION TO OBTAIN U22,V22,W22
  235 DO 236 I=1,NSTAT
      D(I,1)=-DL2*C11*W1X(I)*W1XX(I)/2.+DL2*(N/R)**2*(C12/2.+C66)*W1(
```

```
   1W1X(I)
    E1=DL2*N/(2.*R)*(C12+C66)*W1X(I)**2
    E2=-DL2/2.*(N/R)**3*C22*W1(I)**2
    E3=DL2*N/(2.*R)*C66*(W1XX(I)*W1(I))
    D(I,2)=E1+E2+E3
    E4=K11/2.*(W1XX(I)**2+W1X(I)*W13X(I))
    E5=(N/R)**2*(K12/2.+2.*K66)*W1(I)*W1XX(I)
    E6=((C11*WOXX(I)-C12/R)/4.-(N/R)**2*(3.*K12/2.+2.*K66))*W1X(I)*
    E7=((N/R)**4*K22+(N/R)**2/4.*(C22/R-C12*WOXX(I)))*W1(I)**2
    E8=NX1(I)*W1XX(I)/2.+N/R*NXY1(I)*W1X(I)-(N/R)**2/2.*NY1(I)*W1(I
    D(I,3)=DL2*(E4-E5+E6+E7+E8)
236 D(I,4)=0.
    GO TO (230,231,231),BC
230 DB(1)=-DEL**2*C11*W1X(1)**2/4.
    DB(2)=0.
    DB(3)=0.
    DB(4)=-DEL**2*K11*W1X(1)**2/4.
    DO 800 J=1,4
    DO 800 K=1,4
    DUMA(J,K)=AA(1,J,K)
    DUMC(J,K)=C(NSTAT,J,K)
    DUMAB(J,K)=AB(1,J,K)
800 DUMCB(J,K)=CB(2,J,K)
    CALL MATRIX(INVERT,4,4,0,DUMA,4,DETERMI)
    CALL MATRIX(INVERT,4,4,0,DUMC,4,DETERMI)
    CALL MATRIX(MULTIPL,4,4,4,DUMAB,4,DUMA,4,DUMA,4)
    CALL MATRIX(MULTIPL,4,4,4,DUMCB,4,DUMC,4,DUMC,4)
    DO 801 J=1,4
801 DUMD(J)=D(1,J)
    CALL MATRIX(MULTIPL,4,4,1,DUMA,4,DUMD,4,DUMD,4)
    CALL MATRIX(SUBTRAC,4,1,0,DB,4,DUMD,4,DUMD,4)
    DO 802 J=1,4
802 D(1,J)=DUMD(J)
    DB(1)=-DEL**2*C11*W1X(NSTAT)**2/4.
    DB(2)=0.
    DB(3)=0.
    DB(4)=-DEL**2*K11*W1X(NSTAT)**2/4.
    DO 803 J=1,4
803 DUMD(J)=D(NSTAT,J)
    CALL MATRIX(MULTIPL,4,4,1,DUMC,4,DUMD,4,DUMD,4)
    CALL MATRIX(SUBTRAC,4,1,0,DB,4,DUMD,4,DUMD,4)
    DO 804 J=1,4
804 D(NSTAT,J)=DUMD(J)
```

```
      GO TO 237
  231 DO 232 J=1,4
      D(1,J)=0.
  232 D(NSTAT,J)=0.
C     CALCULATE Z22 BY GAUSSIAN ELIMINATION
  237 CALL POTTER (AA,B,C,D,NSTAT,4,SMAT,DMAT,PP,QQ,Z22, 61,4)
C     CALCULATE W20X,W20XX,W20XXX,W22X,W22XX,W22XXX
      PRINT 25
   25 FORMAT(//*1*,4X*STATION*9X*U20*,17X*V20*,17X*W20*,17X*M20*)
      DO 249 I=1,NSTAT
      U20(I)=Z20(I,1)
      V20(I)=Z20(I,2)
      W20(I)=Z20(I,3)
      M20(I)=Z20(I,4)
      IF(IPRINT.EQ.0) GO TO 249
      PRINT 31,I, U20(I), V20(I), W20(I), M20(I)
  249 CONTINUE
      PRINT 26
   26 FORMAT(//*1*,4X*STATION*,9X*U22*,17X*V22*,17X*W22*,17X*M22*)
      DO 899 I=1,NSTAT
      U22(I)=Z22(I,1)
      V22(I)=Z22(I,2)
      W22(I)=Z22(I,3)
      M22(I)=Z22(I,4)
      IF(IPRINT.EQ.0) GO TO 899
      PRINT 31,I, U22(I), V22(I), W22(I), M22(I)
  899 CONTINUE
      PRINT 500
  500 FORMAT(////4X*STATION*,9X*W20X*,17X*W22X*,17X*W20XX*,17X*W22XX*
      DO 251 I=1,NSTAT
      W20X(I)=DIF(I,1,NSTAT,X,W20)
      U20X(I)=DIF(I,1,NSTAT,X,U20)
      W22X(I)=DIF(I,1,NSTAT,X,W22)
      U22X(I)=DIF(I,1,NSTAT,X,U22)
      V22X(I)=DIF(I,1,NSTAT,X,V22)
      W20XX(I)=K11*(U20X(I)+WOX(I)*W20X(I))/D11+K12*W20(I)/(R*D11)-M2
     1)/D11
      W22XX(I)=K11*(U22X(I)+WOX(I)*W22X(I))/D11+K12*(2.*N*V22(I)/R+W2
     1)/R)/D11+D12*(2.*N/R)**2*W22(I)/D11-M22(I)/D11
      IF(IPRINT.EQ.0) GO TO 251
      PRINT 924, I, W20X(I), W22X(I), W20XX(I), W22XX(I)
  251 CONTINUE
C     CALCULATE NX20,NY20,NX22,NY22,NXY22
```

```
      PRINT 501
  501 FORMAT(////4X*STATION*,9X*NX20*,15X*NY20*,15X*NX22*,15X*NY22*,
     115X*NXY22*)
      DO 302 I=1,NSTAT
      W20XXX(I)=DIF(I,1,NSTAT,X,W20XX)
      W22XXX(I)=DIF(I,1,NSTAT,X,W22XX)
      EPSX=U20X(I)+WOX(I)*W20X(I)
      EPSY=W20(I)/R
      NX20(I)=C11*EPSX+C12*EPSY-K11*W20XX(I)
      NY20(I)=C12*EPSX+C22*EPSY-K12*W20XX(I)
      EPSX=U22X(I)+WOX(I)*W22X(I)
      EPSY=2.*N*V22(I)/R+W22(I)/R
      EPSXY=-2.*N*U22(I)/R+V22X(I)-WOX(I)*2.*N*W22(I)/R
      NX22(I)=C11*EPSX+C12*EPSY-K11*W22XX(I)+(2.*N/R)**2*W22(I)*K12
      NY22(I)=C12*EPSX+C22*EPSY-K12*W22XX(I)+(2.*N/R)**2*W22(I)*K22
      NXY22(I)=C66*EPSXY+2.*K66*2.*N*W22X(I)/R
      IF(IPRINT.EQ.0) GO TO 302
      PRINT 502, I, NX20(I), NY20(I),NX22(I),NY22(I),NXY22(I)
  502 FORMAT(I8,5E20.8)
  302 CONTINUE
C     CALCULATION OF SENSITIVITY INDEX BY PRESENT THEORY
      DO 400 I=1,NSTAT
      DP3(I,1)=-C11*(W1XX(I)*WOXL(I)+W1X(I)*WO2L(I))+(N/R)**2*WOXL(I)
     1W1(I)*C66
      DP3(I,2)=N/R*C66*WO2L(I)*W1(I)+N/R*(C66+C12)*WOXL(I)*W1X(I)
      DP3(I,3)=-W1XX(I)+NX1(I)*WO2L(I)-(N/R)**2*NYOL(I)*W1(I)
     1+C11*WOXX(I)*WOXL(I)*W1X(I)-C12/R*WOXL(I)*W1X(I)
     2+K11*(WOXL(I)*W13X(I)+2.*WO2L(I)*W1XX(I)+WO3L(I)*W1X(I))
     3-2.*(N/R)**2*K66*WO2L(I)*W1(I)-(N/R)**2*(2.*K66+K12)*WOXL(I)
     4*W1X(I)
      DP3(I,4)=0.
      EP3(I,1)=-C11*(W1XX(I)*(W20X(I)+.5*W22X(I))+W1X(I)*(W20XX(I)+.5
     1W22XX(I)))+(N/R)**2*C12*(W1X(I)*W22(I)+W1(I)*W22X(I))
     2+(N/R)**2*C66*(3.*W1X(I)*W22(I)+1.5*W1(I)*W22X(I)+W1(I)*W20X(I)
      EP3(I,2)= N/R*(C12+C66)*(W1X(I)*(W20X(I)+.5*W22X(I)))
     1+N/R*C66*(W1XX(I)*W22(I)+W1(I)*(W20XX(I)-.5*W22XX(I)))
     2+(N/R)**3*C22*W1(I)*W22(I)
      AK1= K11*(W13X (I)*(W20X(I)+.5*W22X(I))+W1XX(I)*(2.*W20XX(I)
     1+W22XX(I))+W1X(I)*(W20XXX(I)+.5*W22XXX(I)))
      AK2=-(N/R)**2*K12*(W1XX(I)*W22(I)+W1X(I)*(W20X(I)+13./2.*W22X(I
     1+W1(I)*W22XX(I))+9.*(N/R)**3*K22*W1(I)*W22(I)
      AK3=-(N/R)**2*K66*(6.*W1XX(I)*W22(I)+W1X(I)*(2.*W20X(I)+9.*W22X
     1)
```

```
   2+W1(I)*(2.*W20XX(I)+3.*W22XX(I)))
    AK4= W0XX(I)*(C11*W1X(I)*(W20X(I)+.5*W22X(I))
   1-(N/R)**2*C12*W1(I)*W22(I))
    AK5=1./R*(C22*(N/R)**2*W1(I)*W22(I)-C12*W1X(I)*(W20X(I)+.5*W22X
   2))
    AK6= W1XX(I)*(3./8.*C11*W1X(I)**2+1./8.*(N/R)**2*C12*W1(I)**2)
    AK7=-(N/R)**2*W1(I)*(3./8.*C12*W1X(I)**2+1./8.*(N/R)**2*C22*W1(
   1*2)
    AK8= .5*(N/R)**2*C66*W1X(I)**2*W1(I)
    AK9= NX1(I)*(W20XX(I)+.5*W22XX(I))+   (NX20(I)+.5*NX22(I))*W1XX
    AK10=-(N/R)**2*(2.*NY1(I)*W22(I)+W1(I)*(NY20(I)+.5*NY22(I)))
    AK11= (N/R)*(2.*NXY1(I)*W22X(I)+NXY22(I)*W1X(I))
    EP3(I,3)=AK1+AK2+AK3+AK4+AK5+AK6+AK7+AK8+AK9+AK10+AK11
400 EP3(I,4)=0.
    DO 410 J=1,4
    DPB3(1,J)=0.
    EPB3(1,J)=0.
    DPB3(2,J)=0.
410 EPB3(2,J)=0.
    GO TO(401,402,403),BC
401 DPB3(1,1)=-C11*W1X(1)*W0XL(1)
    DPB3(1,4)=-K11*W1X(1)*W0XL(1)
    DPB3(2,1)=-C11*W1X(NSTAT)*W0XL(NSTAT)
    DPB3(2,4)=-K11*W1X(NSTAT)*W0XL(NSTAT)
    EPB3(1,1)=-C11*W1X(1)*(W20X(1)+.5*W22X(1))
    EPB3(1,4)=-K11*W1X(1)*(W20X(1)+.5*W22X(1))
    EPB3(2,1)=-C11*W1X(NSTAT)*(W20X(NSTAT)+.5*W22X(NSTAT))
    EPB3(2,4)=-K11*W1X(NSTAT)*(W20X(NSTAT)+.5*W22X(NSTAT))
    GO TO 402
403 DPB3(1,1)=-C11*W1X(1)*W0XL(1)
    EPB3(1,1)=-C11*W1X(1)*(W20X(1)+.5*W22X(1))
    DPB3(2,1)=-C11*W1X(NSTAT)*W0XL(NSTAT)
    EPB3(2,1)=-C11*W1X(NSTAT)*(W20X(NSTAT)+.5*W22X(NSTAT))
    GO TO 402
402 CONTINUE
    TEST3=1.
    M=1.
    GO TO 250
407 CONTINUE
    DO 480 J=1,4
    DO 480 K=1,4
    DUMA(J,K)=AA(1,J,K)
    DUMC(J,K)=C(NSTAT,J,K)
```

```
      DUMAB(J,K)=AB(1,J,K)
480   DUMCB(J,K)=CB(2,J,K)
      CALL MATRIX(INVERT,4,4,0,DUMA,4,DETERMI)
      CALL MATRIX(INVERT,4,4,0,DUMC,4,DETERMI)
      CALL MATRIX(MULTIPL,4,4,4,DUMAB,4,DUMA,4,DUMA,4)
      CALL MATRIX(MULTIPL,4,4,4,DUMCB,4,DUMC,4,DUMC,4)
      DO 481 J=1,4
      DUMD(J)=DP3(1,J)
481   DB(J)=DPB3(1,J)
      CALL MATRIX(MULTIPL,4,4,1,DUMA,4,DUMD,4,DUMD,4)
      CALL MATRIX(SUBTRAC,4,1,0,DB,4,DUMD,4,DUMD,4)
      DO 483 J=1,4
483   DP3(1,J)=DUMD(J)
      DO 484 J=1,4
      DUMD(J)=EP3(1,J)
484   DB(J)=EPB3(1,J)
      CALL MATRIX(MULTIPL,4,4,1,DUMA,4,DUMD,4,DUMD,4)
      CALL MATRIX(SUBTRAC,4,1,0,DB,4,DUMD,4,DUMD,4)
      DO 485 J=1,4
485   EP3(1,J)=DUMD(J)
      DO 486 J=1,4
      DUMD(J)=DP3(NSTAT,J)
486   DB(J)=DPB3(2,J)
      CALL MATRIX(MULTIPL,4,4,1,DUMC,4,DUMD,4,DUMD,4)
      CALL MATRIX(SUBTRAC,4,1,0,DB,4,DUMD,4,DUMD,4)
      DO 487 J=1,4
487   DP3(NSTAT,J)=DUMD(J)
      DO 488 J=1,4
      DUMD(J)=EP3(NSTAT,J)
488   DB(J)=EPB3(2,J)
      CALL MATRIX(MULTIPL,4,4,1,DUMC,4,DUMD,4,DUMD,4)
      CALL MATRIX(SUBTRAC,4,1,0,DB,4,DUMD,4,DUMD,4)
      DO 489 J=1,4
489   EP3(NSTAT,J)=DUMD(J)
      DO 420 J=1,NSTAT
      DO 420 K=1,4
      I=K+4*(J-1)
      Z1V(I)=Z1(J,K)
      DUMDE(I)=EP3(J,K)
420   CONTINUE
      XTE=0.
      XTD=0.
       NVAR=4*NSTAT
```

```
      DO 425 I=1,NVAR
  425 XTE=Z1V(I)*DUMDE(I)+XTE
      DO 430 J=1,NSTAT
      DO 430 K=1,4
      I=K+4*(J-1)
      DUMDE(I)=DP3(J,K)
  430 CONTINUE
      DO 435 I=1,NVAR
  435 XTD=Z1V(I)*DUMDE(I)+XTD
      DO 460 I=1,NSTAT
  460 FOFX(I)=U1(I)**2+V1(I)**2+W1(I)**2
C
      CALL SIMP(DEL,NSTAT,FOFX,AREA)
  637 FORMAT(2X*AREA( U1, V1, W1)=*E16.8)
      PRINT 637, AREA
  638 FORMAT(/2X*XTE=*E16.8)
      PRINT 638, XTE
  639 FORMAT(/2X*XTD=*E16.8)
      PRINT 639, XTD
      BCARD=-2.*T**2*A*XTE/(NXB*XTD*AREA)
      PRINT 635, BCARD
  635 FORMAT(2X*SENSITIVITY INDEX BY PRESENT THEORY B=*1E20.8)
C     CALCULATION OF SENSITIVITY INDEX BY BUDIANSKY THEORY
      DO 470 I=1,NSTAT
  470 FOFX(I)= W1X(I)**2*(NX20(I)+.5*NX22(I))+(N/R*W1(I))**2*(NY20(I)
     1-.5*NY22(I))-(N/R)*NXY22(I)*W1X(I)*W1(I)
     2+3./8.*C11*W1X(I)**4+1./4.*(N/R)**2*C12*W1X(I)**2*W1(I)**2
     3+3./8.*(N/R)**4*C22*W1(I)**4+.5*(N/R)**2*C66*(W1X(I)*W1(I))**2
      CALL SIMP(DEL,NSTAT,FOFX,AREA1)
      PRINT 640, AREA1
  640 FORMAT(2X*AREA1=*E16.8)
      DO 471 I=1,NSTAT
  471 FOFX(I)= NX1(I)*W1X(I)*(W20X(I)+.5*W22X(I))
     1+(N/R)**2*NY1(I)*W1(I)*W22(I)
     2-N/R*NXY1(I)*W1X(I)*W22(I)-N/R*NXY1(I)*W1(I)*(W20X(I)-.5*W22X(I
      CALL SIMP(DEL,NSTAT,FOFX,AREA2)
      PRINT 641, AREA2
  641 FORMAT(2X*AREA2=*E16.8)
      DO 472 I=1,NSTAT
  472 FOFX(I)=-W1X(I)**2+(N/R)**2*NYOL(I)*W1(I)**2
     1+WOXL(I)*(2.*NX1(I)*W1X(I)-2.*N/R*NXY1(I)*W1(I))
      CALL SIMP(DEL,NSTAT,FOFX,AREA3)
      PRINT 642, AREA2
```

```
642 FORMAT(2X*AREA3=*E16.8)
    BBUD=-(AREA1+2.*AREA2)/(NXB*AREA3)
    PRINT 636, BBUD
636 FORMAT(/2X*SENSITIVITY INDEX BY BUDIANSKY THEORY B=*1E20.8)
    GO TO 1000
    END
```

PROGRAM LENGTH INCLUDING I/O BUFFERS
045532

FUNCTION ASSIGNMENTS

STATEMENT ASSIGNMENTS

1	-	000632	2	-	001027	3	-	001207	4	-	001451
5	-	001220	6	-	001223	7	-	001232	10	-	007334
11	-	007356	12	-	007365	13	-	007370	14	-	007375
15	-	007401	16	-	007404	17	-	007407	18	-	007412
19	-	007423	20	-	007426	21	-	007432	22	-	007435
23	-	007475	24	-	007503	25	-	007554	26	-	007563
30	-	007506	31	-	007514	51	-	000341	52	-	000272
55	-	001457	80	-	000267	99	-	001554	101	-	002163
102	-	002322	103	-	002364	105	-	002507	137	-	003213
138	-	003253	160	-	003312	170	-	003515	172	-	003474
181	-	003633	200	-	003644	201	-	003764	202	-	004103
210	-	004107	211	-	003052	212	-	004517	220	-	004237
221	-	004467	225	-	004107	227	-	004500	230	-	004704
231	-	005137	235	-	004521	237	-	005150	249	-	005220
250	-	001464	251	-	005402	300	-	003045	302	-	005553
401	-	006216	402	-	006276	403	-	006255	407	-	006301
425	-	006647	435	-	006674	460	-	006702	483	-	006434
485	-	006500	487	-	006545	489	-	006612	500	-	007572
501	-	007601	502	-	007612	635	-	007642	636	-	007662
637	-	007627	638	-	007634	639	-	007637	640	-	007651
641	-	007654	642	-	007657	701	-	004350	702	-	004404
703	-	004424	704	-	004460	801	-	005015	802	-	005051
803	-	005074	804	-	005130	899	-	005255	921	-	007517
922	-	007526	923	-	007531	924	-	007540	999	-	007451
1000	-	000003									

BLOCK NAMES AND LENGTHS

VARIABLE ASSIGNMENTS

A	-	041304	AA	-	011401	AB	-	017161	AK1	-	041444
AK10	-	041455	AK11	-	041456	AK2	-	041445	AK3	-	041446
AK4	-	041447	AK5	-	041450	AK6	-	041451	AK7	-	041452
AK8	-	041453	AK9	-	041454	AN	-	017521	ANS	-	041342
AR	-	041314	AREA	-	041460	AREA1	-	041462	AREA2	-	041463
AREA3	-	041464	AS	-	041321	B	-	013321	BB	-	017221

BBUD	-	041465	BC	-	041245	BCARD	-	041461	BETA	-	041350
BETAL	-	041352	BN	-	017541	BS	-	041324	B1	-	017461
B1LL	-	041406	B11	-	010773	B12	-	011017	B22	-	011043
B66	-	011163	C	-	015241	CB	-	017261	CC	-	041356
CS	-	041357	CXCX	-	041402	CXSX	-	041404	C1	-	017501
C11	-	041327	C12	-	041330	C22	-	041331	C66	-	041332
D	-	025741	DB	-	036411	DBAR	-	041364	DEL	-	041411
DELBAR	-	041305	DETERMI	-	041440	DETERM1	-	041416	DETRI	-	041421
DL2	-	041432	DMAT	-	030245	DPB3	-	041216	DP3	-	036613
DUMA	-	017321	DUMAB	-	017401	DUMB	-	017341	DUMBB	-	017421
DUMC	-	017361	DUMCB	-	017441	DUMD	-	036415	DUMDE	-	037563
D11	-	041335	D12	-	041336	D22	-	041337	D66	-	041340
EPB3	-	041226	EPSX	-	041427	EPSXY	-	041431	EPSY	-	041430
EP3	-	037177	ER	-	041313	ES	-	041320	EX	-	010603
EY	-	010627	E1	-	041433	E2	-	041434	E3	-	041435
E4	-	041436	E5	-	041437	E6	-	041441	E7	-	041442
E8	-	041443	FOFX	-	040533	FOL	-	041374	F1	-	041372
F1L	-	041375	F1LL	-	041405	F2	-	041373	F2L	-	041376
G	-	041371	GAMA	-	041351	GAMAL	-	041353	GRJR	-	041316
GSJS	-	041323	GXY	-	010723	G1	-	041362	G1L	-	041365
G1LL	-	041407	G12	-	041367	G2	-	041363	G2L	-	041366
G21	-	041370	H	-	010747	I	-	041341	II	-	041424
INVERT	-	041414	IPRINT	-	041312	IR	-	041236	IS	-	041237
J	-	041377	K	-	041413	K11	-	041240	K12	-	041241
K22	-	041242	K66	-	041243	L	-	041325	LAM11	-	041250
LAM12	-	041251	LAM13	-	041252	LAM14	-	041265	LAM15	-	041266
LAM16	-	041267	LAM17	-	041253	LAM21	-	041254	LAM22	-	041255
LAM23	-	041256	LAM24	-	041257	LAM25	-	041270	LAM26	-	041271
LAM31	-	041272	LAM32	-	041260	LAM33	-	041273	LAM34	-	041274
LAM35	-	041275	LAM36	-	041276	LAM41	-	041261	LAM42	-	041262
LAM43	-	041263	LAM44	-	041277	LAM45	-	041264	LAYER	-	041307
M	-	041247	MODRES	-	041300	MT	-	041417	MULTIPL	-	041415
M1	-	023770	M20	-	034374	M22	-	034760	N	-	041306
NEND	-	041412	NORM	-	041311	NSTAT	-	041310	NS1	-	041423
NUX	-	010653	NUY	-	010677	NVAR	-	041457	NXB	-	041244
NXY1	-	025644	NXY22	-	036314	NX1	-	025452	NX20	-	035730
NX22	-	036122	NYOL	-	011207	NY1	-	025547	NY20	-	036025
NY22	-	036217	P	-	017561	PD	-	024455	PI	-	023461
PIM1	-	023421	PP	-	030631	P1	-	041354	QQ	-	032551
R	-	041303	RGB	-	041346	RGG	-	041347	RG1	-	041343
RG2	-	041344	RG3	-	041345	RI	-	023441	RS	-	041317
R1	-	021501	S	-	011067	SC	-	041355	SCALE	-	041420
SHCH	-	041360	SMAT	-	026325	SNCN	-	041361	SS	-	011113

SSS	-	011137	ST	-	041246	SUBTRAC	-	041301	SXCX	-	041403
SXSX	-	041401	S1	-	041333	S2	-	041334	T	-	041410
TEST3	-	041326	TRANSPO	-	041302	U1	-	023501	U1X	-	024577
U20	-	034105	U20X	-	035152	U22	-	034471	U22X	-	035247
V1	-	023576	V1X	-	024674	V20	-	034202	V22	-	034566
V22X	-	035344	WMAX	-	041422	WO	-	010217	WOL	-	011304
WOX	-	010314	WOXL	-	010506	WOXX	-	010411	WO2L	-	025163
WO3L	-	025355	W1	-	023673	W1X	-	024771	W1XX	-	025066
W13X	-	025260	W20	-	034277	W20X	-	035055	W20XX	-	035536
W20XXX	-	036421	W22	-	034663	W22X	-	035441	W22XX	-	035633
W22XXX	-	036516	X	-	024502	XB	-	041400	XTD	-	040631
XTE	-	040630	Z	-	024451	ZD	-	024476	ZMAG2	-	041425
ZNORM	-	041426	ZR	-	041315	ZS	-	041322	Z1	-	024065
Z1SQ	-	024475	Z1T	-	040147	Z1V	-	040632	Z20	-	033135
Z22	-	033521									

START OF CONSTANTS
007326

START OF TEMPORARIES
007671

START OF INDIRECTS
010053

UNUSED COMPILER SPACE
003400

```
                SUBROUTINE SUM (I,L,X,Y,ANS)
000006          DIMENSION X(L), Y(L)
000006          ANS=0.
000007          DO 1 J=I,L
000010        1 ANS=ANS+X(J)*Y(J)
000015          RETURN
000016          END
```

```
SUBPROGRAM LENGTH
000026

FUNCTION ASSIGNMENTS

STATEMENT ASSIGNMENTS
1       -  000010

BLOCK NAMES AND LENGTHS

VARIABLE ASSIGNMENTS
J       -  000025

START OF CONSTANTS
000020

START OF TEMPORARIES
00C021

START OF INDIRECTS
000023

UNUSED COMPILER SPACE
033100
```

```
                SUBROUTINE SIMP (DEL,NSTAT,FOFX,AREA)
000006          DIMENSION FOFX(NSTAT)
000006          MS=(NSTAT-1)/2
000010          TOT=0.
000011          DO 480 K=1,MS
000012      480 TOT=TOT+4.*FOFX(2*K)+2.*FOFX(2*K+1)
000023          AREA=DEL/3.*(FCFX(1)+TOT-FOFX(2*MS+1))
000030          RETURN
000030          END
```

```
SUBPROGRAM LENGTH
000051

FUNCTION ASSIGNMENTS

STATEMENT ASSIGNMENTS
480     -  000013

BLOCK NAMES AND LENGTHS

VARIABLE ASSIGNMENTS
K       -  000050     MS      -  000046     TOT     -  000047

START OF CONSTANTS
000032

START OF TEMPORARIES
000036

START OF INDIRECTS
000042

UNUSED COMPILER SPACE
033100
```

```
$INPUT
R       =  0.1E+02,
A       =  0.7E+01,
DELBAR  =  0.5E-01,
BC      =  1,
NXB     =  0.4374E+04,
N       =  7,
EX      =  0.105E+08,  0.203E+07, I, I, I, I, I, I, I, I, I, I, I, I, I, I, I, I, I, I,
EY      =  0.105E+08,  0.3025E+08, I, I, I, I, I, I, I, I, I, I, I, I, I, I, I, I, I, I,
NUX     =  0.3E+00,  0.23E-01, I, I, I, I, I, I, I, I, I, I, I, I, I, I, I, I, I, I,
NUY     =  0.3E+00,  0.346E+00, I, I, I, I, I, I, I, I, I, I, I, I, I, I, I, I, I, I,
GXY     =  0.4038E+07,  0.5249E+06, I, I, I, I, I, I, I, I, I, I, I, I, I, I, I, I, I, I,
H       =  0.5E-01,  0.5E-01, I, I, I, I, I, I, I, I, I, I, I, I, I, I, I, I, I, I,
LAYER   =  2,
ST      =  0,
NSTAT   =  61,
NORM    =  1,
IPRINT  =  1,
$END
```

```
IMPERFECTION SENSITIVITY OF AXIALLY COMPRESSED CYLINDER
CARD-SYKES  A2338  RDF367  OCTOBER,1968)
```

LAYER	EX	EY	NUX	NUY	GXY	H
1	1.050E+07	1.050E+07	3.000E-01	3.000E-01	4.038E+06	5.000E-02
2	2.030E+06	3.025E+07	2.300E-02	3.460E-01	5.249E+05	5.000E-02

```
          11                  12                  22                  66
```

B	1	1.15384615E+07	3.46153846E+06	1.15384615E+07	4.03800000E+06
B	2	2.04628433E+06	7.08014378E+05	3.04926606E+07	5.24900000E+05
C		6.79237293E+05	2.08477642E+05	2.10155611E+06	2.28145000E+05
D		5.66031078E+02	1.73731368E+02	1.75129676E+03	1.90120833E+02
K		-1.18652215E+04	-3.44190510E+03	2.36927488E+04	-4.39137500E+03

BETA= 8.64861327E-01 GAMA= 2.60541762E+00 F1= -3.73726721E-03 F2= -5.06316344E-04

STATION	WO	WOX	WOXX	WOXL	WOL
1	2.77555756E-17	-9.39208292E-02	-2.12972811E-01	-6.38340345E-05	-2.16840434E-19
2	-9.43477662E-03	-6.73307433E-02	2.38094963E-01	-5.45861168E-05	-6.97393851E-06
3	-1.56591006E-02	-3.94024296E-02	2.36612173E-01	-3.96694748E-05	-1.25157747E-05
4	-1.86874509E-02	-1.29633109E-02	2.13512103E-01	-2.15387267E-05	-1.61050842E-05
5	-1.88273106E-02	9.81224981E-03	1.74870363E-01	-2.70999409E-06	-1.75146617E-05
6	-1.65973320E-02	2.74849851E-02	1.27094306E-01	1.45444992E-05	-1.67992660E-05
7	-1.26408642E-02	3.93502793E-02	7.62737380E-02	2.84273546E-05	-1.42528785E-05
8	-7.64363528E-03	4.53702557E-02	2.76784827E-02	3.77581480E-05	-1.03441204E-05
9	-2.26240539E-03	4.60568413E-02	-1.45780364E-02	4.20246368E-05	-5.64042483E-06
10	2.93082941E-03	4.23253691E-02	-4.77087467E-02	4.13511954E-05	-7.31185017E-07
11	7.48675307E-03	3.53374049E-02	-7.02712393E-02	3.64003894E-05	3.84133164E-06
12	1.10984861E-02	2.63490635E-02	-8.20603689E-02	2.82283635E-05	7.63667727E-06
13	1.36046071E-02	1.65776227E-02	-8.39077159E-02	1.81165075E-05	1.03524436E-05
14	1.49781298E-02	7.09526524E-03	-7.74229136E-02	7.40099734E-06	1.18405203E-05
15	1.53049163E-02	-1.24526635E-03	-6.47106142E-02	-2.68118246E-06	1.21042672E-05
16	1.47553472E-02	-7.85204416E-03	-4.80927827E-02	-1.11155839E-05	1.12793952E-05
17	1.35530000E-02	-1.24044245E-02	-2.98600010E-02	-1.71940708E-05	9.60270610E-06
18	1.19437024E-02	-1.48370413E-02	-1.20684496E-02	-2.05554152E-05	7.37356574E-06
19	1.01677135E-02	-1.53032735E-02	3.60792435E-03	-2.11839876E-05	4.91312030E-06
20	8.43704093E-03	-1.41248559E-02	1.59671612E-02	-1.93718532E-05	2.52586750E-06
21	6.91911945E-03	-1.17342989E-02	2.43136233E-02	-1.56525128E-05	4.67394790E-07
22	5.72732590E-03	-8.61621869E-03	2.84437569E-02	-1.07162548E-05	-1.07897797E-06
23	4.91814755E-03	-5.25270695E-03	2.85928363E-02	-5.31763699E-06	-2.01511955E-06
24	4.49429144E-03	-2.07666385E-03	2.53535307E-02	-1.85131595E-07	-2.33024837E-06
25	4.41263876E-03	5.64257145E-04	1.95772032E-02	4.05834697E-06	-2.09311060E-06
26	4.59571219E-03	2.43167610E-03	1.22679684E-02	6.95722096E-06	-1.43586290E-06
27	4.94522392E-03	3.40815449E-03	4.47804212E-03	8.26277345E-06	-5.32013051E-07
28	5.35628760E-03	3.49706533E-03	-2.78888593E-03	7.94822892E-06	4.28834628E-07
29	5.73098460E-03	2.81190581E-03	-8.66133500E-03	6.19950036E-06	1.26656202E-06
30	5.99014918E-03	1.55676931E-03	-1.24674719E-02	3.38379209E-06	1.83371833E-06
31	6.08245709E-03	0.	-1.37842948E-02	0.	2.03393063E-06
32	5.99014918E-03	-1.55676931E-03	-1.24674719E-02	-3.38379209E-06	1.83371833E-06
33	5.73098460E-03	-2.81190581E-03	-8.66133500E-03	-6.19950036E-06	1.26656202E-06
34	5.35628760E-03	-3.49706533E-03	-2.78888593E-03	-7.94822892E-06	4.28834628E-07
35	4.94522392E-03	-3.40815449E-03	4.47804212E-03	-8.26277345E-06	-5.32013051E-07
36	4.59571219E-03	-2.43167610E-03	1.22679684E-02	-6.95722096E-06	-1.43586290E-06
37	4.41263876E-03	-5.64257145E-04	1.95772032E-02	-4.05834697E-06	-2.09311060E-06
38	4.49429144E-03	2.07666385E-03	2.53535307E-02	1.85131595E-07	-2.33024837E-06
39	4.91814755E-03	5.25270695E-03	2.85928363E-02	5.31763699E-06	-2.01511955E-06
40	5.72732590E-03	8.61621869E-03	2.84437569E-02	1.07162548E-05	-1.07897797E-06
41	6.91911945E-03	1.17342989E-02	2.43136233E-02	1.56525128E-05	4.67394790E-07
42	8.43704093E-03	1.41248559E-02	1.59671612E-02	1.93718532E-05	2.52586750E-06
43	1.01677135E-02	1.53032735E-02	3.60792435E-03	2.11839876E-05	4.91312030E-06
44	1.19437024E-02	1.48370413E-02	-1.20684496E-02	2.05554152E-05	7.37356574E-06
45	1.35530000E-02	1.24044245E-02	-2.98600010E-02	1.71940708E-05	9.60270610E-06
46	1.47553472E-02	7.85204416E-03	-4.80927827E-02	1.11155839E-05	1.12793952E-05
47	1.53049163E-02	1.24526635E-03	-6.47106142E-02	2.68118246E-06	1.21042672E-05
48	1.49781298E-02	-7.09526524E-03	-7.74229136E-02	-7.40099734E-06	1.18405203E-05
49	1.36046071E-02	-1.65776227E-02	-8.39077159E-02	-1.81165075E-05	1.03524436E-05

50	1.10984861E-02	-2.63490635E-02	-8.20603689E-02	-2.82283635E-05	7.63667727E-06
51	7.48675307E-03	-3.53374049E-02	-7.02712393E-02	-3.64003894E-05	3.84133164E-06
52	2.93082941E-03	-4.23253691E-02	-4.77087467E-02	-4.13511954E-05	-7.31185017E-07
53	-2.26240539E-03	-4.60568413E-02	-1.45780364E-02	-4.20246368E-05	-5.64042483E-06
54	-7.64363528E-03	-4.53702557E-02	2.76784827E-02	-3.77581480E-05	-1.03441204E-05
55	-1.26408642E-02	-3.93502793E-02	7.62737380E-02	-2.84273546E-05	-1.42528785E-05
56	-1.65973320E-02	-2.74849851E-02	1.27094306E-01	-1.45444992E-05	-1.67992660E-05
57	-1.88273106E-02	-9.81224981E-03	1.74870363E-01	2.70999409E-06	-1.75146617E-05
58	-1.86874509E-02	1.29633109E-02	2.13512103E-01	2.15387267E-05	-1.61050842E-05
59	-1.56591006E-02	3.94024296E-02	2.36612173E-01	3.96694748E-05	-1.25157747E-05
60	-9.43477662E-03	6.73307433E-02	2.38094963E-01	5.45861168E-05	-6.97393851E-06
61	2.77555756E-17	9.39208292E-02	2.12972811E-01	6.38340345E-05	-2.16840434E-19

MODRES= -8.57902481E-03

STATION	U1	V1	W1
1	4.27874577E+02	0.	0.
2	3.68884410E+02	6.32995795E+01	-1.79131629E-01
3	3.24059859E+02	1.23208761E+02	-3.45844320E-01
4	2.92892596E+02	1.76618281E+02	-4.89135773E-01
5	2.71058914E+02	2.21305220E+02	-6.00786467E-01
6	2.53036603E+02	2.56227664E+02	-6.76296108E-01
7	2.34543440E+02	2.81514898E+02	-7.15200574E-01
8	2.13883040E+02	2.98232210E+02	-7.20765051E-01
9	1.91937999E+02	3.08040818E+02	-6.99192072E-01
10	1.71158918E+02	3.12863031E+02	-6.58553378E-01
11	1.54198476E+02	3.14621605E+02	-6.07657672E-01
12	1.42793904E+02	3.15074002E+02	-5.55025237E-01
13	1.37235502E+02	3.15726283E+02	-5.08079383E-01
14	1.36449068E+02	3.17795660E+02	-4.72603199E-01
15	1.38498385E+02	3.22193415E+02	-4.52460365E-01
16	1.41231000E+02	3.29512718E+02	-4.49546951E-01
17	1.42827650E+02	3.40019966E+02	-4.63926709E-01
18	1.42118431E+02	3.53657475E+02	-4.94100912E-01
19	1.38641740E+02	3.70067262E+02	-5.37368404E-01
20	1.32506789E+02	3.88641394E+02	-5.90236538E-01
21	1.24160756E+02	4.08596884E+02	-6.48846188E-01
22	1.14158859E+02	4.29065796E+02	-7.09374473E-01
23	1.03002921E+02	4.49186738E+02	-7.68379678E-01
24	9.10698621E+01	4.68183456E+02	-8.23057218E-01
25	7.86136552E+01	4.85419537E+02	-8.71384739E-01
26	6.58042848E+01	5.00423956E+02	-9.12148347E-01
27	5.27678145E+01	5.12888345E+02	-9.44858207E-01
28	3.96068892E+01	5.22642050E+02	-9.69577181E-01
29	2.64003884E+01	5.29613956E+02	-9.86698008E-01
30	1.31945510E+01	5.33790900E+02	-9.96710530E-01
31	5.79721572E-04	5.35181365E+02	-1.00000000E+00
32	-1.31934056E+01	5.33791041E+02	-9.96710842E-01
33	-2.63992831E+01	5.29614238E+02	-9.86698591E-01
34	-3.96058450E+01	5.22642474E+02	-9.69577954E-01
35	-5.27668447E+01	5.12888915E+02	-9.44859065E-01
36	-6.58033942E+01	5.00424681E+02	-9.12149174E-01
37	-7.86128400E+01	4.85420436E+02	-8.71385425E-01
38	-9.10691097E+01	4.68184558E+02	-8.23057685E-01
39	-1.03002210E+02	4.49188092E+02	-7.68379901E-01
40	-1.14158159E+02	4.29067465E+02	-7.09374502E-01
41	-1.24160022E+02	4.08598952E+02	-6.48846169E-01
42	-1.32505966E+02	3.88643962E+02	-5.90236728E-01
43	-1.38640762E+02	3.70070443E+02	-5.37369177E-01
44	-1.42117232E+02	3.53661390E+02	-4.94102757E-01
45	-1.42826180E+02	3.40024734E+02	-4.63930215E-01
46	-1.41229253E+02	3.29518447E+02	-4.49552778E-01
47	-1.38496422E+02	3.22200193E+02	-4.52469197E-01
48	-1.36447044E+02	3.17803542E+02	-4.72615684E-01
49	-1.37233671E+02	3.15735282E+02	-5.08096054E-01

50	-1.42792601E+02	3.15084076E+02	-5.55046419E-01
51	-1.54198064E+02	3.14632649E+02	-6.07683396E-01
52	-1.71159717E+02	3.12874866E+02	-6.58583293E-01
53	-1.91940210E+02	3.08053175E+02	-6.99225388E-01
54	-2.13886699E+02	2.98244729E+02	-7.20800513E-01
55	-2.34548436E+02	2.81527127E+02	-7.15236500E-01
56	-2.53042773E+02	2.56239074E+02	-6.76330484E-01
57	-2.71066189E+02	2.21315241E+02	-6.00817102E-01
58	-2.92901156E+02	1.76626352E+02	-4.89160506E-01
59	-3.24070207E+02	1.23214404E+02	-3.45861254E-01
60	-3.68897304E+02	6.33028653E+01	-1.79139344E-01
61	-4.27890803E+02	0.	2.26829198E-06

STATION	U1	V1	W1	M1
1	1.13129929E-02	0.	0.	0.
2	9.75329445E-03	1.67364985E-03	-1.79131629E-02	-2.98697318E+01
3	8.56813445E-03	3.25763651E-03	-3.45844320E-02	-5.62318563E+01
4	7.74407280E-03	4.66978285E-03	-4.89135773E-02	-7.57065770E+01
5	7.16679081E-03	5.85130441E-03	-6.00786467E-02	-8.59047813E+01
6	6.69028137E-03	6.77465294E-03	-6.76296108E-02	-8.59423329E+01
7	6.20132260E-03	7.44324675E-03	-7.15200574E-02	-7.65125451E+01
8	5.65506215E-03	7.88525205E-03	-7.20765051E-02	-5.95900447E+01
9	5.07483583E-03	8.14459139E-03	-6.99192072E-02	-3.79239207E+01
10	4.52543744E-03	8.27209061E-03	-6.58553378E-02	-1.44844699E+01
11	4.07700378E-03	8.31858723E-03	-6.07657672E-02	8.01080816E+00
12	3.77546721E-03	8.33054861E-03	-5.55025237E-02	2.74201653E+01
13	3.62850318E-03	8.34779491E-03	-5.08079383E-02	4.23300436E+01
14	3.60770990E-03	8.40250917E-03	-4.72603199E-02	5.20594359E+01
15	3.66189379E-03	8.51878570E-03	-4.52460365E-02	5.65638317E+01
16	3.73414406E-03	8.71230789E-03	-4.49546951E-02	5.62919935E+01
17	3.77635943E-03	8.99011927E-03	-4.63926709E-02	5.20375922E+01
18	3.75760770E-03	9.35069467E-03	-4.94100912E-02	4.48079726E+01
19	3.66568409E-03	9.78456901E-03	-5.37368404E-02	3.57137642E+01
20	3.50347613E-03	1.02756686E-02	-5.90236538E-02	2.58725518E+01
21	3.28280724E-03	1.08032912E-02	-6.48846188E-02	1.63190273E+01
22	3.01835734E-03	1.13444887E-02	-7.09374473E-02	7.92006583E+00
23	2.72339461E-03	1.18764860E-02	-7.68379678E-02	1.30096610E+00
24	2.40788484E-03	1.23787587E-02	-8.23057218E-02	-3.20585198E+00
25	2.07854305E-03	1.28344802E-02	-8.71384739E-02	-5.57837291E+00
26	1.73986362E-03	1.32311967E-02	-9.12148347E-02	-6.08214277E+00
27	1.39517967E-03	1.35607548E-02	-9.44858207E-02	-5.20791769E+00
28	1.04720515E-03	1.38186425E-02	-9.69577181E-02	-3.57828578E+00
29	6.98025599E-04	1.40029795E-02	-9.86698008E-02	-1.83750192E+00
30	3.48863594E-04	1.41134178E-02	-9.96710530E-02	-5.41600312E-01
31	1.53278237E-08	1.41501817E-02	-1.00000000E-01	-6.55972735E-02
32	-3.48833309E-04	1.41134216E-02	-9.96710842E-02	-5.41709583E-01
33	-6.97996375E-04	1.40029870E-02	-9.86698591E-02	-1.83770581E+00
34	-1.04717754E-03	1.38186537E-02	-9.69577954E-02	-3.57855561E+00
35	-1.39515403E-03	1.35607699E-02	-9.44859065E-02	-5.20821202E+00

36	-1.73984007E-03	1.32312158E-02	-9.12149174E-02	-6.08240945E+00
37	-2.07852149E-03	1.28345040E-02	-8.71385425E-02	-5.57855196E+00
38	-2.40786495E-03	1.23787878E-02	-8.23057685E-02	-3.20587938E+00
39	-2.72337582E-03	1.18765218E-02	-7.68379901E-02	1.30115385E+00
40	-3.01833882E-03	1.13445329E-02	-7.09374502E-02	7.92052636E+00
41	-3.28278784E-03	1.08033459E-02	-6.48846169E-02	1.63198065E+01
42	-3.50345437E-03	1.02757365E-02	-5.90236728E-02	2.58736773E+01
43	-3.66565823E-03	9.78465311E-03	-5.37369177E-02	3.57152387E+01
44	-3.75757600E-03	9.35079817E-03	-4.94102757E-02	4.48097666E+01
45	-3.77632058E-03	8.99024533E-03	-4.63930215E-02	5.20396372E+01
46	-3.73409786E-03	8.71245938E-03	-4.49552778E-02	5.62941760E+01
47	-3.66184189E-03	8.51896493E-03	-4.52469197E-02	5.65659903E+01
48	-3.60765639E-03	8.40271758E-03	-4.72615684E-02	5.20613637E+01
49	-3.62845478E-03	8.34803284E-03	-5.08096054E-02	4.23314989E+01
50	-3.77543275E-03	8.33081497E-03	-5.55046419E-02	2.74208924E+01
51	-4.07699289E-03	8.31887926E-03	-6.07683396E-02	8.01057054E+00
52	-4.52545856E-03	8.27240351E-03	-6.58583293E-02	-1.44858485E+01
53	-5.07489428E-03	8.14491811E-03	-6.99225388E-02	-3.79265118E+01
54	-5.65515888E-03	7.88558307E-03	-7.20800513E-02	-5.95937764E+01
55	-6.20145470E-03	7.44357009E-03	-7.15236500E-02	-7.65171808E+01
56	-6.69044448E-03	6.77495462E-03	-6.76330484E-02	-8.59474759E+01
57	-7.16698315E-03	5.85156934E-03	-6.00817102E-02	-8.59099117E+01
58	-7.74429912E-03	4.66995626E-03	-4.89160506E-02	-7.57111183E+01
59	-8.56840804E-03	3.25778572E-03	-3.45861254E-02	-5.62352613E+01
60	-9.75363534E-03	1.67372615E-03	-1.79139344E-02	-2.98715665E+01
61	-1.13134220E-02	0.	2.26829198E-07	0.

STATION	W1X	U1X	V1X	W1XX
1	-1.58863798E-01	-1.49740093E-02	1.47298410E-02	1.11916155E-03
2	-1.48218994E-01	-1.17636793E-02	1.39612993E-02	9.12411761E-02
3	-1.32858919E-01	-8.61094991E-03	1.28405700E-02	1.72074401E-01
4	-1.09260920E-01	-6.00575845E-03	1.11157196E-02	2.32462715E-01
5	-8.02115725E-02	-4.51624898E-03	9.02087179E-03	2.65526106E-01
6	-4.90346170E-02	-4.13772091E-03	6.82261004E-03	2.68935987E-01
7	-1.90581181E-02	-4.43665381E-03	4.75971050E-03	2.44946853E-01
8	6.86078625E-03	-4.82780045E-03	3.00576276E-03	1.99377221E-01
9	2.66621454E-02	-4.84124876E-03	1.65787951E-03	1.40074651E-01
10	3.92290287E-02	-4.27642309E-03	7.45696464E-04	7.53576338E-02
11	4.43692034E-02	-3.21415814E-03	2.50534286E-04	1.27596463E-02
12	4.26764094E-02	-1.92214544E-03	1.25175766E-04	-4.17789723E-02
13	3.53237306E-02	-7.18959870E-04	3.08402421E-04	-8.42669499E-02
14	2.38367223E-02	1.43102627E-04	7.32817662E-04	-1.12653192E-01
15	9.88124905E-03	5.41860660E-04	1.32770878E-03	-1.26583493E-01
16	-4.91414732E-03	4.90567033E-04	2.02000102E-03	-1.27051874E-01
17	-1.90945547E-02	1.00558471E-04	2.73594334E-03	-1.16040824E-01
18	-3.14750125E-02	-4.74322889E-04	3.40478460E-03	-9.61955957E-02
19	-4.12009825E-02	-1.08913528E-03	3.96417396E-03	-7.05353182E-02
20	-4.77761930E-02	-1.64090079E-03	4.36595239E-03	-4.21825761E-02

21	-5.10591150E-02	-2.07908055E-03	4.58065780E-03	-1.40960875E-02
22	-5.12286385E-02	-2.39748267E-03	4.59940594E-03	1.11899711E-02
23	-4.87211768E-02	-2.61631070E-03	4.43258542E-03	3.17950871E-02
24	-4.41450261E-02	-2.76364957E-03	4.10568981E-03	4.66532105E-02
25	-3.81819123E-02	-2.86294809E-03	3.65330574E-03	5.55715968E-02
26	-3.14886292E-02	-2.92870017E-03	3.11260537E-03	5.91703990E-02
27	-2.46123573E-02	-2.96853632E-03	2.51762505E-03	5.87085480E-02
28	-1.79313434E-02	-2.98780318E-03	1.89524876E-03	5.58231191E-02
29	-1.16285781E-02	-2.99289236E-03	1.26332277E-03	5.22242850E-02
30	-5.70085373E-03	-2.99147259E-03	6.30866394E-04	4.93938478E-02
31	-1.34012557E-07	-2.99012959E-03	1.59941271E-08	4.83327760E-02
32	5.70060391E-03	-2.99147873E-03	-6.30834415E-04	4.93941597E-02
33	1.16283806E-02	-2.99290383E-03	-1.26329070E-03	5.22248689E-02
34	1.79312252E-02	-2.98781853E-03	-1.89521618E-03	5.58238967E-02
35	2.46123346E-02	-2.96855373E-03	-2.51759097E-03	5.87094064E-02
36	3.14887031E-02	-2.92871768E-03	-3.11256814E-03	5.91711972E-02
37	3.81820664E-02	-2.86296376E-03	-3.65326291E-03	5.55721736E-02
38	4.41452246E-02	-2.76366142E-03	-4.10563819E-03	4.66533959E-02
39	4.87213645E-02	-2.61631658E-03	-4.43252119E-03	3.17947157E-02
40	5.12287419E-02	-2.39748006E-03	-4.59932496E-03	1.11888976E-02
41	5.10590459E-02	-2.07906668E-03	-4.58055602E-03	-1.40979714E-02
42	4.77758537E-02	-1.64087313E-03	-4.36582635E-03	-4.21853242E-02
43	4.12002733E-02	-1.08909268E-03	-3.96402135E-03	-7.05389113E-02
44	3.14738412E-02	-4.74267201E-04	-3.40460476E-03	-9.61999244E-02
45	1.90928481E-02	1.00620599E-04	-2.73573767E-03	-1.16045672E-01
46	4.91186450E-03	4.90622972E-04	-2.01977318E-03	-1.27056905E-01
47	-9.88410270E-03	5.41892008E-04	-1.32746484E-03	-1.26588248E-01
48	-2.38400812E-02	1.43087620E-04	-7.32566083E-04	-1.12657099E-01
49	-3.53274576E-02	-7.19041545E-04	-3.08154059E-04	-8.42693537E-02
50	-4.26802896E-02	-1.92230618E-03	-1.24943930E-04	-4.17791948E-02
51	-4.43729464E-02	-3.21439633E-03	-2.50334830E-04	1.27622210E-02
52	-3.92322823E-02	-4.27672026E-03	-7.45547749E-04	7.53634493E-02
53	-2.66645226E-02	-4.84157279E-03	-1.65780190E-03	1.40083860E-01
54	-6.86190525E-03	-4.82811608E-03	-3.00577726E-03	1.99389580E-01
55	1.90585836E-02	-4.43693829E-03	-4.75983619E-03	2.44961658E-01
56	4.90368851E-02	-4.13797908E-03	-6.82286034E-03	2.68952081E-01
57	8.02157048E-02	-4.51651987E-03	-9.02125011E-03	2.65541973E-01
58	1.09266792E-01	-6.00610670E-03	-1.11162155E-02	2.32476666E-01
59	1.32866212E-01	-8.61144095E-03	-1.28411576E-02	1.72084825E-01
60	1.48227224E-01	-1.17643454E-02	-1.39619388E-02	9.12467946E-02
61	1.58872683E-01	-1.49748540E-02	-1.47305095E-02	1.11927182E-03

STATION	NX1	NY1	NXY1	NYOL
1	-2.29851527E+01	-7.27850388E+00	2.53052034E+03	-3.17916866E-01
2	-2.28147090E+02	-1.56830261E+03	2.34620711E+03	-1.74861622E+00
3	-4.38673734E+02	-2.98889820E+03	2.16034766E+03	-2.88541230E+00
4	-6.14815772E+02	-4.13432232E+03	1.86971991E+03	-3.62010975E+00
5	-7.48950954E+02	-4.90725825E+03	1.50079939E+03	-3.90657018E+00

6	-8.42140079E+02	-5.24970402E+03	1.08641051E+03	-3.75656675E+00
7	-9.00767759E+02	-5.14917468E+03	6.62164909E+02	-3.23093538E+00
8	-9.32482617E+02	-4.63949754E+03	2.62692818E+02	-2.42626175E+00
9	-9.43416484E+02	-3.79537928E+03	-8.18588385E+01	-1.45928193E+00
10	-9.37464050E+02	-2.72144103E+03	-3.48625141E+02	-4.51095177E-01
11	-9.17188248E+02	-1.53763149E+03	-5.23796256E+02	4.87009673E-01
12	-8.85302018E+02	-3.63633603E+02	-6.03207130E+02	1.26475826E+00
13	-8.45752856E+02	6.95081348E+02	-5.91772022E+02	1.82029297E+00
14	-8.03927663E+02	1.55750505E+03	-5.01962552E+02	2.12347334E+00
15	-7.66033376E+02	2.17261658E+03	-3.51647109E+02	2.17525954E+00
16	-7.38040382E+02	2.52021825E+03	-1.61655900E+02	2.00375664E+00
17	-7.24638397E+02	2.60793678E+03	4.65892958E+01	1.65777415E+00
18	-7.28529321E+02	2.46565133E+03	2.53117913E+02	1.19890313E+00
19	-7.50191921E+02	2.13863200E+03	4.40961311E+02	6.93138923E-01
20	-7.88088504E+02	1.68044968E+03	5.97141028E+02	2.02995399E-01
21	-8.39179903E+02	1.14641334E+03	7.13099734E+02	-2.19108625E-01
22	-8.99572954E+02	5.88023364E+02	7.84633538E+02	-5.35631119E-01
23	-9.65133732E+02	4.87413382E+01	8.11419440E+02	-7.26544464E-01
24	-1.03194735E+03	-4.38745186E+02	7.96253699E+02	-7.89764608E-01
25	-1.09657446E+03	-8.53682478E+02	7.44128812E+02	-7.39532816E-01
26	-1.15612420E+03	-1.18686432E+03	6.61278834E+02	-6.03097453E-01
27	-1.20821159E+03	-1.43886435E+03	5.54313647E+02	-4.16179227E-01
28	-1.25088126E+03	-1.61720243E+03	4.29541435E+02	-2.17783623E-01
29	-1.28256052E+03	-1.73289805E+03	2.92545875E+02	-4.49484240E-02
30	-1.30206656E+03	-1.79695563E+03	1.48043452E+02	7.20141581E-02
31	-1.30865394E+03	-1.81734356E+03	2.02500284E-03	1.13295408E-01
32	-1.30206682E+03	-1.79695720E+03	-1.48039465E+02	7.20141581E-02
33	-1.28256104E+03	-1.73290027E+03	-2.92542038E+02	-4.49484240E-02
34	-1.25088202E+03	-1.61720353E+03	-4.29537727E+02	-2.17783623E-01
35	-1.20821262E+03	-1.43886189E+03	-5.54309875E+02	-4.16179227E-01
36	-1.15612553E+03	-1.18685540E+03	-6.61274587E+02	-6.03097453E-01
37	-1.09657616E+03	-8.53664050E+02	-7.44123437E+02	-7.39532816E-01
38	-1.03194956E+03	-4.38714395E+02	-7.96246304E+02	-7.89764608E-01
39	-9.65136661E+02	4.87867629E+01	-8.11408923E+02	-7.26544464E-01
40	-8.99576929E+02	5.88084697E+02	-7.84618653E+02	-5.35631119E-01
41	-8.39185370E+02	1.14649045E+03	-7.13079190E+02	-2.19108625E-01
42	-7.88096034E+02	1.68054065E+03	-5.97113618E+02	2.02995399E-01
43	-7.50202195E+02	2.13873284E+03	-4.40926074E+02	6.93138923E-01
44	-7.28543091E+02	2.46575576E+03	-2.53074309E+02	1.19890313E+00
45	-7.24656414E+02	2.60803634E+03	-4.65373901E+01	1.65777415E+00
46	-7.38063310E+02	2.52030250E+03	1.61715267E+02	2.00375664E+00
47	-7.66061684E+02	2.17267379E+03	3.51712193E+02	2.17525954E+00
48	-8.03961530E+02	1.55752315E+03	5.02030638E+02	2.12347334E+00
49	-8.45792107E+02	6.95049255E+02	5.91839455E+02	1.82029297E+00
50	-8.85346112E+02	-3.63724462E+02	6.03269462E+02	1.26475826E+00
51	-9.17236325E+02	-1.53778559E+03	5.23848516E+02	4.87009673E-01
52	-9.37515018E+02	-2.72165737E+03	3.48662225E+02	-4.51095177E-01
53	-9.43469102E+02	-3.79565050E+03	8.18759885E+01	-1.45928193E+00
54	-9.32535524E+02	-4.63980970E+03	-2.62699493E+02	-2.42626175E+00
55	-9.00819418E+02	-5.14950791E+03	-6.62197928E+02	-3.23093538E+00
56	-8.42188665E+02	-5.25003397E+03	-1.08647060E+03	-3.75656675E+00
57	-7.48994272E+02	-4.90755819E+03	-1.50088519E+03	-3.90657018E+00
58	-6.14851329E+02	-4.13456559E+03	-1.86982789E+03	-3.62010975E+00
59	-4.38699044E+02	-2.98906080E+03	-2.16047221E+03	-2.88541230E+00
60	-2.28160185E+02	-1.56836548E+03	-2.34634087E+03	-1.74861622E+00
61	-2.29864352E+01	-7.22995077E+00	-2.53066237E+03	-3.17916866E-01

STATION	U2C	V2C	W2C	M2C
1	2.41273601E-02	0.	0.	1.01896513E+00
2	2.13269831E-02	0.	-1.97657114E-02	-3.20432184E+01
3	1.93071340E-02	0.	-3.56372344E-02	-6.35451996E+01
4	1.79693584E-02	0.	-4.68868029E-02	-8.92656410E+01
5	1.70953699E-02	0.	-5.31752511E-02	-1.04189883E+02
6	1.64421698E-02	0.	-5.45586954E-02	-1.04903861E+02
7	1.58235981E-02	0.	-5.14701927E-02	-9.11309865E+01
8	1.51554210E-02	0.	-4.46668458E-02	-6.58459794E+01
9	1.44552341E-02	0.	-3.51430195E-02	-3.41547830E+01
10	1.38060730E-02	0.	-2.40198473E-02	-1.64196988E+00
11	1.33046449E-02	0.	-1.24271216E-02	2.70780646E+01
12	1.30165558E-02	0.	-1.39489205E-03	4.91651691E+01
13	1.29530808E-02	0.	8.23092779E-03	6.36445928E+01
14	1.30723843E-02	0.	1.58405432E-02	7.09840125E+01
15	1.32984847E-02	0.	2.10783089E-02	7.24552172E+01
16	1.35469518E-02	0.	2.38311879E-02	6.95426326E+01
17	1.37473104E-02	0.	2.41956742E-02	6.35542572E+01
18	1.38562412E-02	0.	2.24322239E-02	5.54744536E+01
19	1.38603356E-02	0.	1.89151310E-02	4.60091938E+01
20	1.37706268E-02	0.	1.40835843E-02	3.57274431E+01
21	1.36127682E-02	0.	8.39741455E-03	2.51978658E+01
22	1.34167499E-02	0.	2.29945202E-03	1.50497556E+01
23	1.32089918E-02	0.	-3.81436439E-03	5.93590994E+00
24	1.30081215E-02	0.	-9.61621570E-03	-1.57654950E+00
25	1.28242773E-02	0.	-1.48581851E-02	-7.13179143E+00
26	1.26607744E-02	0.	-1.93742183E-02	-1.06698764E+01
27	1.25166408E-02	0.	-2.30727241E-02	-1.24350281E+01
28	1.23888272E-02	0.	-2.59214261E-02	-1.29046665E+01
29	1.22735347E-02	0.	-2.79272468E-02	-1.26635390E+01
30	1.21667257E-02	0.	-2.91148460E-02	-1.22600221E+01
31	1.20642136E-02	0.	-2.95076971E-02	-1.20796955E+01
32	1.19616995E-02	0.	-2.91151449E-02	-1.22608780E+01
33	1.18548845E-02	0.	-2.79278128E-02	-1.26651858E+01
34	1.17395827E-02	0.	-2.59221977E-02	-1.29069768E+01
35	1.16117573E-02	0.	-2.30736150E-02	-1.24378182E+01
36	1.14676102E-02	0.	-1.93751238E-02	-1.06729160E+01
37	1.13040930E-02	0.	-1.48589903E-02	-7.13481736E+00
38	1.11202342E-02	0.	-9.61680552E-03	-1.57928304E+00
39	1.09193494E-02	0.	-3.81463400E-03	5.93374460E+00
40	1.07115781E-02	0.	2.29958606E-03	1.50484133E+01
41	1.05155490E-02	0.	8.39800382E-03	2.51975647E+01
42	1.03576838E-02	0.	1.40846392E-02	3.57283518E+01
43	1.02679749E-02	0.	1.89166137E-02	4.60114189E+01
44	1.02720775E-02	0.	2.24340442E-02	5.54780252E+01
45	1.03810258E-02	0.	2.41976901E-02	6.35591085E+01
46	1.05814095E-02	0.	2.38332111E-02	6.95485724E+01
47	1.08299056E-02	0.	2.10801155E-02	7.24618991E+01
48	1.10560321E-02	0.	1.58418914E-02	7.09909102E+01
49	1.11753506E-02	0.	8.23158018E-03	6.36509993E+01

50	1.11118726E-02	0.	-1.39514209E-03	4.91702391E+01
51	1.08237583E-02	0.	-1.24284224E-02	2.70809163E+01
52	1.03222844E-02	0.	-2.40222635E-02	-1.64208996E+00
53	9.67306355E-03	0.	-3.51465125E-02	-3.41582972E+01
54	8.97281262E-03	0.	-4.46712635E-02	-6.58527922E+01
55	8.30457539E-03	0.	-5.14752709E-02	-9.11403898E+01
56	7.68594871E-03	0.	-5.45640712E-02	-1.04914601E+02
57	7.03268932E-03	0.	-5.31804874E-02	-1.04200410E+02
58	6.15861785E-03	0.	-4.68914202E-02	-8.92744838E+01
59	4.82071072E-03	0.	-3.56407468E-02	-6.35513219E+01
60	2.80065950E-03	0.	-1.97676631E-02	-3.20461907E+01
61	0.	0.	0.	1.01907911E+00

STATION	U22	V22	W22	M22
1	-8.90431061E-02	0.	0.	1.01896513E+00
2	-7.30274709E-02	-1.47056488E-02	1.90802936E-01	4.00389061E+02
3	-5.98268948E-02	-2.81948330E-02	3.68258957E-01	7.56210448E+02
4	-4.94258779E-02	-3.93821705E-02	5.17653284E-01	1.01719279E+03
5	-4.07019003E-02	-4.75223112E-02	6.27833896E-01	1.14673573E+03
6	-3.22518435E-02	-5.23278785E-02	6.92788854E-01	1.13440683E+03
7	-2.31462475E-02	-5.39431811E-02	7.12166139E-01	9.97377371E+02
8	-1.32884908E-02	-5.28227558E-02	6.90661604E-01	7.73382881E+02
9	-3.31278379E-03	-4.95779861E-02	6.36561711E-01	5.09255811E+02
10	5.81176682E-03	-4.48436764E-02	5.59912293E-01	2.49383911E+02
11	1.32167244E-02	-3.91909742E-02	4.70780565E-01	2.72955045E+01
12	1.84165903E-02	-3.30881266E-02	3.77941921E-01	-1.38195068E+02
13	2.13749670E-02	-2.68956694E-02	2.88135857E-01	-2.42526636E+02
14	2.24033374E-02	-2.08792292E-02	2.05865908E-01	-2.91979372E+02
15	2.19890953E-02	-1.52271703E-02	1.33607926E-01	-2.99054597E+02
16	2.06377118E-02	-1.00665471E-02	7.22493148E-02	-2.78130674E+02
17	1.87729674E-02	-5.47563787E-03	2.15960230E-02	-2.42279200E+02
18	1.66994393E-02	-1.49364345E-03	-1.91696766E-02	-2.01502490E+02
19	1.46087670E-02	1.87146689E-03	-5.11428886E-02	-1.62214313E+02
20	1.26064397E-02	4.63638191E-03	-7.54764994E-02	-1.27584730E+02
21	1.07417548E-02	6.83695614E-03	-9.32717798E-02	-9.83517507E+01
22	9.03222625E-03	8.52369422E-03	-1.05546956E-01	-7.37778267E+01
23	7.48022923E-03	9.75798056E-03	-1.13248665E-01	-5.25283102E+01
24	6.08279775E-03	1.06086897E-02	-1.17276720E-01	-3.33394079E+01
25	4.83618762E-03	1.11488153E-02	-1.18502191E-01	-1.54188429E+01
26	3.73657465E-03	1.14519095E-02	-1.17768973E-01	1.41458219E+00
27	2.77808997E-03	1.15883464E-02	-1.15877499E-01	1.67979706E+01
28	1.94954076E-03	1.16216106E-02	-1.13554875E-01	3.00159444E+01
29	1.23136027E-03	1.16048978E-02	-1.11418357E-01	4.02329592E+01
30	5.94214910E-04	1.15782889E-02	-1.09939291E-01	4.67022969E+01
31	1.19329737E-07	1.15666698E-02	-1.09413405E-01	4.89179500E+01
32	-5.93990977E-04	1.15784734E-02	-1.09941485E-01	4.67019157E+01
33	-1.23118019E-03	1.16052611E-02	-1.11422694E-01	4.02320725E+01
34	-1.94943272E-03	1.16221409E-02	-1.13561249E-01	3.00143279E+01
35	-2.77808065E-03	1.15890252E-02	-1.15885739E-01	1.67953403E+01
36	-3.73668885E-03	1.14527109E-02	-1.17778836E-01	1.41063903E+00
37	-4.83644820E-03	1.11497051E-02	-1.18513354E-01	-1.54243809E+01
38	-6.08322599E-03	1.06096249E-02	-1.17288769E-01	-3.33467974E+01
39	-7.48084544E-03	9.75890899E-03	-1.13261091E-01	-5.25378040E+01
40	-9.03305065E-03	8.52455469E-03	-1.05559152E-01	-7.37897183E+01
41	-1.07428080E-02	6.83767907E-03	-9.32830363E-02	-9.83664228E+01
42	-1.26077426E-02	4.63689042E-03	-7.54860001E-02	-1.27602676E+02
43	-1.46103387E-02	1.87167846E-03	-5.11497029E-02	-1.62236093E+02
44	-1.67012931E-02	-1.49381483E-03	-1.91727513E-02	-2.01528586E+02
45	-1.87751033E-02	-5.47627903E-03	2.15978683E-02	-2.42309751E+02
46	-2.06401051E-02	-1.00677423E-02	7.22573798E-02	-2.78165092E+02
47	-2.19916824E-02	-1.52289975E-02	1.33623595E-01	-2.99091122E+02
48	-2.24060007E-02	-2.08817551E-02	2.05890574E-01	-2.92014672E+02
49	-2.13775249E-02	-2.68989433E-02	2.88170792E-01	-2.42555611E+02

50	-1.84187998E-02	-3.30921733E-02	3.77988078E-01	-1.38211053E+02
51	-1.32183037E-02	-3.91957848E-02	4.70838332E-01	2.72999944E+01
52	-5.81243829E-03	-4.48491961E-02	5.59981218E-01	2.49415844E+02
53	3.31323694E-03	-4.95841015E-02	6.36640249E-01	5.09319862E+02
54	1.32901772E-02	-5.28292821E-02	6.90746958E-01	7.73479591E+02
55	2.31491552E-02	-5.39498540E-02	7.12254264E-01	9.97501776E+02
56	3.22558814E-02	-5.23343576E-02	6.92874670E-01	1.13454815E+03
57	4.07069894E-02	-4.75281994E-02	6.27911734E-01	1.14687849E+03
58	4.94320548E-02	-3.93870525E-02	5.17717513E-01	1.01731937E+03
59	5.98343705E-02	-2.81983293E-02	3.68304684E-01	7.56304544E+02
60	7.30365966E-02	-1.47074726E-02	1.90826646E-01	4.00438889E+02
61	8.90542355E-02	-7.18922196E-17	0.	1.01907911E+00

STATION	W20X	W22X	W20XX	W22XX
1	-1.86109762E-01	1.69265480E+00	2.05070256E-01	2.00151799E-01
2	-1.52731005E-01	1.57825267E+00	2.86103633E-01	-9.80589652E-01
3	-1.16233249E-01	1.40078721E+00	3.39572170E-01	-2.06167554E+00
4	-7.51629285E-02	1.11246402E+00	3.64490476E-01	-2.88100759E+00
5	-3.28795391E-02	7.50581015E-01	3.60367627E-01	-3.32270110E+00
6	7.30739294E-03	3.61423901E-01	3.28551207E-01	-3.34856371E+00
7	4.23936411E-02	-9.11678781E-03	2.72927332E-01	-3.00356238E+00
8	6.99735994E-02	-3.24018581E-01	1.99871953E-01	-2.39476093E+00
9	8.84871362E-02	-5.60354187E-01	1.17502964E-01	-1.65669974E+00
10	9.73538482E-02	-7.10490625E-01	3.44978124E-02	-9.17067761E-01
11	9.69640941E-02	-7.79873023E-01	-4.11793106E-02	-2.72344780E-01
12	8.85344974E-02	-7.82763033E-01	-1.03328061E-01	2.22801749E-01
13	7.38661510E-02	-7.37468630E-01	-1.48129306E-01	5.53673738E-01
14	5.50602047E-02	-6.62262560E-01	-1.74258345E-01	7.35573166E-01
15	3.42456203E-02	-5.72642541E-01	-1.82563101E-01	8.00770026E-01
16	1.33601369E-02	-4.80051015E-01	-1.75473758E-01	7.86513279E-01
17	-5.99556017E-03	-3.91795678E-01	-1.56338191E-01	7.26435355E-01
18	-2.26308991E-02	-3.11738192E-01	-1.28839047E-01	6.45978678E-01
19	-3.57798838E-02	-2.41314955E-01	-9.65721197E-02	5.61276822E-01
20	-4.50759278E-02	-1.80552391E-01	-6.27886350E-02	4.80367134E-01
21	-5.05034242E-02	-1.28873387E-01	-3.02541605E-02	4.05558644E-01
22	-5.23361954E-02	-8.56152245E-02	-1.16477463E-03	3.36009854E-01
23	-5.10671474E-02	-5.02704172E-02	2.29198844E-02	2.69901129E-01
24	-4.73306601E-02	-2.25151095E-02	4.11341829E-02	2.05904145E-01
25	-4.18200111E-02	-2.10965406E-03	5.33340850E-02	1.43903662E-01
26	-3.52051670E-02	1.12486807E-02	6.00632429E-02	8.50963624E-02
27	-2.80594619E-02	1.80604187E-02	6.24345594E-02	3.16762890E-02
28	-2.08050975E-02	1.91106084E-02	6.19259728E-02	-1.36730378E-02
29	-1.36860855E-02	1.54953610E-02	6.01142322E-02	-4.83026303E-02
30	-6.77335827E-03	8.59264914E-03	5.83896638E-02	-7.00295739E-02
31	-1.28099958E-06	-9.40478538E-06	5.77030893E-02	-7.74342077E-02
32	6.77093272E-03	-8.61123860E-03	5.83920030E-02	-7.00258005E-02
33	1.36840594E-02	-1.55132720E-02	6.01187408E-02	-4.82947724E-02
34	2.08037045E-02	-1.91273320E-02	6.19323180E-02	-1.36605409E-02

35	2.80588881E-02	-1.80753739E-02	6.24422576E-02	3.16941071E-02
36	3.52055345E-02	-1.12612072E-02	6.00716800E-02	8.51201798E-02
37	4.18213642E-02	2.10028927E-03	5.33425443E-02	1.43934045E-01
38	4.73329557E-02	2.25096962E-02	4.11418809E-02	2.05941502E-01
39	5.10702496E-02	5.02697852E-02	2.29260154E-02	2.69945740E-01
40	5.23398764E-02	8.56202352E-02	-1.16098558E-03	3.36061974E-01
41	5.05073708E-02	1.28884937E-01	-3.02533963E-02	4.05618630E-01
42	4.50797566E-02	1.80571429E-01	-6.27914184E-02	4.80435511E-01
43	3.57831641E-02	2.41342495E-01	-9.65787385E-02	5.61354200E-01
44	2.26331847E-02	3.11775305E-01	-1.28849480E-01	6.46065401E-01
45	5.99642944E-03	3.91843419E-01	-1.56352039E-01	7.26530831E-01
46	-1.33610343E-02	4.80110259E-01	-1.75490196E-01	7.86614998E-01
47	-3.42485130E-02	5.72713691E-01	-1.82580868E-01	8.00872407E-01
48	-5.50651512E-02	6.62345129E-01	-1.74275786E-01	7.35666528E-01
49	-7.38730005E-02	7.37560732E-01	-1.48144488E-01	5.53743813E-01
50	-8.85428682E-02	7.82860886E-01	-1.03338959E-01	2.22830264E-01
51	-9.69733776E-02	7.79970600E-01	-4.11840591E-02	-2.72378036E-01
52	-9.73632433E-02	7.10579642E-01	3.45006479E-02	-9.17181240E-01
53	-8.84957142E-02	5.60424600E-01	1.17514136E-01	-1.65690520E+00
54	-6.99803933E-02	3.24060067E-01	1.99891365E-01	-2.39505821E+00
55	-4.23977475E-02	9.11876390E-03	2.72953992E-01	-3.00393556E+00
56	-7.30807043E-03	-3.61467986E-01	3.28583329E-01	-3.34898016E+00
57	3.28827903E-02	-7.50673529E-01	3.60402854E-01	-3.32311486E+00
58	7.51703165E-02	-1.11260164E+00	3.64526167E-01	-2.88136709E+00
59	1.16244673E-01	-1.40096086E+00	3.39605659E-01	-2.06193380E+00
60	1.52746058E-01	-1.57844865E+00	2.86132367E-01	-9.80713967E-01
61	1.86128167E-01	-1.69286528E+00	2.05091820E-01	2.00174153E-01

STATION	NX20	NY20	NX22	NY22	NXY22
1	-4.27003039E+03	-1.35158486E+03	-4.16901593E+03	-1.31959751E+03	-2.23187264E+04
2	-4.06421640E+03	-5.33200981E+03	-3.66613286E+02	6.26714377E+03	-1.95453261E+04
3	-3.37714006E+03	-8.36574437E+03	3.71615523E+03	1.40231381E+04	-1.76081687E+04
4	-2.42938575E+03	-1.03720080E+04	7.49929425E+03	2.11220980E+04	-1.46462810E+04
5	-1.49755248E+03	-1.13664915E+04	1.05550344E+04	2.67224818E+04	-1.08542438E+04
6	-8.04822677E+02	-1.14293995E+04	1.26172957E+04	3.00381546E+04	-6.50262129E+03
7	-4.47337874E+02	-1.06792557E+04	1.36194109E+04	3.05571851E+04	-1.92972325E+03
8	-3.86621531E+02	-9.25978969E+03	1.36579782E+04	2.82186119E+04	2.48795372E+03
9	-4.98240165E+02	-7.33704050E+03	1.29205064E+04	2.34532354E+04	6.38553889E+03
10	-6.41997742E+02	-5.09815089E+03	1.16178044E+04	1.70746541E+04	9.46646939E+03
11	-7.18598211E+02	-2.74443877E+03	9.94268943E+03	1.00716883E+04	1.15482566E+04
12	-6.93974291E+02	-4.76566854E+02	8.05526466E+03	3.38241232E+03	1.25835847E+04
13	-5.91729934E+02	1.52509610E+03	6.08413171E+03	-2.27908768E+03	1.26523361E+04
14	-4.66542021E+02	3.11925355E+03	4.13284049E+03	-6.50572736E+03	1.19298862E+04
15	-3.74207917E+02	4.21648400E+03	2.28566176E+03	-9.19084712E+03	1.06431397E+04
16	-3.49923770E+02	4.78343842E+03	6.10979102E+02	-1.04594777E+04	9.02678721E+03
17	-3.99698834E+02	4.83860283E+03	-8.37596680E+02	-1.05741349E+04	7.28916146E+03
18	-5.03952428E+02	4.44179293E+03	-2.02199172E+03	-9.84632641E+03	5.59212668E+03
19	-6.28820562E+02	3.68038622E+03	-2.92173154E+03	-8.57198265E+03	4.04482643E+03

20	-7.39598614E+02	2.65517210E+03	-3.53615986E+03	-6.99573546E+03	2.70807466E+03
21	-8.11515472E+02	1.46799996E+03	-3.88517453E+03	-5.29968743E+03	1.60495442E+03
22	-8.34986350E+02	2.12480308E+02	-4.00705004E+03	-3.60821173E+03	7.33395067E+02
23	-8.14896701E+02	-1.03189937E+03	-3.95298490E+03	-2.00035746E+03	7.75432299E+01
24	-7.65558684E+02	-2.20256351E+03	-3.77944156E+03	-5.23709516E+02	-3.83901715E+02
25	-7.04100385E+02	-3.25422568E+03	-3.54033885E+03	7.93686732E+02	-6.72925490E+02
26	-6.44928537E+02	-4.15758172E+03	-3.28117130E+03	1.93455763E+03	-8.10558067E+02
27	-5.96814115E+02	-4.89688377E+03	-3.03621699E+03	2.88677090E+03	-8.17329540E+02
28	-5.62743410E+02	-5.46676731E+03	-2.82872040E+03	3.64032816E+03	-7.14649243E+02
29	-5.41632867E+02	-5.86862541E+03	-2.67297662E+03	4.18634649E+03	-5.26118866E+02
30	-5.30672591E+02	-6.10689814E+03	-2.57697678E+03	4.51736682E+03	-2.78160077E+02
31	-5.27344328E+02	-6.18578545E+03	-2.54462006E+03	4.62829596E+03	2.57939538E-01
32	-5.30671976E+02	-6.10695932E+03	-2.57705998E+03	4.51731329E+03	2.78671261E+02
33	-5.41631839E+02	-5.86874132E+03	-2.67314167E+03	4.18623641E+03	5.26615773E+02
34	-5.62742352E+02	-5.46692548E+03	-2.82896457E+03	3.64015558E+03	7.15121731E+02
35	-5.96813516E+02	-4.89706667E+03	-3.03653595E+03	2.88652720E+03	8.17766538E+02
36	-6.44928850E+02	-4.15776801E+03	-3.28155890E+03	1.93423176E+03	8.10947198E+02
37	-7.04101819E+02	-3.25439189E+03	-3.54078664E+03	7.93265502E+02	6.73252689E+02
38	-7.65560975E+02	-2.20268593E+03	-3.77993815E+03	-5.24241070E+02	3.84150822E+02
39	-8.14898970E+02	-1.03195622E+03	-3.95351536E+03	-2.00101533E+03	-7.73908428E+01
40	-8.34987174E+02	2.12506610E+02	-4.00759535E+03	-3.60901151E+03	-7.33360719E+02
41	-8.11513255E+02	1.46812056E+03	-3.88571137E+03	-5.30064159E+03	-1.60506197E+03
42	-7.39592261E+02	2.65538955E+03	-3.53666070E+03	-6.99684899E+03	-2.70834973E+03
43	-6.28810306E+02	3.68069279E+03	-2.92216522E+03	-8.57324672E+03	-4.04529453E+03
44	-5.03940539E+02	4.44216957E+03	-2.02232442E+03	-9.84771039E+03	-5.59281010E+03
45	-3.99689844E+02	4.83901912E+03	-8.37793265E+02	-1.05755778E+04	-7.29007469E+03
46	-3.49923886E+02	4.78385390E+03	6.10953220E+02	-1.04608810E+04	-9.02793115E+03
47	-3.74223470E+02	4.21685088E+03	2.28583840E+03	-9.19207295E+03	-1.06444954E+04
48	-4.66577147E+02	3.11952095E+03	4.13324601E+03	-6.50660414E+03	-1.19314093E+04
49	-5.91784143E+02	1.52521542E+03	6.08478409E+03	-2.27942751E+03	-1.26539537E+04
50	-6.94040987E+02	-4.76636093E+02	8.05617046E+03	3.38278478E+03	-1.25851962E+04
51	-7.18665421E+02	-2.74472349E+03	9.94384079E+03	1.00728985E+04	-1.15497401E+04
52	-6.42051866E+02	-5.09866039E+03	1.16191760E+04	1.70767397E+04	-9.46769355E+03
53	-4.98272441E+02	-7.33776436E+03	1.29220523E+04	2.34561186E+04	-6.38637825E+03
54	-3.86635251E+02	-9.26069792E+03	1.36596286E+04	2.82220931E+04	-2.48830576E+03
55	-4.47352913E+02	-1.06803003E+04	1.36210706E+04	3.05609648E+04	1.92992391E+03
56	-8.04873731E+02	-1.14305170E+04	1.26188470E+04	3.00418799E+04	6.50339429E+03
57	-1.49767934E+03	-1.13676044E+04	1.05563471E+04	2.67258067E+04	1.08555614E+04
58	-2.42961784E+03	-1.03730272E+04	7.50024509E+03	2.11247382E+04	1.46480731E+04
59	-3.37748139E+03	-8.36657151E+03	3.71665178E+03	1.40249042E+04	1.76103309E+04
60	-4.06463862E+03	-5.33254283E+03	-3.66612457E+02	6.26794750E+03	1.95477296E+04
61	-4.27047979E+03	-1.35172710E+03	-4.16948156E+03	-1.31974489E+03	2.23214739E+04

AREA(U1, V1, W1)= 3.32926879E-02

XTE= -1.37353058E+04

XTD= 1.40413805E+00
SENSITIVITY INDEX BY PRESENT THEORY B= 9.40435297E+00
AREA1= 4.18255826E+01
AREA2= 1.97430955E+02
AREA3= 1.97430955E+02

SENSITIVITY INDEX BY BUDIANSKY THEORY B= 2.39133287E+00

```
05/22/69   LRC CM SCOPE 3.0  6600D-131K 04/16/69
16.34.32.SRD6698.        -  0522  1325
16.34.32.                     LRC COMPUTER COMPLEX
16.34.32.JOB,1,0400,70000.         A2338,      2,
16.34.32.  MICHAEL CARD,  RDF367,1148,201I,
16.34.33.RUN(S)
16.34.50.NOMAP.
16.34.50.SETINDF.
16.34.52.LGO.
16.35.06.MEMORY  062000 CM
16.35.10.EOF ENCOUNTERED BY NAMELIST
16.35.10.EXIT
16.35.11.SPPRINT(OUTPUT,5)
16.35.13.CPU    13.111505 SEC.
16.35.13.PPU    41.054208 SEC.
16.35.13.DATE     05/22/69
16.55.15. SRD6698. PRINT-PP 01723. LINES,LP 26
```

TABLE I.- ELASTIC CONSTANTS FOR MATERIALS USED IN

IMPERFECTION SENSITIVITY STUDY

Constituent material	Young's modulus, ksi	Poisson's ratio
Glass fiber	10,500	0.23
Boron fiber	60,000	0.30
Aluminum	10,500	0.30
Epoxy	500	0.40

Properties of Helically Wrapped Layers (see refs. 33 and 35)

Material	v_f	α	E_x, ksi	E_y, ksi	μ_x	μ_y	G_{xy}, ksi
Glass-epoxy	0.65	0	7,000	2,562	0.283	0.104	709
		15	6,102	2,419	0.420	0.167	1,054
		30	3,878	2,117	0.649	0.354	1,744
		45	2,270	2,270	0.600	0.600	2,089
		60	2,117	3,878	0.354	0.649	1,744
		75	2,419	6,102	0.167	0.420	1,054
		90	2,562	7,000	0.104	0.283	709
Boron-epoxy	0.50	0	30,250	2,030	0.346	0.023	525
		15	23,800	1,900	1.179	0.094	2,339
		30	7,762	1,608	1.655	0.342	5,967
		45	1,977	1,977	0.844	0.884	7,782
		60	1,608	7,762	0.343	1.655	5.967
		75	1,900	23,800	0.094	1.179	2,339
		90	2,030	30,250	0.023	0.346	525

TABLE II.- TEST CYLINDER CONSTITUENT PROPERTIES

Material	Young's modulus, ksi	Poisson's ratio	Density lb/cu. in.
ERL-2256 epoxy	635	0.40	0.0445
TYPE E glass fiber	10,500	0.23	0.0930

*Cured at 250° F for 2 hours.

TABLE III.- TEST CYLINDER DIMENSIONS AND EXPERIMENTAL RESULTS

(Inside diameter, 30 in.; length 30 in.)

Cylinder	Type*	α, deg	t, in.	v_f	v_r	v_v	$\bar{E}_{x_{exp}}$, ksi	$\bar{\mu}_{x_{exp}}$, ksi	λ_{exp} lb/in.	λ_{cr} lb/in.
1	H + C	15	0.0796	53.8	42.1	4.1	4,780	0.165	567	711
2	H + C	15	0.0948	55.1	40.2	4.7	4,540	0.233	804	1043
3	H + C	30	0.0722	47.8	50.4	1.8	3,310	0.264	360	511
4	H + C	30	0.0717	47.2	50.3	2.5	3,210	0.289	322	511
5	H + C	45	0.0720	53.1	43.6	3.3	2,560	0.268	430	501
6	H + C	45	0.0697	55.0	41.4	3.6	2,750	0.229	404	501
7	H	15	0.0943	45.9	50.4	3.7	5,060	0.463	717	789
8	H	15	0.0974	54.5	41.6	3.9	5,620	0.484	711	1037
9	H	30	0.0765	43.0	48.6	8.4	3,280	0.562	386	464
10	H	30	0.0704	51.9	44.1	4.0	3,500	0.605	341	447
11	H	45	0.0670	57.2	36.3	6.5	2,780	0.427	341	386
12	H	45	0.0669	52.7	41.1	6.2	2,180	0.512	311	386

*H + C - helically and circumferentially wrapped.
H - helically wrapped.